ALTERNATIVE OXIDANTS AND PROCESSING PROCEDURES FOR PYROTECHNIC TIME DELAYS

ISABEL MARIA MOREIRA RICCO

A dissertation submitted in partial fulfilment of the requirements for the degree of

MASTER OF ENGINEERING (CHEMICAL ENGINEERING)

In the

Faculty of Engineering, Built Environment and Information Technology

University of Pretoria

2004

ALTERNATIVE OXIDANTS AND PROCESSING PROCEDURES FOR PYROTECHNIC TIME DELAYS

Isabel Maria Moreira Ricco

Supervisor: Professor W. W. Focke
Department: Department of Chemical Engineering
University: University of Pretoria
Degree: Master of Engineering (Chemical Engineering)

SYNOPSIS

This study was directed at the pyrotechnic time delay compositions that are used in detonator assemblies. The objectives were to:

- Investigate effective alternatives for the barium and lead-based oxidants currently used, maintaining the use of silicon as fuel
- Develop easy to use, realistic measurement techniques for burn rates and shock tube ignitability
- Determine the variables that affect burn rate, and
- Evaluate alternative processing routes to facilitate intimate mixing of the component powders.

Lead chromate and copper antimonite were found to be suitable oxidants for silicon in time delay compositions. They were ignitable by shock tubing, a relatively weak ignition source. The measured burn speeds for these systems showed a bimodal dependence on stoichiometry. Measured burn rates varied between 6-28 mm/s. Lead chromate is potentially a suitable alternative to the oxidant currently used in the

medium burn rate commercial composition. It burns faster than copper antimonite. The latter is potentially a suitable replacement oxidant for the *slow* and *medium* compositions.

Antimony trioxide-based compositions exhibited unreliable performance with respect to ignition with shock tubing.

The addition of aluminium powder or fumed silica was found to reduce the burn rate. Increasing the silicon particle size (<3,5μm) also decreased the burn speed for copper antimonite and lead chromate compositions. Addition of fumed silica improved the flow properties of the lead chromate, copper antimonite and antimony trioxide powders allowing for easier mixing.

The silicon powder was found to react violently with water in alkaline solutions. This makes particle dispersion in a wet-mixing process problematic.

Keywords: pyrotechnic, time delay, copper antimonite, burn speed, silicon, lead chromate, antimony trioxide, detonator.

ALTERNATIEWE OKSIDEERMIDDELS EN PROSSESSERING VAN PIROTEGNIESE TYD VERTRAGERS

Isabel Maria Moreira Ricco

Promotor: Professor W. W. Focke
Department: Department of Chemical Engineering
Universiteit: University of Pretoria
Graad: Magister in Ingenieurswese (Chemies Ingenieurswese)

SINOPSIS

Hierdie studie was gerig op pirotegniese tydvertragersamestellings wat in slagdoppies gebruik word. Die doelwit was om:

- Effektiewe alternatiewe vir die barium- en loodgebaseerde oksideermiddels te vind wat tans saam met silikon as brandstof gebruik word
- Eenvoudige en realistiese meettegnieke vir ontsteekbaarheid en die brandtempo van tydvertrager formulasies te ontwikkel
- Te bepaal watter veranderlikes brandtempos beïnvloed, en
- Alternatiewe prosesserings roetes te ondersoek om goeie vermenging van die komponentpoeiers te verseker.

Dit is gevind dat loodchromaat en koperantimoniet geskikte oksideermiddels is vir silikon in tydvertragendesamestellings. Hulle kon ontsteek word met behulp van ‘n skokbuis, ‘n relatief lae intensiteit ontstekingsbron. Die brandtempos toon ‘n bimodale afhanklikheid van stoichiometrie. Die gemete waardes het variëer oor die gebied 6-28 mm/s. Loodchromaat is ‘n potensiële alternatief vir die oksideermiddels wat tans in die “medium” kommersiëele samestelling gebruik word. Dit brand

vinniger as koperantimoniet. Laasgenoemde is ‘n potensiële alternatief vir die oksideermiddels in die “stadige” en “medium” samestellings.

Antimoon trioksied gebasseerde sametstellings het wisselende resultate in terme van aansteekbaarheid met skokbuise getoon.

Toevoegings van aluminium of gerookte silika poeiers het brandtempos verlaag. Die brandtempos van die koperantimoniet en loodchromaat samestellings het ook afgeneem met toename in die silikon partikelgrootte. Gerookte silika het ook die vloei eienskappe van loodchromaat, koperantimoniet en antimoontrioksied poeiers verbeter en sodoende beter vermenging bewerkstellig.

Silikon reageer heftig met water in die teenwoordigheid van alkalies. Dus is die dispersie van die partikels in ‘n nat vermengingsproses problematies.

Sleutelwoorde: pirotegnies, koperantimoniet, brandtempo, silikon, loodchromaat, antimoontrioksied, slagdoppie

ACKNOWLEDGEMENTS

I wish to express my appreciation to the following organisations and persons who made this dissertation possible:

- This dissertation is based on a research project of African Explosives Limited (AEL). Permission to use the material is gratefully acknowledged. The opinions expressed are those of the author and do not necessarily represent the policy of AEL.

- AEL for financial support, the provision of data and the use of facilities and expertise.

- The following persons are gratefully acknowledged for their assistance during the course of the study:
    - Mr C. Conradie, Mrs L. Cloete, Hilton Lange (AEL)
    - Dr S. van der Walt who wrote and rewrote Capture until perfect, designed the electronic interface, got the data capture card to work, and still had the patience to teach me. A true gentleman who kept his word and was proud of his work.
    - Serei Sefanyetso
    - Leon de Jager from Poretech who willingly did particle size analysis for us at his own cost.
    - Dr B. Kosowski from Mach I who supplied and couriered the Nanocat from the US at his own cost.
    - All other organisations who supplied free samples: Hayley from Rolfes pigments, Bayer, Steve Swart from Delta EMD, Chemimpo, Rhombus Vanadium Mine, Degussa, Bayer
    - SEM, XRD and XRF staff.

- Professor W. W. Focke, my supervisor for his guidance and support.
- My family for the encouragement and support during the study, in particular my sister, Marisa, who helped brush mix and crimp detonators for hours on end.

- Eddie Ferreira, my partner for life, who listened to endless ideas and helped me implement quite a few of them. Your support, enthusiasm to better the world around you and belief in my abilities inspired me through the good and bad.

CONTENTS

TABLES

FIGURES

NOMENCLATURE

a	Filtration parameter for first order data filter
a_o	Initial thickness of metal A (half effective particle size of the discontinuous phase (cm)
b	Reaction zone width
b_1	Fraction of inert or product diluent
c	Specific heat capacity
c_1	Heat capacity of the gaseous products
c_p, c_s, c_f	Specific heat capacity of solid
d	Particle size
d_1	Particle size of fine particles
d_2	Particle size of coarse particles
d_B^{st}	Diameter of reactant B in a corresponding stoichiometric mixture
d_{eff}	Effective particle size
d_{max}	Maximum particle size
d_{min}	Minimum particle size
D	Mass diffusivity
D_{rc}	Diameter of the reaction cell.
E	Activation energy
f	Fraction of the surface covered by the adsorbate
f(d)	Dependence of v on particle size
f(n)	Reaction order function
F	Van der Waal's force between particles
F(T)	Dependence of v on temperature
G	Thermal power arising from heat effects of all changes
h	Lateral heat transfer coefficient
H_R	Heat of reaction at 298K
H_f	Heat of formation at 298K
k	Boltzmann constant
K_{ads}	Adsorption constant
K_o	Preexponential constant for kinetics
l	Order of reaction

L	Distance between centres of two particles
Le	Lewis number
m	Combustion mass velocity
m_1	Mass fraction of fine particles
MW_i	Molecular mass of component i
n	Reaction order
P	Vapour pressure of most volatile component or product dissociation pressure at the combustion temperature
P_o	External gas pressure
Q	Heat of reaction
r	Radius of spherical particle
R	Ideal gas constant
s	Distance between two particles
S	Surface area
t*	Rise time of inert forewave
t_{th}	Thermal relaxation time
T	Absolute temperature
T^*	Conversion controlling the combustion front
T_a	Ambient temperature
T_c	Combustion temperature
T_f	Flame temperature
T_g	Gas temperature
T_m	Melting point
T_s	Condensed phase temperature
T_0	Initial temperature of porous solid
u	Attraction energy
U	Temperature excess
v	Velocity of the combustion front
v_1	Mass fraction of gas in the reaction products
v_i	Volume of component i
w	Rate of heat evolution per unit mass of reaction mixture
w_1	Thickness ratio of metals A and B
W	Constant for calculation of van der Waal's forces
W_1	Energy required to produce a dispersion

x	Spatial coordinate in travelling wave frame
x_T	Characteristic length of thermal relaxation in combustion wave
x_n	Measured value at time n.
y	Reaction velocity
y_n	Filtered value corresponding to x at time n
y_{n-1}	Filtered value corresponding to x at time n-1

α	Tamman temperature ratio
α_1	Thermal diffusivity
α_2	Coefficient of interphase heat transfer
β_1	Heating rate
β_2	Pore shape parameter
β, γ	Wave stability parameters
$\chi(d)$	Particle size distribution
δ	Product layer thickness
δ_1	Length which surfactant extends into liquid
ϕ	Volume fraction of component
γ_1	Surface tension
η	Reactant conversion
η^*	Conversion controlling the combustion front
η_1	Degree of reaction
ι	Confinement parameter (fraction of the gas that passes through the flame)
λ	Thermal conductivity
ρ	Density
ρ_o	Initial effective solid density (mass per unit volume of porous solid)
ρ_∞	Final effective solid density (fully reacted)
ξ	Gas direction flow parameter

1. INTRODUCTION

Delay detonators are self-contained pyrotechnic devices that allow a desired interval (burning time) between an impulse and a later action. The delay elements which are contained in the delay detonators involve reactions between a fuel and an oxidiser. At present African Explosives Limited (AEL) manufactures various grades of these shock tube delay and carrick detonators as well as detonating relays. A single fuel, silicon, is used in conjunction with three possible oxidisers: red lead (Pb_3O_4), lead dioxide (PbO_2) and barium sulphate ($BaSO_4$) to obtain burn rates varying between 4 and 250mm/s for the delay elements.

The formulation of the pyrotechnic compositions in these elements was developed by a former ICI Explosive company in Canada. Since then, ICI Explosives has split and AEL and the company are competitors, leaving AEL with a range of powders which function satisfactorily, but when a problem occurs it is difficult to obtain information to solve the problem and to continue production (Taylor, 2000). Further problems encountered by AEL include:

- The lead-based compounds are toxic and the mixtures are very sensitive to ignition during mixing, making them difficult and dangerous to process. Furthermore they are not environmentally friendly.
- The barium sulphate-based composition has exhibited variable performance. Mixtures sometimes fail to initiate, propagate or burn at a consistent burn rate within a single batch.
- The powders coming directly from the dry mixer have poor flow properties and cause difficulty during downstream processing i.e. jams, increased processing time, high wastage levels and a higher incidence of fires. In order to overcome this problem, AEL have granulated the powder using a nitrocellulose binder. However, the binder is a gas generator which affects the burn rates of the powders, an undesirable situation.
- Currently AEL use 6 different types of silicon.

In light of these problems the following long term solutions were proposed by AEL:

- To critically analyse the available literature on pyrotechnic mixtures and delay elements in order to gain a better theoretical, scientific understanding of how these and other pyrotechnic formulations function and the variables which influence them.
- To replace the three oxidisers with oxidisers that are more environmentally friendly, easily sourced, cost effective, whilst rationalising the range of silicon and still obtaining the required burn rates and ignition reliability.
- To improve the processing of the powders such that the final product is a free flowing powder that burns in a lead tube by considering the use of dispersions, controlled precipitation or dry mixing using flow conditioners.
- To investigate the possibility of using thermoset resins or filled thermoplastic compositions as a novel processing technology.

Based on the above the main objectives of this investigation were:

- To obtain insight, through a critical literature review, into how delay elements and pyrotechnic formulations work and the variables which influence them. Also, to understand AEL's needs in terms of product range and AEL's existing processes and equipment (not discussed here).
- To find alternative oxidants that are easily sourced and cost effective, whilst maintaining the use of silicon as a fuel. The compositions also had to be ignited using shock tube and comply with the required burn rates.
- To establish safe and cheap experimental procedures and equipment in the laboratory to characterise (in particular the burn rates) the existing (not discussed here) and new formulations in an environment as close to reality as possible. The following equipment was used: TGA-DTA, the data acquisition computer, particle size analysers, XRD, XRF and SEM. Analysis of the reaction products was not conducted.
- To investigate experimentally, the influence of the most important variables, which were to be identified during the literature review, on the new compositions' burn rates.

- To investigate on a laboratory scale and through literature, the feasibility and repercussions of using dispersions, flow conditioners and thermoset resins or filled thermoplastic compositions in terms of burn rates etc.

Figure 1-1 is a schematic of the methodology used in this investigation.

Literature Review to evaluate and understand pyrotechnic reactions and delay detonators i.e.

- Insight into the solid state (Section 2.1) and reaction propagation mechanism and stability (Section 2.2)
- Understanding of the processing of delay compositions, AEL specific needs in terms of burn rate, etc. (Section 3)
- Knowledge of the variables affecting burn rate and the mathematical expression of these variables (Section 4), as well the properties of reagents and Si-based compositions used by AEL and in this investigation (Section 5). A critical analysis of the mathematical modelling presented previously will not be conducted.

Equipment and Experimental Procedures Development

Develop (trial and error) an easy, close-to-reality technique to measure burn rates and suggest further improvements to enable a better setup and augmentation of burn rate measurements of compositions (Sections 6.1-3) as well as determine reagent properties (Section 6-4)

Measure Burn Rates for *Existing Compositions* (Not discussed here)

Find Alternative Oxidants by evaluating thermochemistry (Section 7.1), AEL Trials (Section 7.2) and Initial Trials (Section 7.3) using Si as fuel

Modification of Burn Rates for alternative oxidants by varying stoichiometry (Sections 8.1 and 8.2), varying particle size (Sections 8.3 and 8.4) and aluminium addition (Section 8.5).

Evaluate Different Processing Routes. Dry mixing using flow conditioner additives (Section 9), wet mixing using dispersions (Section 10) and incorporation into a thermoset or thermoplastic (Section 11).

Figure 1-1: Investigation Methodology

2. THE SOLID STATE AND PYROTECHNIC REACTIONS

2.1 The Solid State

2.1.1 Crystals

The reactivity of a solid is dependent on the departures from bulk properties. When two particles are placed in intimate contact, something must cross the boundary for a reaction to occur i.e. something must diffuse out and must have a place to diffuse to. It is the imperfections in the solid that makes reactions possible and determines the reactivity (McLain, 1980:9).

Most solids are crystalline in nature i.e. a homogeneous structure in which the constituent atoms are arranged in a regular repeated pattern. Crystalline solids are categorised according to the chemical bonds that hold the atoms or molecules together. In descending order of strength the bonds are covalent (held together by electron-pair bonds e.g. diamond, Si, grey tin and graphite), ionic (large differences in electronegativity produces an attraction between the constituents' unlike charges, e.g. alkali metal halides and metallic oxides and hydroxides), metallic (electrons are shared broadly without preferential directions defined by atom pairs i.e. elemental metals), hydrogen and van der Waals. Many crystals are simultaneously ionic and covalent (McLain, 1980:12).

The physical properties of a solid depend largely on the crystal bonding forces and specific crystal structure, i.e.

- *Hardness*. Diamond is very hard partly because the covalent crystal bonds are very strong. The close packing of the carbon atoms in diamond also affects the hardness as the forces between the atoms are increased and prevents easy displacement by external pressures.
- *Melting point*. The melting point tends to be higher for crystals with stronger bonds as the atoms are more difficult to separate.

- *Malleability and ductility*. Metals are generally more malleable and ductile than other solids because the bonding forces have no preferred orientation and the assembly of atoms tolerates deformation without bond rupture (McLain, 1980:12).

Crystal structures are characterised by the geometric symmetries of the unit cell that is repeated throughout the lattice and the closeness of packing. Spheres, which include metal crystals, naturally assemble with either cubic or hexagonal symmetry whilst other crystals arrange either side by side (plate-like and stick-like molecules) or cluster in various configurations (pear-shaped molecules) (McLain, 1980:12-13).

2.1.2 Crystal Imperfections

The relationship between the physical properties of a solid and the chemical and geometric crystal classification is not exact due to crystals' imperfect ions e.g. dislocations, cracks and lattice defects (McLain, 1980:13).

A crystal may contain structural dislocations along the grain boundaries as a result of the manner of crystal growth and the acquisition of impurities (occupy sites for which they are too large or small). Cracks and dislocations influence the chemical reactivity of solids as they result in a larger surface area and in more edges and corners where material may be lost at the crystal decomposition temperature, i.e.:

- Reaction of a solid with a liquid begins at defects where the bonds are weakened and,
- The rates of adsorption, decomposition and solution increase with greater surface area (McLain, 1980:14).

Inherent lattice or Schottky and Frenkel defects occur when there are absences or displacements of atoms from their normal lattice sites and does not involve the intrusion of impurities. The defective crystal is more thermodynamically stable because of a proportionately compensating increase in configurational entropy. Other lattice defects are due to impurities being included in the crystal structure and nonstoichiometric defects (McLain, 1980:15-6).

Several compounds, e.g. ZnO, NiO, Cu_2O, Fe_3O_4, PbO_2, Pb_3O_4 and $CaSi_2$, deviate from stoichiometry due to the vacancy of one specie and not of the other or the preferential acceptance of one specie into interstitial sites. Ionic crystals must remain electrically neutral therefore, if a crystal has an excess of interstitial cations, there must be an equal excess of trapped electrons. The electronic properties of the crystal will therefore be affected. These nonstoichiometric crystals are further classified into two semiconductor categories: n-type and p-type. A semiconductor differs from a metallic conductor in that its resistivity decreases with an increase in temperature. Silicon is an intrinsic semiconductor. If the Si crystal were perfect, all of the electrons would be used for bonding and none would have the mobility necessary for conduction. As the crystal is not perfect, Si is able to conduct and heating the crystal gives more vibrational freedom and mobility to the carrier electrons. If an impurity that has five electrons in its valence shell, is introduced into the Si crystal, the crystal is an n-type conductor. If however, the impurity has only three electrons in its valence shell the crystal is p-type semiconductor. The conductivity of nonstoichiometric crystals may be altered i.e.:

- n-type nonstoichiometric semiconductors – the conductivity may be decreased by doping with foreign ions of higher ionic charge and increased by doping with ions with a lower ionic charge
- p-type nonstoichiometric semiconductors– the conductivity may be decreased by doping with foreign ions of lower ionic charge and increased by doping with ions with a higher ionic charge.

The semiconductor properties depend on the extent of the impurity and the chemical identity of the impurity (McLain, 1980:15-8).

The nature of a reaction of a solid with a gas, liquid or another solid is dependent on the chemical composition of the solid but the rate of the reaction is affected by the mode of pre-treatment of the solid (McLain, 1980:25).

2.2 Reaction Propagation Mechanism

The usefulness of pyrotechnic reactions derives from their being exothermic, self-sustaining and self-contained (Conkling, 1996:680).

In general the principal components of pyrotechnic compositions are (Figure 2-1):

- Reducing agent or fuel (metals, non-metals, carbohydrates, inorganic and organic compounds.
- Oxidising agent (nitrates, perchlorates, chlorates, chromates, peroxides, oxides and halogen-containing substances.
- Catalysts (Fe_2O_3, V_2O_5 etc.)
- Binders (natural and synthetic resins) and
- Formulation aids (anticaking agents and lubricants) (Krone and Lancaster, 1992:438).

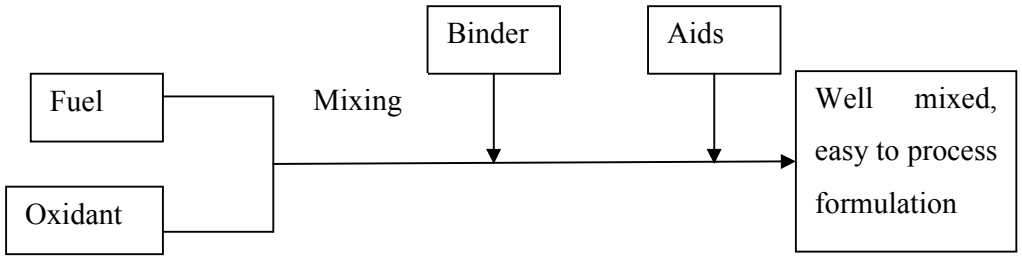

Figure 2-1: Principal Components of Pyrotechnic Composition

Considerable research has been undertaken to understand the mechanisms of various solid-state reactions and a large number of rate equations have been proposed and tested with varying success. The complexity of various solid-state systems has made the understanding of the reaction mechanisms difficult (Beretka, 1984). A fundamental question which arises in pyrotechnic reactions is whether the reaction is a genuine solid-solid reaction, a solid-liquid reaction involving a molten fuel or oxidant or whether the fuel reacts only with gaseous oxygen (or some other gaseous species) formed by the prior thermal decomposition of the oxidant or whether by combination of these processes (Rugunanan and Brown, 1991).

The theory of pyrotechnic reactions is based largely on the work of Spice and Staveley (quoted by McLain, 1980:4-5). They proved that for an iron-potassium dichromate mixture and an iron-barium dioxide mixture, that two reactions were occurring: ignition and preignition (PIR). They concluded that the PIR reaction for these mixtures was a genuine solid-solid reaction mechanism, as the rate increased

with increased packing density in terms of the increased contact surface between the particles. The effects of compaction and inert dilution are useful for determining if a pyrotechnic system is also a solid-solid reaction. If the PIR is a necessary precursor to the bulk, incandescent, self-propagating reaction, then it plays a vital role in the reactivity of the mixture. Thus, by controlling the onset of the PIR and the slope of its self-heating curve, the bulk reaction may be controlled (quoted by McLain, 1980:4-5, quoted by Drennan and Brown, 1992a). They have further suggested that the burning characteristics are more dependent on the properties of the oxidant than on the fuel (quoted by Drennan and Brown, 1992a).

Hill *et al* (quoted by Drennan and Brown, 1992a) on the other hand proposed that the burning rates were dependent on a thermal conduction mechanism. This is further echoed by Fordham (1980:117). According to Fordham (1980:117), by analysing the temperature profile of the reaction front it can be deduced that the reaction is solid-solid reaction initiated by thermal conduction of heat through the unreacted material. Thus to obtain reproducible reaction rates there must be a constant amount of solid to solid contact and constant thermal conductivity (Fordham, 1980:117).

According to McLain (1980:20), the reaction between a metal and a non-metal may proceed by two possible mechanisms. Either the metal migrates through the product layer to the non-metal or the non-metal migrates in the opposite direction. The reaction will not proceed if the product layer is not capable of conducting electrons, which accompany the ionic migration of the ions (McLain, 1980:20). He has also compared an oxidation-reduction reaction with semiconductor activity as it necessitates the transfer of electrons. The reducing agent is the electron donor and the oxidising agent is the electron acceptor. This is analogous to the activity at an *np* semiconductor junction where the n-type crystal creates the space charge potential by donating electrons to the p-type crystal. Therefore a n-type reducing agent should be more reactive than a p-type and a p-type oxidising agent is more reactive than a n-type (McLain, 1980:23). Therefore as Si is a semiconductor, this property of doping with foreign ions can be used to modify the burn rate. The Si can be doped with foreign ions of a higher ionic charge to increase its conductivity and become an n-type conductor. This will subsequently increase the overall reaction rate. The opposite

effect can also be brought about by doping with ions of lower ionic charge if a slower reaction rate is desired.

For gasless delay compositions, McLain (1980:3) has found that the failure of the reaction to propagate through the entire length of the column in metal tubes with small column diameters and at low temperatures is as a result of the rapid heat loss which is promoted by these conditions. This is because the burning is a series of reignitions along the length of the delay column from layer to layer of the compressed mixture, i.e. the burning of a column of delay composition takes place by the passage of a reaction front along the column. McLain (1980:50) supports the view that burning propagates by reignition from layer to layer along the burning path and therefore depends in the thermal conductivity of the mixture. His study of a Pb_3O_4-Si-Al mix, showed that the burn rate varied with train cross section and packing density and indicated a planar transfer mechanism. The addition of inert materials with relatively low thermal conductivity reduced the rate of heat transfer through the mixture and slowed the reaction. Conversely, the addition of thermally conductive material (i.e. fine Cu and Al powders) has been found to increase the burn rate of gasless delay mixtures (McLain, 1980:50).

Further evidence which supports that a solid-solid reaction is taking place is that the mass burning rates are relatively constant with loading pressure, or increase with rising consolidation and level off as maximum density is approached. An example which has been quoted by McLain (1980:51-52) is the B-$BaCrO_4$ system. He concluded that the reaction was truly solid-solid and that a 10:90 (B:$BaCrO_4$) system was more dependent on density than a 5:95 system because it was more nearly stoichiometric and the excess, unreacted material contained less inert, insulating $BaCrO_4$ and more conducting B. There was however scatter in the burn rate data at low consolidation pressures due to the poor contact and heat transfer between the particles and the low rate of heat generation was too slow to overcome radiation losses (McLain, 1980:52).

The reaction for a solid-solid reaction proceeds according to the simplified schematic diagrams in Figure 2-2.

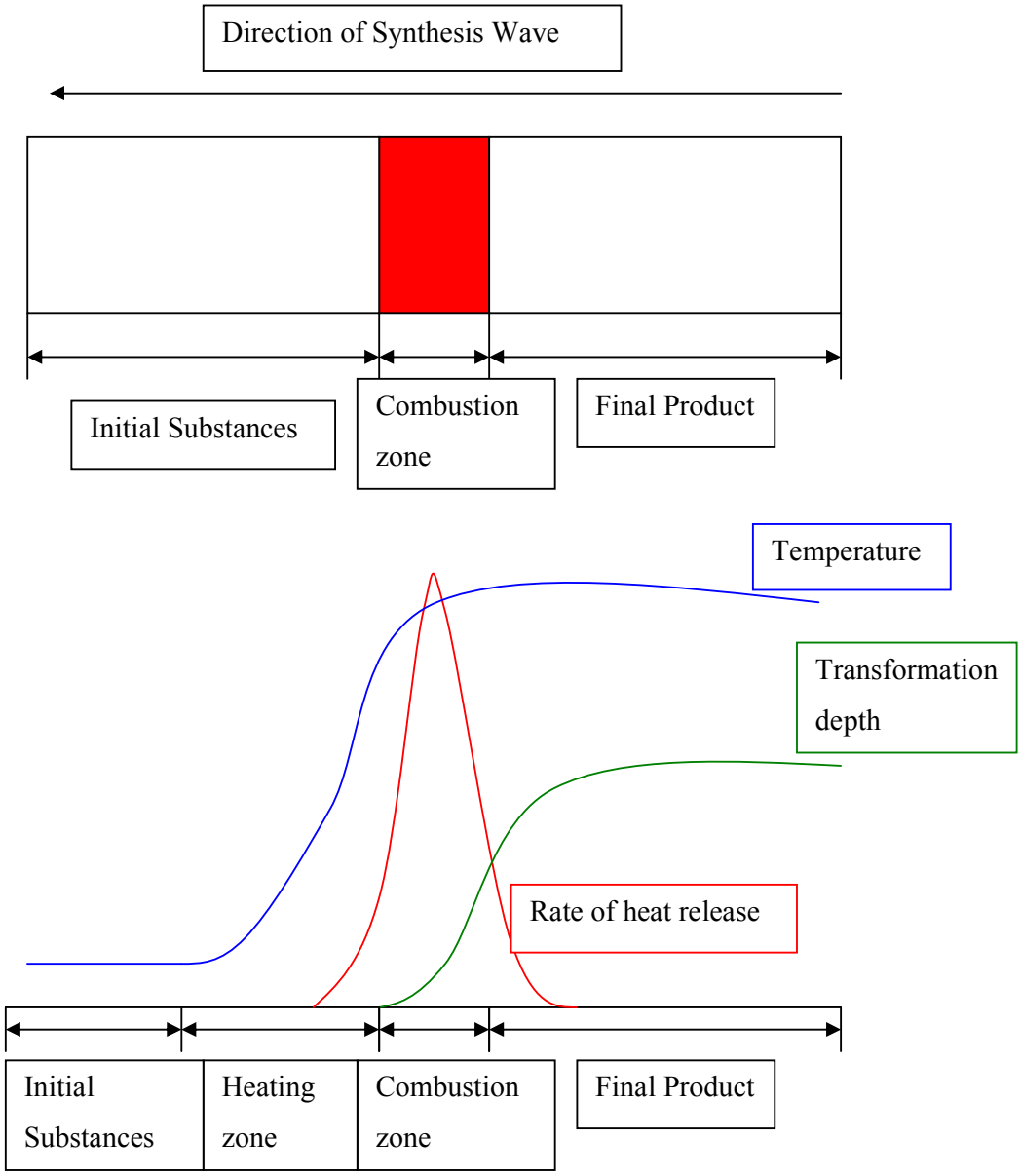

Figure 2-2: Simplified Schematic Diagrams of an Equilibrium Combustion Wave (Crider, 1982).

Therefore the determination of whether a solid-solid reaction is taking place can be conducted by analysing the effect of cross sectional area and packing density on the reaction rate (on a mass basis) and the temperature profile independently of analysing the reaction products of samples that have been frozen.

According to Hardt and Holsinger (1973) whether a condensed-phase reaction goes to completion spontaneously after initiation depends on whether the heat transfer is sufficiently low to allow accumulation of heat in the reaction zone and system characteristics of particle size and fusion temperatures sufficiently small to promote a high rate of mass transfer.

2.3 Combustion Wave Stability

Instability of the combustion wave can come from insufficient heat generation due to weak exothermic reactions (Munir, 1988). Zeldovich *et al* (quoted by Varma *et al*, 1998) found from classic combustion theory that the following two conditions must be satisfied for a constant pattern combustion wave with a thin reaction zone to be self-propagating:

$$\beta = \frac{RT_c}{E} << 1 \text{ and } \gamma = \frac{cRT_c^{\,2}}{QE} << 1 \quad \text{.....(2-1, 2-2)}$$

However using numerical results Aldushin *et al* (quoted by Varma *et al*, 1998) found that

$$\gamma - \beta = \frac{RT_oT_c}{E(T_c - T_o)} << 1 \quad \text{.....} \quad (2\text{-}3)$$

was sufficient. Margolis (quoted by Varma *et al*, 1998) modified the stability criterion for melting reactants i.e.

$$\frac{E(T_c - T_o)}{2RT_c^{\,2}\left\{1 - \exp\left[\frac{E(T_c - T_o)}{RT_c^{\,2}}\right]\right\}} < (2 + \sqrt{5}) \quad \text{.....(2-4)}$$

According to this equation it can be deduced that for gasless combustion, unstable combustion is more likely to occur for higher melting temperatures and higher activation energies and lower combustion temperatures. The higher melting temperatures will absorb energy that will have been used for conduction to the next zone for ignition. Also the higher activation energy means that more energy is required before the reaction commences and releases its own energy. Therefore compositions with high melting points and activation energies will exhibit unstable combustion.

3. EXISTING PRACTICES FOR THE MANUFACTURE OF DELAY DETONATORS

3.1 Delay Detonators

Delay Detonators, both electric and non-electric are used in mining, quarrying and other blasting operations for the sequential initiation of explosive charges (Beck and Flanagan, 1992, Davitt and Yuill, 1983). The delays between the sequential initiation is commonly referred to as a millisecond delay blasting operation. It is effective in controlling the fragmentation and throw of the rock being blasted and reduces the ground vibration and air blast noise (Beck and Flanagan, 1992, Davitt and Yuill, 1983). It is thus evident that reliable ignition is paramount owing to its safety implications. Repeatable burn rates are important for efficient use of the explosive during mining and quarrying. Short period delays (25-1000ms) usually allow for the best results in terms of fragmentation, however, where excessive throw and concussion (such as tunnelling and shaft sinking) are problematic, long period delays are used (Beck, 1984). Electronic delay detonators in which the desired delay time may be programmed into a microchip timing circuit within the detonator; are more precise and accurate but are considerably more expensive (Rugunanan, 1991).

Commercial delay detonators are essentially metallic shells which are closed at one end and which contain in sequence from the closed end, a base charge of a detonating high explosive e.g. PETN, a primer charge of a heat-sensitive detonable material e.g. lead azide and an amount of deflagrating or burning composition which provides the desired delay time in the manner of a fuse (Beck, 1984, Beck and Flanagan, 1992, Davitt and Yuill, 1983). In some cases the primer charge of a heat sensitive material may be omitted if the delay composition has been designed to have sufficient ignitable power (Fordham, 1980:119). A non-electric delay detonator is depicted in Figure 3-1 .The burning composition may be ignited by an ignition charge using an electrically heated bridge wire or by the heat and flame of a low energy detonating cord or shock wave conductor (Beck and Flanagan, 1992, Davitt and Yuill, 1983).

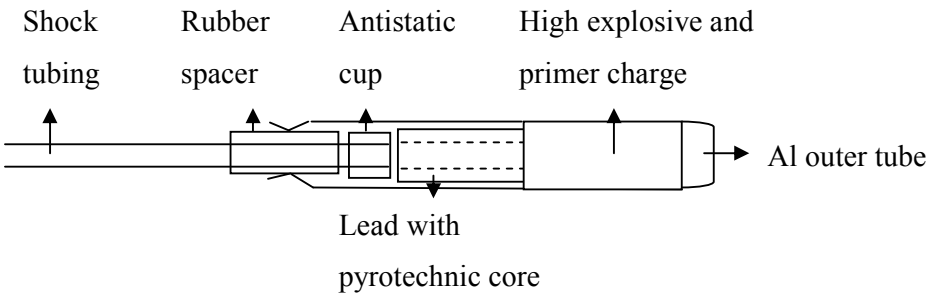

Figure 3-1: Non-Electric Delay Detonator

A pyrotechnic delay composition consists of an intimate mixture of solid, powdered fuels and oxidants capable of a highly exothermic propagating oxidation-reduction reaction. The delay times are linearly related to the length of the element (Beck, 1984).

3.2 Delay Element Requirements

Numerous delay compositions have been used with varying degrees of success. In general delay element compositions and elements have the following requirements:

- Must be essentially gasless. The evolution of large amounts of gaseous by-products will interfere with the functioning of the delay detonator i.e. gas-producing delays are vented and can only operate at low altitude whilst gasless delays are unvented and may be used at any altitude (Watkins *et al*, 1968:62). The description "gasless" is usually applied to mixtures that release during combustion, less than $10cm^3$ of gas per g of mixture (Charsley *et al*, 1980). Wang *et al* (1993) have stated that the criterion for defining gasless combustion as $P(T_c) << P_0$ where P is the vapour pressure of the most volatile component (or dissociation pressure of the products) at the combustion temperature T_c and P_0 is the external gas pressure.
- Must be safe to handle (both from a health and explosive viewpoint). This is to avoid problems during manufacture, to reduce emissions and also to lessen the problem of exposure at the point of end use. For these reasons it is desirable that

charges be prepared without using solvents and that special precautions are implemented when a compound is dangerous (e.g. $BaCrO_4$ is recognised as carcinogenic and requires special procedures (Boberg *et al*, 1997 and Davitt and Yuill, 1983).

- Must be resistant to moisture.
- Must not deteriorate over periods of storage, i.e. there must be no change over in burning characteristics over time. Brauer (1974:16-17) has discussed the problem of storage and temperature. He stated that the delay time may be affected by as much as 16%.
- Must be simply compounded and economical to manufacture.
- Must be adaptable for use in a wide range of delay units within the limitations of space available inside a detonator shell (Beck and Flanagan, 1992, Davitt and Yuill, 1983). Some compositions have a very high burn rate and are therefore very difficult to incorporate in delay detonators having short delay periods. These result in variations in the delay times within groups of detonators intended to have equal delay times. The same can be said of compositions having slow burn rates (Davitt and Yuill, 1983).
- Must have the reduced possibility of "flash past", particularly in the shorter delay periods where the length of the elements used are at a minimum. In the past this problem was overcome by introducing a layer of delay composition above the initiating explosive before placing in the delay element. This is no longer done due to improved overall design and technique (Fordham, 1980:119).
- Must have minimal effect due to the liberation of gas. As the speed of the delay composition is affected by pressure, the free space within the detonator should be controlled. The plug, which seals the leading wires in place, should be able to withstand this pressure for more than the delay period of the detonator. Conduction along the metal walls of the detonator shell of the heat which is liberated by the fusehead and delay composition, is likely to soften plastic plugs in particular. These may be ejected from the detonator with probable failure of the burning of the delay column (Fordham, 1980:119).
- Delay detonators that are to be used in coal mines should be constricted such that they do not ignite methane-air mixtures even if fired outside the cartridge of the blasting explosive. This requires careful selection of the fusehead and the use of a delay composition which will not produce large particles of slag on burning.

Carrick detonators have been developed for this application. They are of the lead type with five or six narrow cores instead of the single central column (Fordham, 1980: 119-120).

3.3 Delay Element Manufacture

The general processing procedures and equipment used for pyrotechnics have been discussed by McLain (1980: 201-213).

Two methods may be used for the manufacture of delay detonators. The first method requires that the delay composition be pressed into preformed zinc, brass or aluminium tubes which are a sliding fit into the detonator shell and which are thick enough to withstand the consolidating pressure (the rigid element). The second method entails filling a lead tube with composition and drawing it down in diameter by conventional means. The required length of lead tube is then cut (Fordham, 1980:118). There is a desire in the industry to phase out the use of drawn-lead containment and use only drawn elements of another metal such as aluminium or rigid elements (Beck and Flanagan, 1992). Beck and Flanagan (1992) have however found that the heat-sink effect of the metal containment of the column of delay composition may result in quenching the exothermic reaction of the composition. This is a problem particularly in the use of rigid elements using zinc and also drawn aluminium tubes, but not lead-drawn tubes.

Regardless of the method used, the delay composition has to be made in a free-flowing form. The fine powders may be mixed and then pelletised in a press. The pellets are then broken down and sieved to remove the fines. If it is difficult to pelletise the mixture, the mixture is granulated with a small amount of nitrocellulose solution in a suitable mixer (Fordham, 1980:118).

It is essential that a constant thermal conductivity and constant solid-solid contact is maintained to ensure repeatability in terms of burn speed and ignitability. To achieve adequate solid contact between the reacting solids, it is necessary to use the ingredients in fine condition and bring them into contact by pressure, whilst to

maintain constant solid contact and thermal conductivity, the density of the column has to be controlled at a uniform value. It is thus essential that the ingredients are suitably sized and are adequately mixed and accurately pressed (Fordham, 1980:117).

3.4 AEL Practices

AEL currently manufactures 5 compositions with burn rates varying between 3-250mm/s. These have been renamed for the purposes of this document as being starter, sealer, slow, medium and fast compositions (AEL Product Specification, 2000a & 2000b).

4. REACTIVITY, BURN SPEED AND MODELLING OF REACTIONS

4.1 Variables Affecting Reactivity and Burn Speed

According to McLain (1980:31) and Brown (1989) the following interrelated variables influence reactivity and in turn the burn speed:

- Deviations from the normal crystallographic amorphous structure of a substance.
- Lattice defects in the form of hereditary structures.
- Formation of imperfect structures, i.e. transitions from one modification to another or thermal decomposition.
- Impurity and presence of guest particles in the lattice.
- Mechanical treatment such as grinding or pressing.
- Differences in the crystallographic formation of different surfaces.
- Gases which are dissolved in the lattice but which are not chemically reactive.
- Corrosion.
- Adsorption and catalysis.
- Irradiation by absorbable wave lengths.
- Changes in the magnetic state and
- Changes in the electric state.

A number of variables which affect the burn speeds have been discussed in literature:

i) *Nature of the Oxidant* - In general the rate of reaction of a metal to form an oxide depends on the physical state of the oxide, the nature of the transport processes within it and its ability to maintain physical continuity between the reactant phases. Thermodynamic driving forces for reaction determine which phases form and in what sequence. The defects in each phase and their mobilities largely determine the rates of growth. If the oxide is solid, a number of processes may occur:

- Nucleation of the oxide at the metal-gas interface may be slow or at preferential sites. Or it may absorb uniformly and oxidation may initiate by the metal and oxygen atoms exchanging places.
- Transport across the metal-oxide, oxide-oxide or oxide-oxygen interface may be slow enough to control the rate of reaction. The slow step could be the decomposition of the oxidant.
- Growth of thick, compact adherent scales occurs by diffusion of ions through the solid oxide, usually cations are more mobile than oxide ions.
- Oxygen may dissolve and diffuse further into the metal before and during the growth of the reaction layer on the surface (Birchenall, 1986:3355).

There is a relationship between the lattice vibrations and chemical reactivity. As the temperature increases, crystals vibrate with increasing amplitude about their average positions in the lattice. When the amplitude is great enough, diffusion is enhanced and the atoms may exchange positions. At low temperatures this may result in a solid transition and at higher temperatures the solid may melt. During such transitions the reactivity is enhanced as the lattice units are more loosely bound. This is known as the *Hedvall* effect (McLain, 1980:30).

The *Tamman* temperature ratio (α) scales the actual temperature of the solid to its melting point. It may be used as a rough measure of lattice loosening. Ionic surface mobility becomes effective at $\alpha \approx 0.3$ and lattice diffusion at $\alpha \approx 0.5$ (McLain, 1980:30).

Spice and Staveley (quoted by McLain, 1980:40) found that the rate of burning was more sensitive to the chemical nature of the oxidising agent than to the metal. This may be explained by the fact that the oxidiser generally has the lower melting point (Tamman), transition temperature (Hedvall) or decomposition temperature. This was noted by Rugunanan and Brown (1994b) who found that changing oxidant has the greatest effect on burn rate. It influences the reaction by its role, through thermal decomposition to supplying gaseous O_2 for the fuel oxidation or by simultaneous diffusion of the species through a developing layer of solid product. The size and charge of the diffusing species may be important, as well as maintenance of contact at

the origins of the diffusion paths. Melting and or vaporisation of the oxidant will be important in the maintenance of such contact (Rugunanan & Brown, 1994b).

The ignition temperature of a mixture is largely determined by the decomposition temperature of the oxidant (Conkling, 1996:684). Chernenko *et al* (quoted by Wang *et al*, 1993) classified oxides according to the following criteria:

- Chemically and physical stable oxides – These oxides (NiO, TiO_2, Cr_2O_3, Al_2O_3, Ta_2O_5 and Nb_2O_5) are essentially inert up to the moment of ignition. Generally when used with Al, the oxidation of Al by atmospheric oxygen precedes and initiates the combustion of the mixture.
- Chemically stable but physically unstable oxides – These oxides include B_2O_3 which melts at 450°C, MoO_3 and WO_3 which sublime. The appearance of a liquid oxide or gaseous oxide phase increases the rate of the oxidation-reduction reaction and thus enhances ignitability. It has been found that oxidisers with high vapour pressures (such as WO_3 and MoO_3) gave the greatest rates of combustion.
- Chemically unstable oxides that decompose – The ignition process for these oxides (V_2O_5, CrO_3, Li_2O_2 and BaO_2) is more complex because the oxygen liberated from the decomposition of the oxide plays a significant role in initiating the reaction.
- Chemically unstable oxides that undergo further oxidation – Further oxidation takes place in air and the heat liberated from this reaction heats the specimen to ignition point (Wang *et al*, 1993).

ii) *Preparation of Constituents and Compositions*– During processing a number of variables such as addition of impurities, grinding, adsorption (e.g. H_2O), surface oxidation of the fuel and partial decomposition of the oxidant may occur and affect the reaction. Grinding, rolling and milling a solid crystal will create new surfaces, edges and corners at which atoms are not bonded as strongly as the internal atoms as well as loosen the crystal lattice. The lattice may also be "loosened" by adding dopants, i.e. Si and Li have been added to Al weakening the Al-Al bonds. This results in increased reactivity (McLain, 1980:35).

An example of how the preparation of an oxidant may affect the reactivity is the dependence of Fe_2O_3 reactivity on the method of preparation. Hedvall and Sandberg

(quoted by McLain, 1980:31) found that Fe_2O_3 prepared from iron sulphate was three times more reactive than that derived from iron oxalate, despite the average particle size of the sulphate-derived oxide being larger. X-ray powder diffraction patterns of the sulphate-derived iron oxide showed a less ordered crystal structure, i.e. less sharply defined, below 650°C compared to the patterns of the oxalate-derived iron oxide. Furthermore, it was observed that at temperatures exceeding 900°C, the oxalate-derived iron oxide was more reactive. By annealing the sulphate-derived iron oxide at 900°C, the lattice was found to be more sharply defined and its reactivity over the full temperature range was found to be more like that of the oxalate-derived iron oxide.

The effect of mechanical and heat pre-treatment of the reagents was not evaluated in this study and is recommended for future work.

iii) *Irradiation by absorbable wave lengths*. Radiation of high enough energy can dislodge atoms from their normal lattice positions to create vacancies and interstitial atoms. In many semiconductors, irradiation increases the conductivity because it increases the abundance of imperfections. The opposite is true for metals. Irradiation also increases the chemical reactivity of semiconductors (McLain, 1980:34). The effect of irradiating the Si was not investigated during this study and it is recommended that this be completed, noting the effects of aging on the burn rates of irradiated compositions.

iv) *Stoichiometry* – Stoichiometry, heat of reaction and burning rate are all interrelated (McLain, 1980:53). The early work by Spice and Staveley (quoted by McLain, 1980:47) provided the following relationships and conclusions concerning the stoichiometry, heat of reaction and burn rate:

- The delivered heats of reaction were never as high as calculated.
- A composition that gave the maximum burning rate usually gave the maximum heat of reaction.
- Burning rate and sensitivity to ignition spark depended mainly on the nature of the oxidant.

- Stoichiometry could be determined from a plot of Q (the heat emitted by that quantity of mix containing a gram formula weight of the oxidiser) versus the percent reductant (McLain, 1980:47).

McLain (1980:53) has demonstrated the relationship between these factors using the PbO_2-Si as an example. He compared a graph for the measured heats of reaction versus varied amount of Si with a graph of the theoretical values calculated from heats of formation of possible reactions. He stated the following reactions take place for the system (Table 4-1):

Table 4-1: Possible Reactions for PbO_2-Si as the Si Content is Varied (McLain, 1980:53)

% Silicon	**Reaction**
2.3	$Si + 4PbO_2 \rightarrow Pb_4SiO_6 + O_2$
3.1	$Si + 3PbO_2 \rightarrow SiO_2 + 3PbO + 3/2\ O_2$
4.8	$Si + 2PbO_2 \rightarrow Pb_2SiO_4$
6.0	$2Si + 3PbO_2 \rightarrow 2PbSiO_3 + Pb$
8.7	$Si + PbO_2 \rightarrow SiO_2 + Pb$
12.6	$3Si + 2PbO_2 \rightarrow SiO_2 + 2SiO + 2Pb$
16.1	$2Si + PbO_2 \rightarrow SiO_2 + 2Pb$
22.3	$3Si + PbO_2 \rightarrow Pb + Si + 2SiO$

McLain (1980:53) observed that the heat of reaction reaches a maximum near 10% Si for PbO-Si. A plot for Pb_3O_4-Si reached a plateau above 20% Si. The measured burning rates for both these systems were a maximum at or near the exothermic maximum (McLain, 1980:53).

Conkling (1996:684) stated that the stoichiometric mixture generates the maximum heat output, but is not always the fastest burning composition. McLain (1980:55) has confirmed that the maximum burning rate occurs at a somewhat higher reductant content than does the maximum heat of reaction (Figure 4-1). This displacement was generally greater for metal reductants such as Fe, Sb and Mn and smaller for non-metals such as S and C and metalloids such as B and Si (McLain, 1980:55).

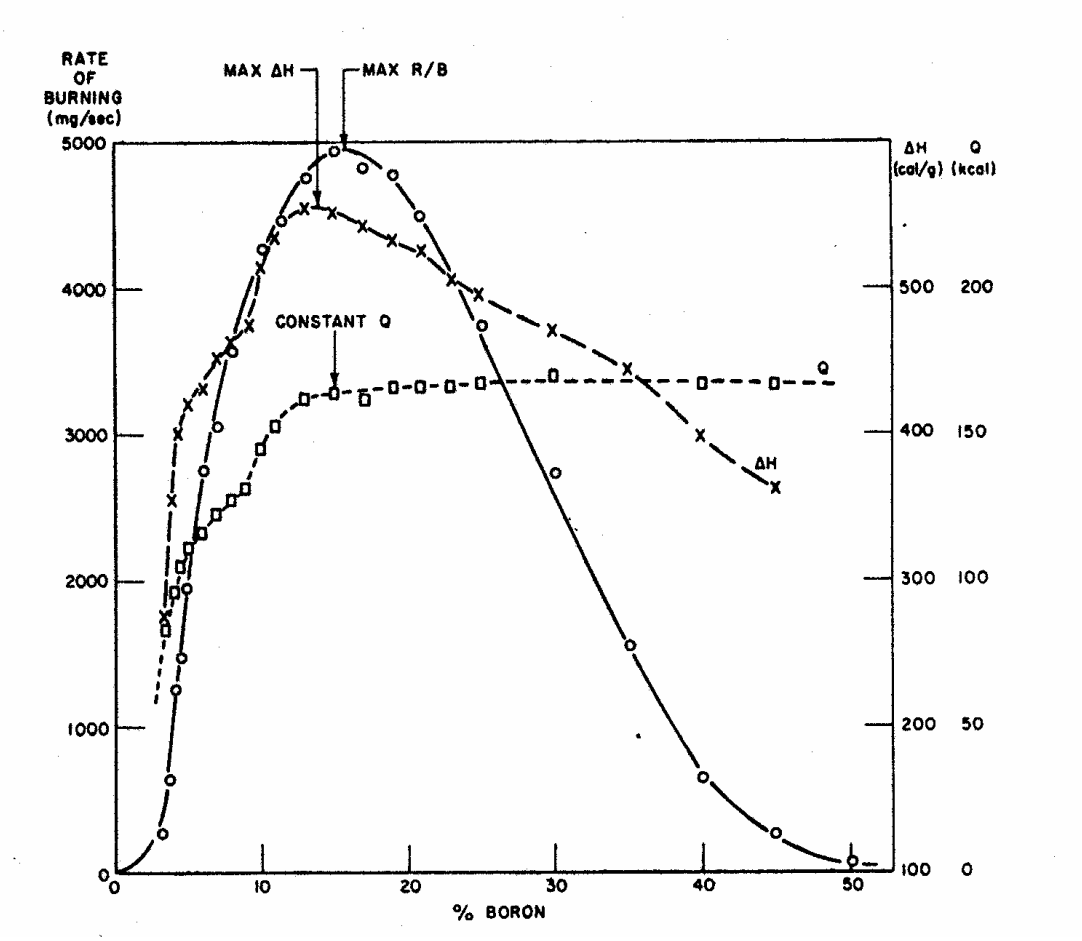

Figure 4-1: Thermal Characteristics of B-$BaCrO_4$ (McLain, 1980:55)

This points to the effect of heat transfer on columnar burning. The addition of a good heat conductor may cause departure from stoichiometry, and may increase the thermal conductivity sufficiently to cause a net increase in the burning rate (McLain, 1980:56).

Spice and Staveley, as well as Hill *et al* (quoted by McLain, 1980:56) found that the smaller the heat of reaction, the more the peak in burning rate is displaced from the peak in heat of reaction. Furthermore, the slope of the burning rate curve is always steeper below the maximum percentage reductant below stoichiometric than above the maximum percentage. This is due to the fact that the region below the maximum represents excess oxidiser, which is an inert diluent and heat insulator that retards burning. Addition of the thermally conductive reductant has a relatively large effect

on accelerating the burning rate. Above the maximum, there is excess reductant which maintains a relatively high burning rate despite the departure from stoichiometry (McLain, 1980:56).

Optimum delay performance is generally expected for stoichiometric compositions because they ignite and propagate more readily. However, if a slower burn rate is necessary, the percentage reductant may be reduced. It is however, much better to rather increase the reductant concentration until the desired burn rate is achieved. The larger addition is more easily mixed and departures from homogeneity will have less of an effect as this portion of the curve is less steep (Figure 4-1). Note, however, that inhomogeneities are less critical near the stoichiometric composition (McLain, 1980:60).

v) *Particle Size and Shape* –The kinetics of solid state reactions are dependent on the initial dispersion of the reactants and thus are affected by the particle size (Munir, 1988). Generally the combustion velocity decreases with increasing particle size. Models have been developed to account for particle size (Appendix A). There has been an exception to this trend e.g. for the Ta-N system the temperature and propagation velocity were independent of the Ta particle size as the coarser particles were more porous than the finer particles and thus acted as a large number of nonporous grains (Varma *et al*, 1998).

According to Cardellini, Mazzone and Antisari (1996) an irregular type of powder morphology (flaky powders) reacts more readily than a regular more uniform type of powder morphology upon application a shock-compression wave. The influence of the type of crystal form on the impact sensitivity and reactivity has also been noted by McLain (1980:33). He mentioned that the reactivity of $KClO_3$ decreases as the crystal form varies from needles to thin lamellae (McLain, 1980:34). The shape of the particles used in this investigation was not varied. It would perhaps be beneficial to note whether the particle shape does influence the burn rate in particular in the case of the precipitated oxidants as it is easy to modify particle size and shape through the use of surfactants, seed particles and varying temperature and concentrations of starting reagents.

vi) *Additives* – Additives may inhibit the reaction by decreasing the contact area between the fuel and oxidant particles or by changing the heat capacity and/or thermal conductivity of the mixture sufficiently to alter the burn rate (Drennan and Brown, 1992a Wang *et al*, 1993 Varma *et al*, 1998 McLain, 1980:60). The addition of fluxing additives such as CaO can be added to the mixtures to form lower melting slags and increase the burn rate. The addition of small amounts of salts of alkali metals and alkaline earth metals and cryolite ($NaAlF_2$) can effectively increase the mass combustion rate of a thermite composition. It has been proposed that the salt additive reduces the temperature at which the reaction occurs. In Al-based compositions, the salt disintegrates the barrier oxide layer on the Al at a lower temperature (Wang *et al*, 1993). McLain (1980:56) recommends that different burn rates should be obtained by adding inert, thermally insulating ingredients to retard the burn rate, or adding metal powder to accelerate the burn rate (McLain, 1980:56). McLain (1980:57) recommends that dilutions of a stoichiometric mix with inert material should not exceed 4%, whether to retard or accelerate the burn rate.

vii) *Compact Density* – The compact density affects the thermal conductivity of the compositions (Wang *et al*, 1993). Goodfield and Rees (1985) have found that the response to variation in consolidation pressure for SnO_2, PbO – Si compositions can be divided into three distinct types of behaviour with respect to the oxidant/fuel ratio in which they are observed, i.e.

- At high oxidant levels where the reaction temperature is high (1700°C), the propagation rate decreases with increasing consolidation pressure. They proposed that this is as a result of the large amounts of relatively volatile metallic reaction products which are formed and allow for the transfer of heat by mass transfer processes as the dominant propagation mechanism.
- At low oxidant levels (lower reaction temperature - 1250°C), the propagation rate increases as a result of heat transfer by conduction being the dominant process.
- At intermediate oxidant levels, the response is more complex as a result of the fact that no one process dominates the consolidation process (Goodfield and Rees, 1985).

Varma *et al* (1998) noted that the combustion velocity often shows a maximum at some intermediate density value. They proposed that the effect can be attributed to the following:

- As the density increases, intimate contact between the reactant particles is augmented, which enhances the reaction and the front propagation.
- The increased thermal conductivity at higher densities however, means that a greater heat is lost due to conduction from the reaction zone to the unreacted portion inhibiting front propagation.
- Contact resistance has not been accounted for previously and may have an effect.

Vadchenko *et al* (quoted by Varma *et al*, 1998) on the other hand have found that the density and absorbed gaseous impurities may have an interrelated effect on the combustion i.e.

- For low sample densities, escape of the desorbed gases is not limited by permeation and occurs without destruction of the reactant medium structure. Thus increasing the density results in increasing thermal diffusivity of the medium and hence increased velocity.
- At higher sample densities, absorbed gases are unable to escape due to sample permeability. As the temperature increase, the gas pressure inside the pores also increases, forming cracks in the sample, lowering the effective thermal conductivity.

It has been found that a pellet with a higher initial density resulted in a product with a lower density than pellets with a lower initial density (Varma *et al*, 1998).

viii) *Ambient Pressure* – The burning rate may be affected by ambient pressure. This has been associated with vaporisation of the starting components at the temperature reached in the combustion front. It has been noted that in some systems, the combustion rate increases with pressure, reaching a maximum, and then decreases with further increase in pressure. Examples include: BaO_2-Zr, MoO_3-Mg and PbO_2-Mg. Because of the high volatility of the reactants, vapours are formed owing to the heat of combustion. The rise of combustion rate at the low range of pressure is associated with the rise in the extent of the vapour phase penetrating the pores as the ambient pressure is increased. However, at higher pressure the gas formation is

suppressed and the melt formed in the combustion process can selectively wet the pores, thereby inhibiting the reaction. The ambient pressure may also affect the dissolved hydrogen and nitrogen gas.

ix) *Cross Sectional Area and Surrounding Material* – The reduction in cross sectional area is accompanied by an increasing lateral heat loss which becomes the dominant variable as the point of failure is approached with about 60% of the evolved heat being lost during the reaction (Boddington *et al*, 1986). Boddington *et al* (1986) have found that the use of glass channels rather than steel did not give very different results except under conditions close to those which give rise to failure. They have therefore concluded that the cross sectional area of the pyrotechnic column is of prime importance in determining lateral heat loss. Increasing the sample diameter (D) increases the ratio of volumetric heat generation ($\propto D^3$) to surface heat loss ($\propto D^2$). By increasing the diameter above a critical value, the combustion temperature approaches the adiabatic value and the burn speed becomes constant (Varma *et al*, 1998). McLain recommends that for slow compositions, containers with large diameters and low thermal conductivity be used (McLain, 1980:60). Beck and Brown (1986) have experimented with the use of plastic materials with low thermal diffusivities as containers but found that the pressure of the gaseous polymer degradation products cause a problem. In the future it would be beneficial to investigate the use of alternative materials (such as metal-lined polymeric rigid elements) as opposed to lead as a result of the environmental and health implications of using lead.

x) *Binder*. Organic binders are reported to lower the ignition temperatures of pyrotechnic systems. It has been found that the addition of boiled linseed oil (<2%) to 15% Sb/$KMnO_4$ (Does not burn on own) resulted in a composition that ignited and burned. The temperature profile indicated that the binder acts as a fuel and increases the combustion temperature (Beck and Brown, 1986). Hardt and Holsinger (1973) however have found that a mixture of gum arabic and water could be used as a binder and have no effect on the reaction characteristics of intermetallic reactions.

Ellern (1968:312-318) offers a detailed discussion on the binders used in the pyrotechnic industry. Boberg *et al* (1997) report the successful use (little gas

production) of carboxymethylcellulose (CMC) in pyrotechnic delay mixtures containing Si. It would be beneficial to investigate the effect of various binders on the burning characteristics and safety of the delay compositions and the implications in terms of processing and cost of implementing the new binder.

xi) *Fluxes*. The addition of a fluxing agent i.e. a material which reduces the lowest eutectic temperature effective in the mixture and thus introduce a small amount of liquid phase, does accelerate solid-solid reactions. Water vapour is known to accelerate pyrotechnic reactions. Similarly, the mixing, storage and loading of PbO_2-Si mixtures in humidified atmospheres, due to the static hazards, resulted in an increase in the burn rate of these mixtures (McLain, 1980:43). The effect of the addition of a fluxing agent would need to be evaluated.

xii) *Impurity and presence of guest particles in the lattice*. Doping by means of co-crystallisation has made Fe_2O_3 highly reactive. McLain (1980:39) experimented with crystals of $CuSO_4.FeSO_4.xH_2O$ and $NiSO_4.FeSO_4.xH_2O$, which were grown from an acidic solution of the salts. The crystals were then decomposed in a current of O_2 at 200°C-250°C to produce Fe_2O_3 Ti-Fe_2O_3 mixtures prepared using this Fe_2O_3 had an increased calorific value (McLain, 1980:39). Doping (Described in Section 2.1.2) NiO with LiO_2 and Cr_2O_3 affected the reactivity of NiO (McLain, 1980:39). It would be interesting in the future to compare the reactivity of Si as an n or p-type fuel as well as an n or p type oxidant (Section 2.1.2).

Varma *et al* (1998) have graphically summarised the dependencies of the combustion velocity and maximum combustion temperature on some of the above variables in Figure 4-2. Varma *et al* (1998) offer the following explanation for Figure 4-2:

- Velocity and T_c decrease with increasing reactant particle size and with the addition of an inert (non-reactive) diluent to the mixture, while increasingly significantly with increasing initial sample temperature.
- Different trends have been observed when the initial sample density is varied. With increasing density, the combustion front velocity either increases monotonically or goes through a maximum, while the combustion temperature generally remains constant.

- A decrease in the sample size (i.e. diameter) does not influence velocity and T_c when the size is larger than the critical size, since heat losses are negligible compared to the heat release from the chemical reaction. Below the critical sample size both velocity and T_c decrease due to significant heat loss (Varma *et al*, 1998).

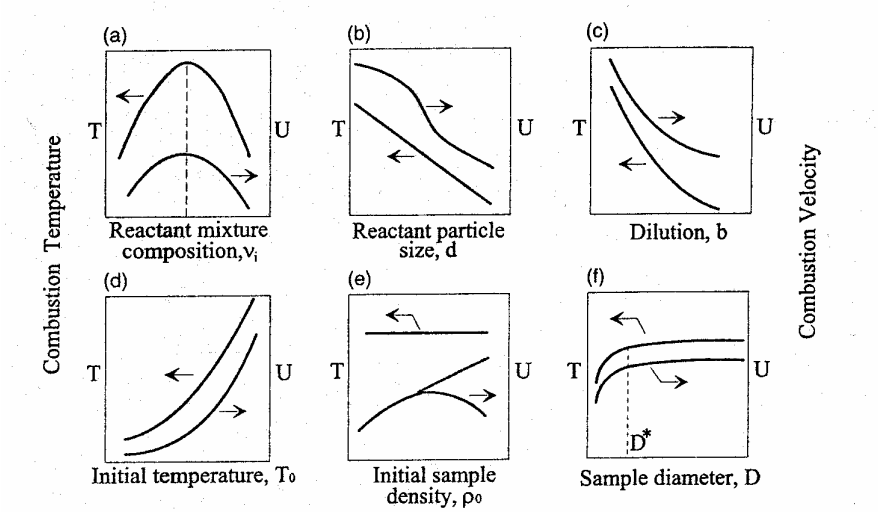

Figure 4-2: Dependence of Combustion Temperature and Velocity on Various Variables (Varma et al, 1998)

Therefore, a number of variables affect reactivity, ignitability and burn rate of delay compositions. The aforementioned variables can be divided into three categories:

- Constituent material properties
- Compositional properties and
- Processing and end use properties.

The easiest variables to manipulate on a laboratory scale using the lead-drawn elements are: the oxidant used, the particle size, the addition of an inert or thermally conductive material and stoichiometry. These variables will also be the most practical to modify on a commercial scale. Should the lead-drawn elements be phased out to use rigid elements, then variables such as the cross sectional area and packing density can also be used.

4.2 Mathematical Modelling of Reactions

A number of authors have attempted to mathematically model the combustion wave with mixed success. As Boddington *et al* (Quoted by Yoganarasimhan, 1988) has stated "The interrelationships which exist between combustion kinetics, heat transfer and burning velocity are complex and simple cause and effect explanations are seldom tenable". This sentiment is echoed by Beretka (1984) who states that due to the complexity of solid state systems, the mechanisms of many reactions are still not understood. Furthermore according to Beretka (1984) in practice reactions rarely reach completion in mixtures of powdered solids due to poor contact of the reacting particles and sintering of the reactants at high temperatures. In addition, the particle size distribution and previous history of the reactants make the interpretation of kinetic measurements difficult (Beretka, 1984). A summary of the mathematical modelling for thermal properties and combustion which have been attempted may be found in Appendix A. This modelling will not be analysed here and it is recommended that the models presented be compared using a chosen formulation that is well understood.

4.3 Combustion versus Thermal Analysis

The use of thermal analysis for the analysis of pyrotechnics has led to controversy. The processes or reactions which occur during combustion of a pyrotechnic composition may be far removed from those identified during thermal analysis experiments where the samples and experimental conditions are such that thermal runaway may be avoided (Rugunanan and Brown, 1991, Beck & Brown, 1991). This is as a result of the different temperature-time histories of the compositions (Rugunanan & Brown, 1991). Laye (1997) on the other hand is of the opinion that it is possible to link the self-sustained combustion process with the presence of reactions identified by thermal analysis.

It has been concluded, however, that caution be exercised when ascribing kinetic parameters to a combustion regime when these have been obtained from studies under

non-ignition conditions where a different rate determining step may operate (Boddington *et al*, 1986, Laye, 1997).

In thermal analysis the values obtained for the activation energy are usually higher than those obtained from combustion studies. In thermal analysis, activation energies are derived under low-heating rates and non-ignition conditions whereas for those derived from temperature profile analysis are dominated by diffusion of heat transfer (Boddington *et al*, 1990 Laye, 1997).

The DTA/DSC measurements are limited by the following variables:

- Al-Kazarji and Rees (1978) have stated that thermal studies usually have been performed on loose powdered mixtures whereas in fuse technology compressed columns of relatively high-density composition are used. While the basic chemical reactions are similar, the mechanism of combustion will differ from the loose powder (Al-Kazarji and Rees, 1978).
- Thermal runaway has been the cause of some concern due to the damage it has caused to thermal analysis equipment, as a result of the increased adiabatic temperature. Thermal runaway occurs only when the rate of heat generation by the reaction is greater than the rate of heat loss to the surroundings (Brown, 1989).
- The isothermal or non-isothermal determination of kinetic parameters has been the source of controversy. Non-isothermal methods require less time and samples whereas isothermal methods are likely to provide more reliable kinetic information. Possible tests include the ASTM test based on Ozawa's method (Brown, 1989). This test involves the measurement of the temperature at the maximum exotherm, T_{max}, on DSC or DTG traces done at different heating rates (β_1). The Arrenhius parameters can then be determined from a plot of ln β_1 against $1/T_{max}$. One problem does exist though. As the use of the temperatures at the peak maximum or times to the maximum rate does not take into account that the activation energy of the induction period (should there be one) may differ widely from that of the main reaction. Rogers and Janney (quoted by Brown, 1989) recommend DSC measurements under isothermal conditions be used and give detailed procedures which include careful temperature calibration of the instrument used and avoidance of emittance errors caused by condensation of

decomposition products on the sample holder. There is also a need to determine the effects of confinement pressure and volume on the kinetic parameters. Rogers and Janney have made effective use of isotopic substitution in determining reaction mechanisms (Brown, 1989).

- According to Beck and Brown (1991) it is uncertain whether the DTA signal obtained from the sample can be regarded as a damped response to the ignition of the pyrotechnic mixture or whether the conditions in the DTA apparatus result in a modified, more controlled reaction in the sample. For this reason Beck and Brown (1991) have modified TOPAZ 2D, a two-dimensional finite element code for heat-transfer analysis, to allow for heat generation by a chemical reaction with specified kinetics in an attempt to simulate the heating of a typical "slow-burning" pyrotechnic composition in DTA. They found during this study that the enthalpy of combustion may be overestimated by altering the thermal response of the instrument (the thermal response is a function of the various thermal resistances in the instrument). The DTA should therefore be calibrated using a material with a thermal resistance comparable to that of the sample being studied. The extraction of kinetic parameters from DTA traces also presented difficulties for Beck and Brown (1991). They recommended that kinetic analysis can be done if confined to the region of the DTA trace corresponding to the initial stages of the reaction and if the instrument is of the type in which the averaged sample temperature is recorded (Beck and Brown, 1991).
- Laye and Charsley (quoted by Beck and Brown, 1991) have stated that the interpretation of DTA curves are difficult when ignition occurs. The ignition temperature may be estimated but the exotherm will show temperature rises of several hundred degrees. Another factor that can not be measured successfully at ignition is the energy, which is released during ignition because of the inability of DTA and DSC to follow the rapid rise in the temperature of the sample. Also the removal of energy by gaseous products cannot be detected in this open form of calorimetric system (Beck and Brown, 1991).

It is therefore felt that the processes observed during thermal analysis can be used to explain the combustion process, however, that the values (i.e. activation energy, kinetic parameters) obtained are not representative of the actual combustion

conditions due to the ignition process difference as well as the difference in compaction and the surroundings.

5. PREVIOUS WORK

5.1 Reagent Properties

A number of authors have reported on the characteristics of some of the reagents which are used by AEL or which have been used in this investigation.

5.1.1 Silicon

Silicon is one of the most widely used fuels in time delays. It is a chemically abundant material readily obtained by chemical reduction of silane or by electrolytic decomposition of molten mixtures of K_2SiF_6-LiF-KF or SiO_2-Na_3AlF_6. When mixed with a suitable oxidant and ignited, it provides relatively high heat outputs (Rugunanan, 1991).

Silicon is generally unreactive except at high temperatures. Hackley *et* al (1997) has stated that oxygen, water and steam have no noticeable effect on silicon. This is due to the presence of a thin, continuous, protective surface layer of SiO_2, which is a few atoms thick. According to Hackley *et al* (1997), the presence of the oxide layer prevents further hydrolysis, but also permits wetting of the powder and promotes the particle dispersion through the development of an electrical double layer resulting from the dissociation of acidic silanol (Si-OH) surface groups. This is despite a clean silicon surface being hydrophobic (Hackley *et al*, 1997). On the other hand, Weiss and Engelhardt (quoted by Pourbaix, 1966:462) have shown that silicon reacts slowly with water. It has been stated that the silicon tends to decompose water with the evolution of hydrogen and gaseous silicon hydride (SiH_4) and the formation of silica or silicates. This is often not apparent at room temperature due to the irreversibility of the oxidation-reduction reactions of Si and the presence of a thin layer passive layer of silica (Pourbaix, 1966:462).

Silicon is however, susceptible to attack by halogens i.e. fluorine at room temperature, chlorine at 300°C and bromine and iodine at 500°C. Molten silicon is extremely reactive. Greenwood and Earnshaw (1984:385) recommend that when using crucibles and molten silicon, the crucibles should be made of refractories such as ZrO_2 or borides of transition metals in Groups IVA and VIA. With non-metals of higher electronegativity, silicon forms non-polar Si_3N_4 and SiC and polar SiO_2 and SiF_4 with an oxidation state of +4.

Silicon is insoluble in water, but does dissolve in hot aqueous alkaline solutions (Greenwood & Earnshaw, 1984:385). Zeulehner *et al* (1993:722) describe this reaction as being extremely violent, even with dilute solutions and it leads to the formation of hydrogen gas. Dillinger *et al* (quoted by Hackley *et al*, 1997) recommend that silicon only be processed in acidic or weakly alkaline solutions as a result of the increased reactivity of the silicon at high pH values. This reactivity is further increased with increasing particle size (Hackley *et al*, 1997). This means that wet mixing of Si and any oxidant is limited by the pH range. This has been discussed in section 10. Silicon is resistant to most acids except to mixtures of HF and HNO_3. According to Zeulehner *et al* (1993:722), the HF etches the thin oxide layer, which is present, and the HNO_3 in the solution reforms the oxide layer and the process is repeated.

According to Davies (1999) silicon is a good fuel for delays as it is reasonably energetic and forms slags which have good heat-retaining properties, however it often reacts sluggishly except for the unusually fast reaction with lead oxides.

Silicon undergoes gaseous oxidation between 990-1200°C which is below its melting point of 1410°C. Amorphous SiO_2 is formed. The oxidation has been found to be accelerated by the presence of water and the formation of Si-O-H bonds has been reported. Oxidation occurs at the Si/SiO_2 interface and therefore oxygen has to diffuse through the oxide layer for the reaction to occur (Rugunanan and Brown, 1991, Rugunanan, 1991). It thus appears that the reaction rate may be limited by the rate of diffusion of oxygen to the Si/SiO_2 interface and the thickness of the SiO_2 layer.

The nitridation of silicon by gaseous N_2 to form Si_3N_4 occurs at temperatures greater then 1200°C (Rugunanan and Brown, 1991, Rugunanan, 1991).

During TG analysis, Rugunanan and Brown (1991) found that in a N_2 atmosphere the silicon experienced a slight mass loss between 50-700°C due to the desorption of surface impurities. Above 700°C there was a mass increase due to the slow reaction with O_2 present in the purge gas and not nitridation which as mentioned previously occurs above 1200°C (Rugunanan & Brown, 1991, Rugunanan, 1991).

Oxygen forms strong bonds with Si. The bond energy has been reported as 25.8kJ and the observed bond length is 0.163nm (Runyan, 1996:834).

From the Ellingham diagram presented by Birchenall (1986:3356) it can be seen that the oxidation of Si is possible by Cu_2O, CuO, Fe_3O_4, ZnO, SnO_2, CoO, NiO, Cr_2O_3 and MnO.

Elemental Si is inert and is only classified as a nuisance particulate with a TLV of $10mg/m^3$. Most Si-compounds are poisonous and the silanes are highly explosive. $SiCl_4$, $SiHCl_3$ and $SiBr_4$ decompose in the presence of moisture and form SiO_2 and the corresponding acid. The long-chain chlorinated silicon polymers are unstable and detonate under mild shock (Runyan, 1996:842).

5.1.2 Antimony Trioxide

Sb_2O_3 has been employed in numerous applications, such as flame retardant in rubber, textiles, paper, plastics and paints, as a stabiliser in plastics and as a catalyst/opacifier in glass, ceramics and vitreous enamels. It can be produced by high temperature oxidation of Sb or SbS_3 or it can be produced electrochemically (Mani *et al*, 1996, Freedman *et al*, 1996:385-6).

Below 570°C antimony trioxide is dimorphic i.e. senarmontite - Sb_4O_6. Sb_2O_3 melts in the absence of O_2 at 656°C and partially sublimes before reaching the boiling temperature of 1425°C. Sb_2O_3 is insoluble in organic solvents and slightly soluble in

water where it forms hydrates that are related to antimonic acid. In an acidic solution, it dissolves to form a series of complex polyantimonic (III) acids. Freshly precipitated antimony trioxide dissolves in strong basic solutions and forms the antimonite ion ($Sb(OH)_6^{3-}$). Other derivatives may be made by heating antimony trioxide with the appropriate metal oxides and carbonates (Freedman *et al*., 1996:385).

Rugunanan and Brown (1991, Rugunanan, 1991) have reported the following thermal behaviour in N_2 for Sb_2O_3 heated to 1000°C in open Pt pans:

- A rapid mass loss (94%) between 500-620°C, which meant that it sublimed before its melting point of 656°C.
- The further mass loss (3.1%) between 620-800°C was the vaporisation of the remainder of the Sb_2O_3.

Rugunanan and Brown (1991, Rugunanan, 1991) have reported the following thermal behaviour in air for Sb_2O_3 heated to 1000°C in open Pt pans:

- An endotherm between 500-650°C which corresponded to the oxidation of Sb_2O_3 by O_2 i.e. $2Sb_2O_3\ (s) + O_2\ (g) \rightarrow 2Sb_2O_4\ (s)$.
- In air the sublimation and oxidation occur simultaneously.
- The mass loss (63%) was less than obtained by heating the Sb_2O_3 in N_2.
- There was a slight mass loss (1.7%) between 600-760°C followed by a mass gain (3.8%) between 760-900°C due to the oxidation of unreacted Sb_2O_3.
- A further mass loss (12-17%) occurred above 910°C as a result of the decomposition of Sb_2O_4.
- The formation of Sb_2O_5 during oxidation was not ruled out as the IR spectrum of Sb_2O_5 closely resembles that of Sb_2O_4.

Long term exposure to Sb_2O_3 has been reported to result in pneumoconiosis and emphysema. It is also a suspected carcinogen for humans as it has been carcinogenic when inhaled by rats. Concentration limits for Sb_2O_3 as reported by Herbst *et al* (1985) are TLV 0.5mg/m^3 (as Sb) and TCLo 4.2mg/m^3 during 52 weeks.

5.1.3 Barium Sulphate

Heating $BaSO_4$ decomposes it, the rate increasing with temperature over the range 100-1500°C. The main products are BaO, SO_2 and O_2. For this reason the melting point differs in literature. $BaSO_4$ is insoluble in water, more soluble in hot concentrated H_2SO_4 and melts of alkali metal salts (Baudis, 1985:330). Beck (1989) however found that $BaSO_4$ undergoes a crystal phase transition around 1156°C. The addition of SiO_2 has been said to have a catalytic effect on the decomposition of $BaSO_4$ which may enhance the initial interaction between Si and $BaSO_4$ (Beck, 1989).This phenomenon may explain the variable performance found for detonators based on this composition. The SiO_2 content is a function of the age of the Si, therefore the difference in SiO_2-content may be found throughout a batch and hence the varying burn speed in batches of this composition.

Insoluble $BaSO_4$ is non-toxic (Wolf, 1985:339).

5.1.4 Nanocat (Super Fine Iron Oxide)

Mach I produce a nano-size iron oxide. The structure of this catalyst has been determined by Zhao *et al* (1993) as being FeOOH. Feng *et al* (1993) found that annealing the Mach I product led to a 12% weight loss, which indicates that the FeOOH converts to Fe_2O_3 by releasing water. The average particle size was also found to be a function of the annealing temperature (Feng *et al*., 1993).

Feng *et al*. (1993) found that the nano-phase powder is water sensitive and may absorb as much as 15% by weight of water upon prolonged exposure to the atmosphere. The particles become linked by the adsorbed water molecules and form a particle cluster (i.e. hydrogen bonding). At elevated temperatures, the water molecules are readily evolved from particle linkages, leading to agglomeration of the small particles (Feng *et al*, 1993).

5.1.5 Iron Oxides

Rugunanan and Brown (1991, Rugunanan, 1991) have found that Fe_2O_3 heated in air and N_2 showed a linear mass loss (0.6%) between 60-940°C. Fe_2O_3 melts at 1457°C (Ellern, 1986:267). Fe_2O_3 has been classified by Conkling (1996:681) as a slow oxidiser due to it high melting point and endothermic decomposition meaning that it will only sustain a self-propagating reaction with the most energetic fuels. This is an example of how the nature of the oxidant affects the reaction rate.

Investigation into the reaction of Fe_2O_3 and Al revealed that three intermediate reaction zones exist between the ferric oxide and Al. It was found that the decomposition of $Fe_2O_3 \rightarrow Fe_3O_4 \rightarrow FeO$ precedes the interaction between the Al and iron oxide (Wang *et al*, .1993).

5.1.6 Lead Oxides

Lead monoxide (PbO) exists in a reddish alpha form up to 489°C. It has a water solubility of 17mg/L at 20°C and is soluble in HNO_3, alkalis, lead acetate, ammonium chloride and chlorides of Ca and St (Carr, 1993:252-253). It melts at 885°C (Ellern, 1968:267).

Lead dioxide (PbO_2) consists of fine flakes in either the orthorhombic alpha of the tetragonal beta form. As mentioned previously, flaky powders react more readily than regular, more uniform powder morphologies. This may be one of the variables that account for the fast reactions encountered with Si-PbO_2 compositions.

PbO_2 decomposes to PbO when heated above 290°C. This is a low temperature decomposition that can also account for the fast burn speed observed with Si. It is practically insoluble in water or alkaline solutions. It dissolves in acetic acid, ammonium acetate, HCl and a mixture of HCl and H_2O_2. It is a vigorous oxidising agent. Pb_3O_4 is insoluble in water and ethanol, but dissolves in acetic acid or hot HCl (Carr, 1993:252-253).

Concentration limits for lead and lead-containing materials have been reported by Adrian (1993:320) as being MAK value (lead) <0.1mg/m^3 and TLV-TWA value (lead) <0.15mg/m^3.

Triblehorn, Venables and Brown (1995) have found the following thermal behaviour for PbO_2 and Pb_3O_4 during a thermoanalytical study:

- DTA curves of PbO_2 in air and nitrogen showed a number of shallow, poorly defined endotherms between 320 and 600°C. TG curves showed 2 overlapping stages over 370-570°C; the first corresponding to the decomposition $PbO_2 \rightarrow Pb_3O_4$ and the second to $Pb_3O_4 \rightarrow PbO$.
- DTA curves showed the endothermic decomposition of Pb_3O_4 at 560°C in N_2 and 580°C in air. The decomposition of Pb_3O_4 to PbO occurred in a single step starting from 550°C.
- DTA curves of PbO in air and N_2 showed 2 small endotherms at 280 and 330°C with a slight mass loss. This is thought to be as a result of $PbCO_3$ on the surface of PbO.

5.1.7 Lead Chromate

The chrome yellow pigments are pure lead chromate or mixed phase pigments with the general formula $Pb(Cr,S)O_4$. They are insoluble in water. Precipitating inert metal hydroxides on the pigment particles may reduce the pigment's solubility in acids and alkalis and discoloration by H_2S and SO_2. Bayer (quoted by Adrian, 1993, 318) has described pigments containing lead chromate stabilised in aqueous slurry with silicate-containing solutions and antimony (III) compounds. Furthermore, Heubach (quoted by Adrian, 1993:318) developed a process for the alternate precipitation of metal oxides and silicates using a homogeniser to disperse the pigment particles during stabilisation. Lead chromate has a low binder demand and good dispersibility (Adrian, 1993:319).

$PbCrO_4$ with Ti metal or W-based compositions have been studied extensively. It was found that for the Ti-based system the oxidation of the Ti was to TiO. The burning rates were linearly dependent on the amount of inert material which was added to the

mixture. The proportionality was also dependent on the fuel/oxidant ratio and increased as the ratio increased. It was deduced that the rate determining step for the Ti-based reaction was not the thermal decomposition of the oxidant but rather the oxidation of the metal. This is unusual for pyrotechnic compositions. For the W/$PbCrO_4$ system the initial reaction step was proposed to be the decomposition of the $PbCrO_4$, followed by diffusion of the decomposition products to the W surface where the W reacts with the oxygen. The volatile WO_3 then combines with the PbO to form $PbWO_4$ or the PbO could decompose further (quoted by Beck, 1984).

$PbCrO_4$ has been classified as a substance suspected of having carcinogenic potential, but as yet epidemiological investigations have given no indication that practically insoluble $PbCrO_4$ has any carcinogenic properties (Adrian, 1993:321).

5.1.8 Copper Oxides

Cu_2O and red phosphorous have been used in the past and yield intermediate time delays. Another alternative has been the use of Cu_2O with Zn by Johnson (quoted by Ellern, 1968:202). Watkins *et al* (1968:80) has also mentioned the use of copper oxides as oxidant. It melts at 1230°C (Ellern, 1968:267).

5.1.9 Manganese Oxides

According to Greenwood and Earnshaw (1984:1048), MnO_2 is an unstable oxide as it decomposes to Mn_2O_3 above 530°C and is a useful oxidising agent. Lower oxides of manganese are basic and react with aqueous acids to give salts of Mn^{2+} and Mn^{3+} cations, whilst higher oxides of manganese are acidic and react with alkalis to yield oxoanion salts (Greenwood and Earnshaw, 1984:1049).

MnO_2 is not extensively used in delay compositions as the dioxide is not stable and its decomposition is largely dependent on its method of manufacture. It has been used with FeSi where it was claimed that the rate of decomposition of MnO_2 was independent of the component ratio and that mixtures with the highest rate of reaction

generated the lowest heat of reaction (quoted by Beck, 1984). Beck (1984) has found that thermal behaviour of MnO_2 was not reproducible and depended on the source. It was also used by Beck (1984) in conjunction with Sb. Thermal analysis of 50% Sb/MnO_2 showed a gradual mass loss (decomposition of MnO_2) followed by a rapid mass gain and strong exotherm around 500°C.

5.1.10 Copper Antimonite

Harding (quoted by Mellors, 1933:432) obtained the compound by adding a dilute solution of copper sulphate to an excess of a saturated solution of antimony trioxide in potash lye. The green crystalline powder that Harding (quoted by Mellors, 1933:432) produced was soluble in hydrochloric, tartaric or citric acid. When heated in an open crucible, it first evolves antimony oxide and then explodes, leaving a residue of antimony trioxide and copper oxide. When heated in a closed vessel, the powder was found to leave a residue containing metallic copper (Mellors, 1933:432).

5.2 Silicon as a Fuel – Compositions Reported in Literature

Figure 5-1 (a and b) contains a summary of Si-based compositions which have been reported in literature. Summaries based on the reported literature of the compositions which are used by AEL or were used in this study follow Figure 5-1 (a and b).

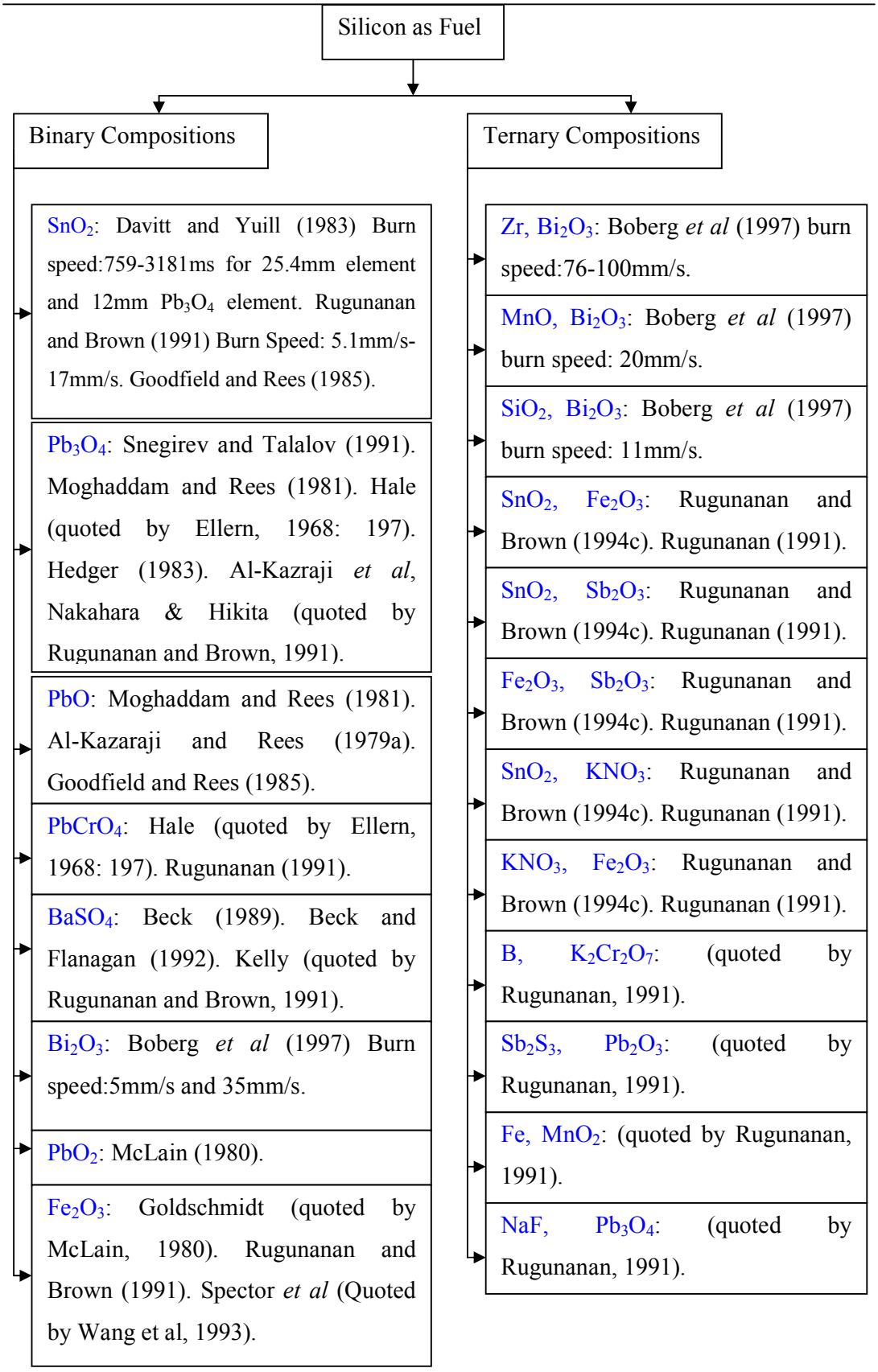

Figure 5-1(a): Si-based Compositions Reported in Literature

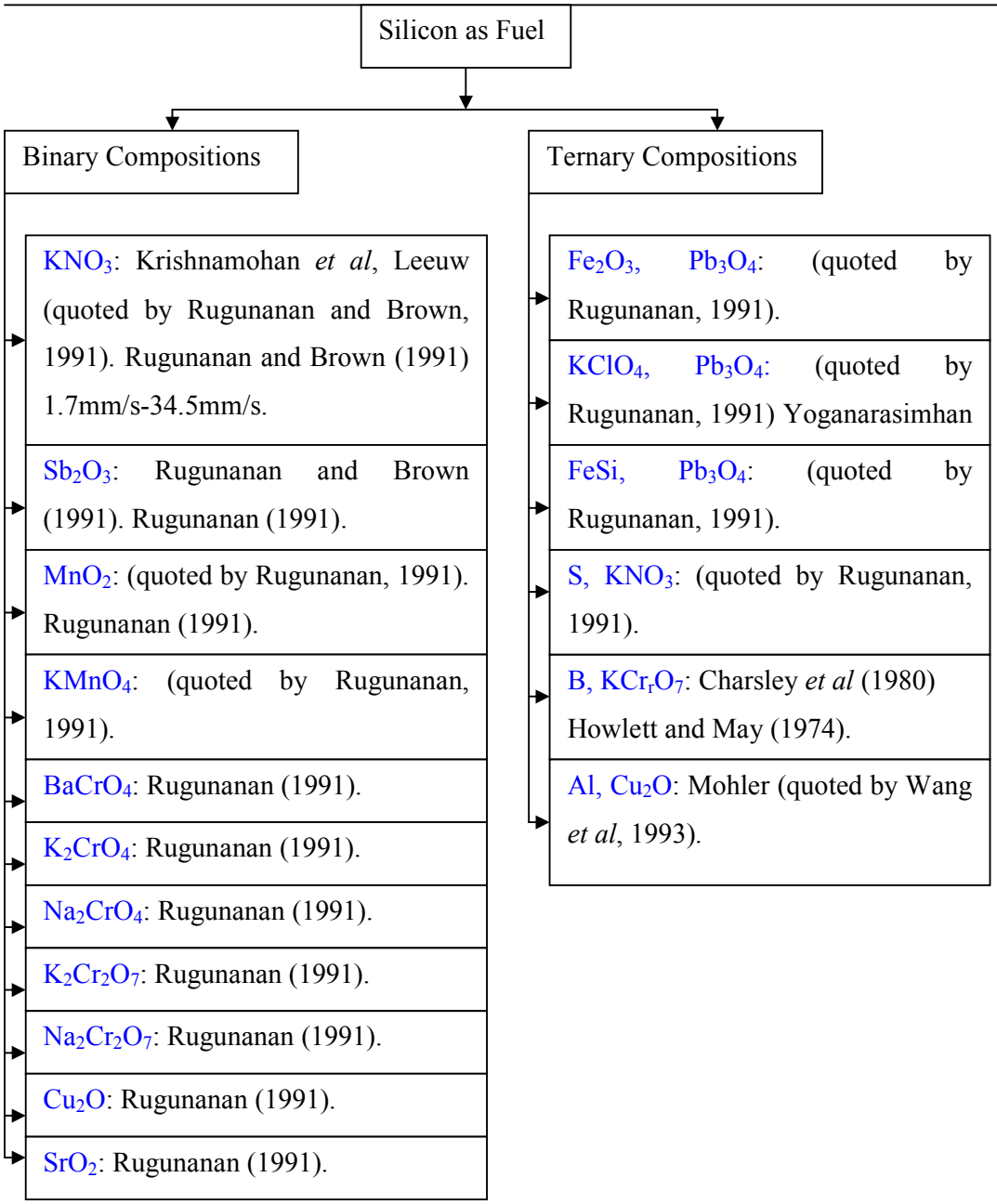

Figure 5-1 (b): Si-based Compositions Reported in Literature

One four component mixture was reported by Boberg *et al* (1997) i.e. Si, Zr, Bi_2O_3 and TiO_2 with a burn rate varying between 7-9mm/s.

5.2.1 Lead Oxides-Si

Hale (quoted by Ellern, 1968:197) reported the first use of Pb_3O_4. He proposed a composition of 84.4% Pb_3O_4, 14.85 Si and 0.8% glycerine (binder) for anti-aircraft fuses.

Thermal Analysis

i) PbO-Si

During DSC studies, Moghaddam and Rees (1981) found that 2 exothermic peaks in N_2 for the PbO-Si system were evident with maxima at 637°C and 709°C respectively. They proposed that the first peak is due to the surface reaction of PbO and Si to form trace amounts of SiO_2 and Pb and the second peak is the bulk reaction whereby the Si atoms penetrate the PbO lattice. This is in contradiction to Rugunanan and Brown (1991) and Rugunanan, (1991) who have stated that the oxidation of Si in air occurs at the Si/SiO_2 interface. The maximum heat release was obtained from the 90:10 (PbO:Si) composition (Moghaddam & Rees, 1981).

However, studies by Al-Kazarji and Rees (1979a) on a 70:30 PbO:Si system yielded the following conclusions:

- The reactions followed the same pattern as those of the Pb_3O_4-Si system i.e. similar temperature occurrence and relative size of the DTA peaks.
- Initially the monoxide was converted to red lead at temperatures above 350°C:

$$6PbO + O_2 \xleftrightarrow{540°C} 2Pb_3O_4$$

$$2Pb_3O_4 + Si \xleftrightarrow{590°C} 6PbO+SiO_2$$

$$PbO + \tfrac{1}{2}O_2 + Si \xleftrightarrow{665°C} SiO_2 + Pb$$

- The excess Si which was present at this concentration meant that the first exothermic reaction occurred on the surface and the second exothermic reaction

was enhanced at the higher temperature to favour the movement of the reactants to penetrate the product layer which formed around the constituents.

- Under nitrogen, the same composition yielded a less violent second reaction due to the absence of oxygen.
- A DTA study of a 70:30 Pb-Si mixture in air showed that the lead melted at 327°C and was partially oxidised to PbO. At temperatures higher than 350°C the monoxide was converted to Pb_3O_4 and the reactions thereafter were similar to those of Pb_3O_4-Si mixtures (Al-Kazarji and Rees, 1979a)

ii) Pb_3O_4-Si

Moghaddam and Rees (1981) detected two exothermic peaks at the same temperature range as PbO-Si for Pb_3O_4-Si mixtures. They also observed the reaction under a hot stage microscope and observed a contraction in volume at the beginning of the reaction. They concluded that the reaction is between lead dioxide (formed by the decomposition of the red lead) and Si.

Zhou Conzhang *et al* (quoted by Davies, 1999) confirmed by chemical analysis and DTA the existence of a solid state non-incandescent pre-ignition reaction starting at 420°C for the Pb_3O_4-Si composition. It was considered to involve the diffusion of oxygen and of lead from red lead to the surface of the Si. $PbSiO_3$ was found in the diffusion layer and the rate of the reaction depended on the thickness of the oxide layer on the Si. Zhong Jun *et al* (quoted by Davies, 1999) on the other hand showed that the thermal ignition of the reaction between red lead and silicon was controlled by the diffusion of Si through its oxide coating and the thickness of the oxide coating affected the burn rate and its reproducibility. Hence again the discrepancy on whether the lead and oxygen diffuse or the Si diffuses to the reaction interface.

Mixtures of Pb_3O_4-Si were also analysed by Al-Kazraji and Rees (1978). A summary of their main findings with regards this system may be found in Table 5-1.

Table 5-1: Thermal Analysis of Pb_3O_4-Si (Al-Kazarji and Rees, 1978)

Pb_3O_4 in air
❑ Endotherm between 540-590°C indicated the decomposition of Pb_3O_4 to PbO and O_2. ❑ Endotherm at 868°C indicated the melting of the PbO which was formed. ❑ TG curve indicated a mass loss due to the decomposition and finally due to the vaporisation of PbO at 950°C.
Si in air
No noticeable peaks were obtained by the DTA until 1000°C.
Pb_3O_4-Si in air
❑ An exotherm was observed between 520°C and 600°C for all the compositions. The reaction was of short duration (200ms) and the formation molten lead and excess molten silicon was confirmed. ❑ An exotherm which commenced slowly at 626°C but rose sharply at 660°C was explained by the oxidation of the molten lead to lead oxide, which then reacted with the excess silicon at 665°C. It was observed that the higher the silicon content of the mixture, the less oxygen is available from the red lead and thus the reactions were less exothermic. ❑ An exotherm was observed between 755-788°C, which indicated the reaction of PbO with lead silicate by migration of lead oxide into the silicate lattice at the silicate melting point. ❑ The TG curve indicated an increase in the mass of the products. The percentage increase increased with increasing Si content due to the reaction of O_2 with excess Si. ❑ The maximum heat evolution occurred for the 90:10 (Pb_3O_4) composition near the stoichiometric amount of silicon (7.6%). ❑ XRD and IR confirmed the presence of PbO, Si and SiO_2.
Pb_3O_4-Si in N_2
❑ Little or no reaction occurs after the first peak at 520-600°C in the DTA as the lead that was formed after the first reaction, was not oxidised to react further. ❑ Reactions were less exothermic than those in air. ❑ XRD indicated that for mixtures 30:70 to 80:20 (Pb_3O_4:Si) heated to 600°C, only crystalline Pb and Si were present. The 90:10 mixture indicated the presence of PbO, Pb and Si under the same conditions.

They also found that at higher %Si compositions (30:70, 40:60 and 50:50) the amount of oxidiser present was insufficient to oxidise the silicon surface available and the heat generated was too small to sustain the burning of delay compositions (Al-Kazarji and Rees, 1978).

Composition, Heats of Reaction and Burn Rate

Glasby (quoted by McLain 1980:58-59) found that the velocity of propagation for the Pb_3O_4-Si system increased with pressure until a limiting velocity at a critical pressure (900-1000 psi i.e. 6.2-6.9MPa) after which is decreased. This effect was due to the stabilisation of the PbO moiety of the red lead. Jakubko (quoted by Davies, 1999) found that the burning of very rich fuel mixtures (55% Si) the composition burned faster under venting than under confinement.

Al-Kazarji and Rees (1979b) did further work on the lead oxides and silicon systems. Their findings confirmed McLain's (1980:53) (Section 4.1 (iv)) concerning the relationship between the stoichiometry, heat of reaction and burning rate particularly for the finer silicon particle sizes. Some of their other observations include the following:

- Compositions containing more than 50%Si failed to maintain sustained reliable combustion. This was particularly evident with the coarser silicon particles that were used.
- The maximum heat of generation occurred at about 10% silicon and then decreased.
- For fine silicon the heat evolved per second reached a peak value at approximately the same percentage silicon as that at which the rate of burning reached its maximum.
- A second peak was found to occur for the coarser grades of silicon. This was been attributed to the high pressure generated in the tubes owing to the high temperature of reaction.
- Theoretically the maximum rate of burning should coincide with the maximum heat of reaction. The discrepancy, in particular for the coarser grades of Si, was due to the fact that the reactions took place at the surface and the Si particles became coated with a layer of SiO_2, which prevents complete reaction of the Si

core even in the molten state. Thus, in approaching the peak of the rate of reaction, the amount of Si is reduced and the layer of product being thicker, causes the rate of reaction and burning rate to drop. This occurs at a point richer in Si than that for the heat-generation maximum.

- For compositions less than 15%Si the rates of reaction were dependent on the pressures formed and the diffusion of the vaporised oxides into the surface of the Si and product layer. Where the Si content was in excess of 20%, solid-solid mechanisms prevail and the surface area of the Si and good fuel/oxidiser contact (controlled by the loading process of the tubes) were the controlling variables.
- XRD and IR confirmed the presence of Pb, fused silica and unreacted Si.
- For compositions containing large amounts of Si, TG showed the loss of some of the oxygen, indicating a solid-solid reaction, whereas compositions with small amounts of Si, the temperature was so high that some of the PbO was vaporised and the solid-solid reactions would not predominate.
- For large excesses of Si, (above 30%), the reactions were incomplete owing to the presence of some Si particles not being in contact with Pb_3O_4 (Al-Kazarji and Rees, 1979b).

Hedger (1983) found and suggested the following for Pb_3O_4-Si :

- The delay time varied with fuel surface area but became independent at high surface areas.
- At fuel surface areas >1m^2/g the delay time curve had a discontinuity between 30 and 40% Si which was attributed to the change in propagation mechanism of the reaction front.
- There was a minimum delay time between 30 and 40% Si.
- The time delay was provided by the initial stage of the reaction which was suggested to be formation of the SiO_2PbO liquid phase.

5.2.2 $BaSO_4$-Si

Kelly (quoted by Rugunanan, 1991) attempted to obtain a burn rate of 4.2mm/s with this composition and found that it could be achieved with a mixture containing 45.5% Si. He found the minimum burn rate (3.8mm/s) was observed at 40% Si. The burn rate

generally increased with increasing SSA of Si. Furthermore, the burn rates were very dependent on the source of the ingredients (Rugunanan, 1991).

Beck and Flanagan (1992) have patented a delay composition comprising a consolidated, particulate mixtures of silicon and $BaSO_4$ and a minor proportion of a dispersed metal compound such as alkali metal salts (sodium chloride, sodium sulphate and potassium sulphate); lead monoxide, antimony tri- and pentoxide and vanadium pentoxide. Of the available oxidisers, Beck and Flanagan (1992) have used $BaSO_4$ but have found Fe_2O_3 to be effective. The metal compound serves as a reaction facilitating flux. The preferred metal compound is vanadium pentoxide as it melts at a temperature of 600°C, which is lower than the ignition temperature of $Si/BaSO_4$ compositions (reported as being 680°C). The molten flux appears to facilitate the $Si/BaSO_4$ reaction without actually participating in any dominant chemical reaction or altering the essential character of the $Si/BaSO_4$ composition as an intermediate to slow burning composition. The V_2O_5 is, however, consumed and becomes involved in complex mixed oxide formation as can be seen from the products, which contain the V^{4+} and V^{5+} species. The presence of the V_2O_5 helps with the composition's resistance to quenching by the heat-sink effect of the metal tubular containment so that the composition is effective in rigid elements. The relative proportions of each ingredient are as follows:

- $Si:BaSO_4$ -55:45 to 30:70 parts by mass
- Flux – preferably 2 to 5 percent by mass. Above 10%, it is believed that the facilitating role of the flux will be offset by the inert diluent effect and tend to quench the reaction.

Table 5-2 summarises Beck and Flanagan's (1992) experimental results. Their formulations were prepared by a wet mixing procedure, drying and sieving. The formulations were tested using two testing procedures i.e.:

1. The first procedure included the consolidation of the compositions to a density of about $2g/cm^3$ in a 22mm zinc delay element (i.d. 3,1mm, o.d. 64mm), containing a 6mm long fast burning igniting sealing composition. The element was then encased in a delay detonator and initiated using a shock wave conductor.
2. The second procedure included the loading of the compositions into a stainless steel combustion channel (dimensions:6mm× 10mm×30mm) with a wall thickness of 1mm

to reduce heat losses. The delay column was then consolidated to a density of about 1.8g/cm^3 and initiation was achieved by an electric fusehead. The delay times were determined by means of two thermocouples embedded in the column and separated by 14mm.

Table 5-2: Beck and Flanagan's (1992) Experimental Results for $BaSO_4$-Si

Reagent Mass Ratios ***(Experimental Procedure)***	**Results**
Si:$BaSO_4$ – 45,5:54,5 (Basic Si-$BaSO_4$ formulation used in the experiments which follow) Si–7m^2/g $BaSO_4$–0,8m^2/g *(1)*	All the attempted samples were incapable of sustaining combustion over an appreciable distance.
V_2O_5 – 1% mass percentage was added to the basic Si-$BaSO_4$ formulation *(1)*	18 out of a sample of 20 detonators fired successfully with an average delay time of 3,550±0.072s. The two misfired detonators revealed that the main delay column had initiated but had failed to propagate along the length of the column
V_2O_5 – 2% by mass was added to the basic Si-$BaSO_4$ formulation *(1)*	All 20 detonators fired with an average delay time of 3,562±0,103s
V_2O_5 – 4.5% by mass was added to the basic Si-$BaSO_4$ formulation *(1)*	All 20 detonators fired with an average delay time of 3.523±0.066s
V_2O_5 – 10% by mass added to the basic Si-$BaSO_4$ formulation *(1)*	All 20 detonators fired with an average delay time of 3,562±0,103s
Sb_2O_3 - 10% by mass was added to the basic Si-$BaSO_4$ formulation *(1)*	12 out of the 20 detonators which were tested fired with an average burning speed of 4.5mm/s

Reagent Mass Ratios *(Experimental Procedure)*	**Results**
Sb_2O_5 - 10% by mass was added to the basic Si-$BaSO_4$ formulation *(1)*	19 out of the 20 detonators which were tested fired with an average burning speed of 4.8mm/s.
Basic Si-$BaSO_4$ formulation *(2)*	An average delay time of 3.900±0.500s was measured.
V_2O_5 – 10% by mass added to the basic Si-$BaSO_4$ formulation *(2)*	An average delay time of 3.840±0.200s was measured.
Si:Fe_2O_3 – 30:70 10% by mass of Na_2SO_4 was intimately mixed with the Si/Fe_2O_3 mixture Si–5.6m^2/g Fe_2O_3–0,8m^2/g *(1)*	A maximum burning speed of about 8.75mm/s was obtained.

According to Beck and Flanagan (1992), these compositions are characterised by low toxicity, moisture resistance and a uniform burn rate.

5.2.3 Fe_2O_3-Si

A number of possible reactions may occur between Si and Fe_2O_3. These include:

- $3Si(s) + 2Fe_2O_3(s) \rightarrow 3SiO_2(s)$ and $4Fe(s)$ (H_r=-355kJ/mol_{Si} and 21% Si) ***(A)***
- $3Si(s) + 2Fe_2O_3(s) \rightarrow SiO_2(s)$ and $4FeO(s)$ (H_r=-325kJ/mol_{Si} and 8% Si) (Rugunanan and Brown, 1994a).
- Fayalite (Fe_2SiO_4) may also be formed. Spector *et al* (quoted by Wang *et al*, 1993) mixed radioactive wastes into a thermite mixture and then ignited the mixture to form highly water insoluble polysilicates which fix the radioactive materials. The principal thermite reaction for this process was $4Fe_2O_3+3Si \rightarrow 3FeSiO_4+2Fe$

(H_r=-245cal – 1026J). The mixture was however preheated before ignition (Wang *et al*, 1993).

Rugunanan and Brown (1991, 1994, Rugunanan, 1991) have found the following:

- The range of compositions which sustained combustion was 20-40% Si (by mass).
- The measured burn rates were 2.3 (20% Si), 3.7 (25% Si), 3.8 (30% Si), 3.6 (35% Si) and 4.5 (40% Si) mm/s.
- The maximum temperature attained during combustion was 1250°C. This indicated that the reaction appeared to occur predominantly between solid oxidant and solid fuel as this temperature is below the melting points of Fe_2O_3 and Si.
- The temperature profiles were complex with three overlapping stages. The first stage was the relatively slow rise in temperature after triggering. The second was a sigmoid segment followed by the third segment which was also a sigmoid segment. This was explained by diffusion of Si or Si^{4+} via the cation vacancies into the condensed Fe_2O_3 layer. The possibility of redox processes such as $Fe^{2+} \rightarrow Fe^{3+}$, with accompanying changes in ionic size, could occur as the reaction proceeds through the SiO_2 layer and could thus not be excluded as also a possible explanation. Another explanation was that the burn front could have been convex-forward resulting in different time responses in the thermocouple.
- The presence of fayalite was confirmed and was formed by SiO_2 and FeO and not by the direct reaction of Fe_2O_3 and Si.
- The heat of reaction at 30%Si was -0.83kJ/g.
- There was only a slight mass loss after burning indicating no significant loss of volatile species.
- SEM showed the formation of solidified melts and the presence of unreacted particles.
- The maximum enthalpy of reaction was found to be at 25% Si which is higher than the 21% indicated for reaction ***A***. This was attributed to the fact that the Si particles become coated with a layer of oxide and this prevents further oxidation of the bulk.
- Varying the loading pressure of the compositions resulted in emphasis of the step-wise nature of the temperature profiles. The linear burn rate initially decreased till a minimum followed by an increase with further increase in density. The mass

burning rate was approximately constant but then increased at higher densities further indicating a solid-solid reaction since the inter-particle contact between the reactants was increased by increasing the compaction of the mixture.

- The burn rate was found to vary only slightly (35%Si) with increasing surface area of the Si particles.
- Burning failed when the addition of additives exceeded 9% for SiO_2 and 7% Al_2O_3. The maximum temperatures were unaffected by the additives. The burning rates decreased sharply with increasing H_2O content whilst the reaction temperature increased. Samples containing 5% water failed to ignite.

Thermal analysis of this composition (35% Si) by Rugunanan and Brown (1991) yielded no significant thermal activity up to 1000°C.

5.2.4 Sb_2O_3-Si

Rugunanan and Brown (1991, 1994b, Rugunanan, 1991) have found the following:

- The range of compositions which sustained combustion was 20-50% Si (by mass). Mixtures with 20-25% Si were slightly gassy (mass loss≈3%) which caused thermocouple shorting and sample movement.
- The measured burn rates were 1.6 (20% Si), 3.3 (25% Si), 6.3 (30% Si), 8.7 (35% Si),8.5 (40% Si),8.7 (45% Si) and 7.25 (50% Si) mm/s. This burn rate was lower than expected because despite the high mobility of Sb_2O_3 through sublimation, it was thought that the adsorption of unchanged Sb_2O_3 on Si surfaces precedes the oxidation of the Si. They felt that the movement of Si^{4+} into Sb^{3+} vacancies in the condensed Sb_2O_3 layer was a possibility, as was the formation of a barrier of the higher oxide, Sb_2O_5 on the surfaces.
- The temperature profiles of mixtures between30-50% showed a smooth rise to the maximum temperature and appeared reproducible.
- The maximum temperature attained during combustion was 1250°C.
- The heat of reaction at 43%Si (which corresponded to the maximum burn rate) was -0.6kJ/g.

- SEM of the combustion products showed the formation of molten material and crystalline structures embedded in the solidified melt. The presence of channels and cavities in the frozen melt formed during the evolution of gaseous products.
- Non-crystalline SiO_2 was detected using IR whilst XRD yielded Si, Sb_2O_3 and Sb. Low intensity XRD peaks were attributed to the formation of antimony silicates and antimony silicides.
- The temperature profiles showed a decrease in the rise-time to the maximum temperature with increasing density. The burn rate and mass burn rate showed an initial increase with compaction followed by a slight decrease with increasing density. This provides further evidence that the system may involve the reaction between molten Sb_2O_3 or even Sb_2O_3 vapour and solid Si.
- There was a slight increase in the burn rate with an increase in the specific surface area of the fuel.
- Both the burn rate and maximum temperature decreased with increasing proportions of additives SiO_2 and Al_2O_3, but the decrease was greater for SiO_2. The presence of water decreased the burn rate even more than SiO_2 and Al_2O_3 and the mixtures containing 3% water failed to ignite. The maximum temperature appeared unchanged after the addition of water, but there was an increase in the induction time of the temperature profile. The effect of enhancing the reactivity of Si in the presence of moisture and oxygen could thus not be confirmed.
- The thermal conductivity of this composition increased linearly with increasing Si content.

DSC analysis of this composition (40%Si) by Rugunanan and Brown (1991, Rugunanan, 1991) yielded the following:

- An exotherm from 590-615°C with change in enthalpy of -0.53kJ/g was evident in N_2. This occurred during the temperature range for the sublimation of Sb_2O_3.
- Similarly an exotherm was evident for air between 600-680°C with a change in enthalpy of -0.74kJ/g.
- The enthalpy values which were measured were not reproducible and varied according to the mass of the sample and the heating rate used.

It thus appears that some reaction occurs between the Si and Sb_2O_3 during the sublimation of Sb_2O_3. In air the reaction is further complicated by the gaseous oxidation of Sb_2O_3.

TG analysis by Rugunanan and Brown (1991, Rugunanan, 1991) found that the reaction was incomplete as only 5% of the Si reacted with the Sb_2O_3 for pans without lids and 20% of the Si reacted for pans with lids compared with the expected 46.5%.

5.2.5 MnO_2-Si

This composition has been reported to be used for long period delays i.e. 0.6 to 12s. A ternary mixture of MnO_2-Fe-Si has been reported as providing millisecond delays (0 to 400ms) (quoted by Rugunanan, 1991).

Rugunanan (1991) found the following for this composition:

- The composition was slightly gassy and very hot.
- The thermocouple melted in all his experiments
- The measured burn rates and mass loss that were reported are summarised in Table 5-3

Table 5-3: MnO_2-Si – Burn Rates and Mass Loss as Reported by Rugunanan (1991)

Mass % Silicon	**Burn rate (mm/s)**	**% Mass loss**
20	5.0	4
30	6.6	4
40	6.6	2

5.2.6 $PbCrO_4$-Si

Rugunanan (1991) found that for 20 and 30% Si mixtures, this composition burned with a 15% mass loss and a burn rate of 7.2 and 13.0 mm/s respectively. Furthermore the gassy nature of the reaction led to shorting of the thermocouples.

6. EQUIPMENT AND EXPERIMENTAL PROCEDURES DEVELOPMENT

6.1 Planning

6.1.1 Experimental Procedures Reported in Literature

Table 6-1 summarises the experimental procedures and equipment (with the exception of thermal analysis) reported in literature as well as any problems which may have been encountered for the analysis of pyrotechnic compositions.

Table 6-1: Experimental Procedures and Equipment Reported for use in Pyrotechnic Composition Analysis

Method and Equipment	**Comments**
Charsley *et al* (1978) *Temperature Profile*: 0.1 mm Pt/Pt10%Rh glass sleeve-insulated thermocouples embedded in steel tube. Fuse ignition. Transient recorder (Data Laboratories DL 905)	
Charsley *et al* (1980) *Velocity*: Electronic timer (Venner, TSA6616) initiated by electric pulse used to ignite fuse and stopped by photo cell which detected burn through. Corrected for time response of apparatus. *Temperature Profile*: Same as for Charsley *et al* (1978).	
Davitt and Yuill (1983) *Velocity*: Nonelectric detonators initiated by Nonel Shock wave conductor.	

Method and Equipment	**Comments**
Drennan and Brown (1992a) *Temperature Profile*: Composition pressed into stainless steel channel. Ignited by starter increment and safety match. 0.05-0.3mm Pt/Pt10%Rh thermocouple. Smoothed temperature profiles using 12-point cubic spline program. *Velocity*: IR detectors triggered and stopped timing circuit.	
Hardt and Holsinger (1973) *Velocity*: Observation of flame front through high speed motion pictures or burn wire technique. Oscillographs of anode current of pyrometer. Ignition by B/$BaCrO_4$ heated nichrome or tungsten bridge wire	
Beck (1989) *Temperature Profile*: Composition pressed into stainless steel channel and ignited with a fusehead and captured with A/D card. Sample frequencies varied between 1109 and 20Hz. 0.1mm Pt/Pt10%Rh thermocouples.	Experienced signal disruption after reaching 1400°C. Attributed to electrical interference as a result of presence of molten Si as thermocouples were undamaged.
Boddington *et al* (1982) *Temperature Profile*: Composition pressed into stainless steel channels and ignited with a fusehead. Recorded using a microprocessor and computer. Signal amplification. Pt/Pt10%Rh thermocouples (0.05, 0.1, 0.2 and 0.3mm diameter). Thermocouple calibration done using British Standards 4937, 1973). Checked using melting point of zinc and gold. *Velocity*: Electronic timer (Venner TSA 6616). Photocell at end of channel stopped signal.	Found that the calculated burning velocities based on temperature profiles were generally less than the experimental results. Attributed this to the size of the thermocouples. Have proposed a method for compensating for the thermocouple size.

Method and Equipment	**Comments**
Boddington *et al* (1986, 1989) *Temperature Profiles*: Composition pressed into steel or machinable glass (Corning, Macor Glass). Pt/Pt 13% Rh thermocouples (0.1, 0.2 and 0.3mm diameter). Captured by high speed analogue to digital converter.	
Boddington *et al* (1990) *Temperature Profiles*: Composition pressed into steel cylinder with septum. Ignited with electric fuse. Used pyrometers with analogue signal. Velocity: Electric timer (Venner, TSA 6616) started by electrical pulse and stopped by signal from photocell.	Corrected for the response time of the pyrometers which lowered the observed maximum temperatures by <30K.
Al-Kazarji and Rees (1979b) *Velocity*. Photoelectric cell connected to Racal Universal Counter/Timer (no9901)	
Hedger (1983) *Velocity*: Conventional Electric Detonators	
Beck (1984) *Temperature Profile*: Composition pressed into channel. Pt/Pt 10% Rh thermocouple (0.05, 0.1, 0.2 and 0.3mm diameter) insulated with thin glass capillaries. Could not initiate using hot wires. Initiated using starter increment of 50% Mn/$KMnO_4$. Originally used digital storage oscilloscope. Replaced with Southwestern Technical Products 6809 microcomputer. Low noise DC amplifier and 12bit analogue to digital converter. Used fourth order polynomial to convert emf to temperature. Electronic CJC. Checked thermocouple calibration using melting points of pure metals and salts. *Velocity*. Used photodetectors. Caused interference in thermocouple signal. Could not measure profiles simultaneously.	Container is reusable.

Method and Equipment	**Comments**
Goodfield and Rees (1985) *Velocity*: Compressed into metal tubes. Ignited by electrically fired fuse head. Time measured with Racal Universal Counter Timer (9901). Photoelectric cell.	
Beck and Brown (1986) *Velocity*. Compared use of aluminium and polymethacrylate (Perspex) tubes.	Found that the results obtained in open laboratory system were different from those obtained from detonators in practice, i.e. Compositions which burned in the channel misfired in the detonators.
Rugunanan (1991) *Temperature Profile*: Pt/Pt 10% Rh (0.1mm diameter). Insulated with asbestos paper. Initiated with starter increment. Calibrated using melting points of Pb and Zn. PC-26A/D card. *Velocity*. IR detectors and manual computing counter clock.	
Laye (1997) *Thermal Conductivity*. Hot wire and laser flash heating techniques.	Neither were reliable.
Rugunanan and Brown (1994a,b) *Temperature Profile*. Pt/Pt 10%Rh. 0.1mm diameter. Composition pressed into stainless steel channel. *Velocity*. Same as for Beck (1985)	

6.1.2 Planned Measurements

Based on the above experiences and the objectives, it was decided to attempt to combine temperature profile capturing and burn rate measurements by embedding two temperature sensing devices along the length of the pyrotechnic column during

combustion. The compositions had to be prepared in real detonator assemblies (excluding explosive) and detonated using shock tube in an attempt to simulate the commercial system as close as possible and evaluate compositions for their ignitability using shock tube. The mixing procedures had to be standardised to prevent difference in burn rate due to mixing. The compaction of the sample also had to be standardised. The reagents would need to be characterised in terms of particle size or surface area. Complementary techniques such as XRD, XRF, SEM etc. were also to be used.

6.2 Equipment

6.2.1 Particle size and BET Measurements

A Flowsorb II 2300 supplied by Micrometrics Instrumentation for single point surface areas was used in the determination of the surface area of the powders and was completed by Serei Sefanyetso (*s.a.)*.

A Saturn Digisizer 5200v1.03 was used for the particle size analysis and was completed by *Poretech*.

6.2.2 Thermal Analysis

A Mettler Toledo TGA/SDTA 851e was used in conjunction STARe Software to do the thermal analysis of various compounds and compositions.

6.2.3 X-Ray Diffraction and Fluorescence

A Siemens D-501 XRD was used with the collection parameters contained in Table 6-2. XRF analysis was executed using a ARL9400XP+ spectrometer using the wide confidence limit program.

Table 6-2: XRD Data Collection Parameters

Radiation	CuK α
Temperature	25°C
Specimen	Flat-plate rotating (30RPM)
Power Setting	40kV, 40mA
Soller Slits	2° (diffracted beam side)
Divergence Slits	1°
Receiving Slits	0.05°
Monochromator	Secondary, graphite
Detector	Scintillation counter
Range of 2θ	4-70°
Step Width	0.04°2θ
Time per step	1.5 seconds

6.2.4 Scanning Electron Microscopy

A JEOL 840 scanning electron microscope was used unless otherwise stated.

6.2.5 Weighing of Compositions

A standard 3-digit laboratory mass balance (Precisa) was used.

6.2.6 Mixing

A box lined with polyurethane attached to rollers and a motor (Figure 6-1) (Tumbler) was used for the end over end tumbling of the compositions.

Figure 6-1: Equipment used for Tumble Mixing of Compositions (Tumbler)

6.2.7 Tube Loading and Composition Compaction

Compositions were loaded incrementally into lead tubes using a metal funnel. Consolidation was achieved by intermediate tapping of the lead tube. The lead tubes were obtained from AEL. The lead tubes had the following dimensions: ID-5mm and OD-10mm. The tube roller with forward-reverse motor and motor control box (Figure 6-2) was supplied by AEL and was used to draw down the lead tubes and compact the compositions.

Figure 6-2: Tube Roller and Motor Control Box

6.2.8 Detonator Assembly

The drawn lead tubes were cut into elements using a standard copper tube or pipe cutter. All other components used in the detonator assembly (Al tubes, antistatic cup etc.) were supplied by AEL. The detonators were crimped using a pneumatic crimper operated with N_2 gas for safety (Figure 6-3).

Figure 6-3: Crimper

6.2.9 Ignition

As mentioned previously, shock tube was used to initiate the compositions. The shock tube was initiated using a "mouse trap" (Figure 6-4) which allows for two probes to pierce the shock tube. An electric spark is generated between the probes initiating the reaction of the composition lining the shock tube. The reaction wave passes down the shock tube into the detonator at a speed of about 2000m/s and breaks the antistatic cup, initiating the pyrotechnic composition. The open end of the shock tube was inserted into a silencer consisting of a sealed plastic container filled with kitchen steel wool.

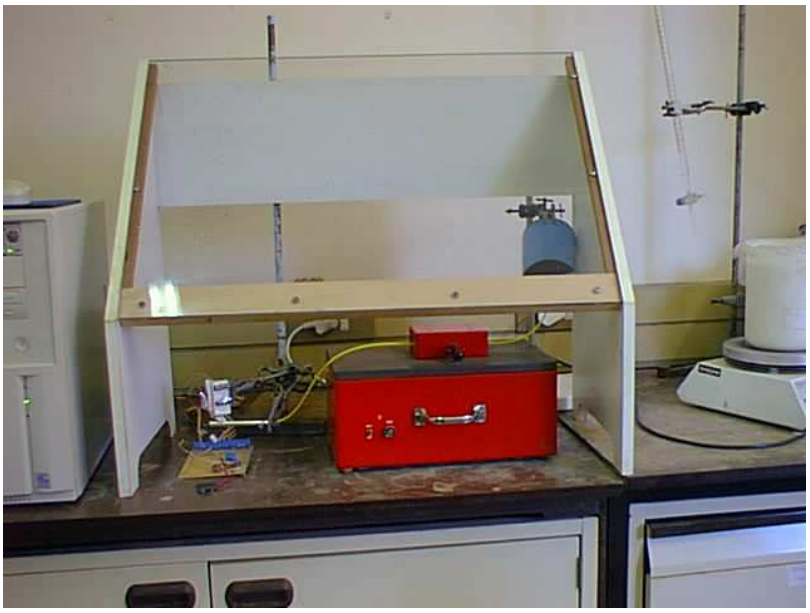

Figure 6-4: "Mouse Trap" and Silencer

6.2.10 Temperature Sensing Devices

Thermocouples were the chosen as temperature sensing device above resistance thermometers as the temperature at a point in the sample was to be monitored and not over the entire length of the sensor.

Type R (Pt/Pt 13% Rh) thermocouples were chosen due to their resistance to extreme oxidising conditions and high melting point. These thermocouples are suitable for temperature measurements up to 1600°C. They do have the disadvantages of a low sensitivity and high cost.

Thin wire thermocouples (0.38mm in diameter) were obtained from WIKA Instrumentation as it was necessary to obtain very rapid response times due to the low thermal inertia of the thin wires. An experiment to gauge the response time of the thermocouples was conducted. A thermally insulted beaker of silicone oil was heated to 196°C and the temperature was kept constant. The data acquisition was initiated (1000Hz) and then a bare thermocouple was plunged into hot oil until the signal stabilised. The data was filtered. The response time of the thermocouple was noted.

Figure 6-5 shows the thermocouple response. The response time of the thermocouple was just over 5ms.

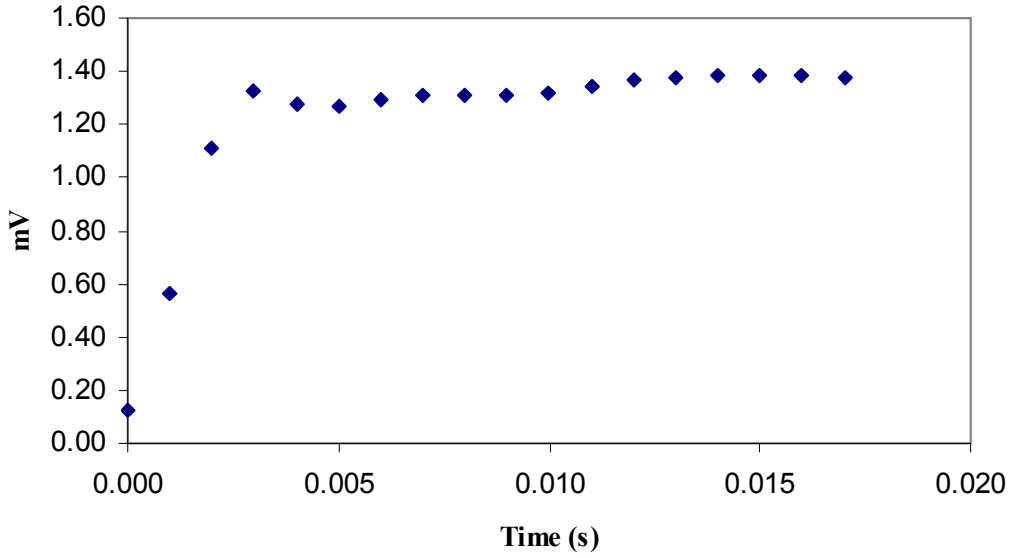

Figure 6-5: Response Time for Bare Wire Type R Thermocouple during heated Silicone Oil Experiment

Spot welding was used for the joining of the thermocouple wires due to its ease. This method has been criticised by Beck (1984) as it does not produce as strong a junction as a gas flame and also possibly introduces a thin oxide layer between the wires in the junction. Pico Technology (2001) however, recommend that welding be used as it ensures that the junction is not limited to the melting point of the solder. It is recommended for future work that the possible inclusion of the oxide layer during spot welding be investigated.

The signals were not corrected for cold junctions (CJC). Typically CJC is sensed by a precision thermistor in good thermal contact with the input connectors of the measuring instrument. The second thermocouple reading, along with the reading from the thermocouple itself is used by the measuring instrument to calculate the true temperature at the thermocouple tip. For less critical temperature measurements, Pico Technology (2001) recommend that CJC be performed by a semiconductor temperature sensor. The combination of this signal and the thermocouple signal will result the correct reading without having to record and store two temperatures (Pico

Technology, 2001). It is recommended that the current set up be modified to include CJC either via having a reference junction at 0°C before feeding the signal to the computer or preferentially installing equipment that models CJC electronically, i.e. a semiconductor temperature sensor. It would be necessary to minimise the number of junctions to reduce noise.

Due to the lack of cold junction compensation the voltage profiles cannot be converted reliably to absolute temperature profiles. It is recommended that once cold junction compensation has been added to the set up, the graph and correlation in Figure 6-6 be used for the conversion. The data points were taken from the CRC Handbook for Chemistry and Physics (1992:15-1) and a correlation and trend fitted to the data. It should be noted that a second order polynomial is used as it results in a better fit to the data than a linear regression. Linear regressions should be used for all thermocouple types excluding those based on Pt/Rh due to the sluggish voltage response at low temperatures. Pico Technology (2001) on the other hand have stated that the relationship between temperature and voltage is a complex polynomial (5^{th} to 9^{th} order). It is therefore recommended that the accuracy of the conversion expression be validated using compounds that undergo visible transitions at known temperatures, i.e. boiling of water, melting point of gold etc or to just use the tables directly.

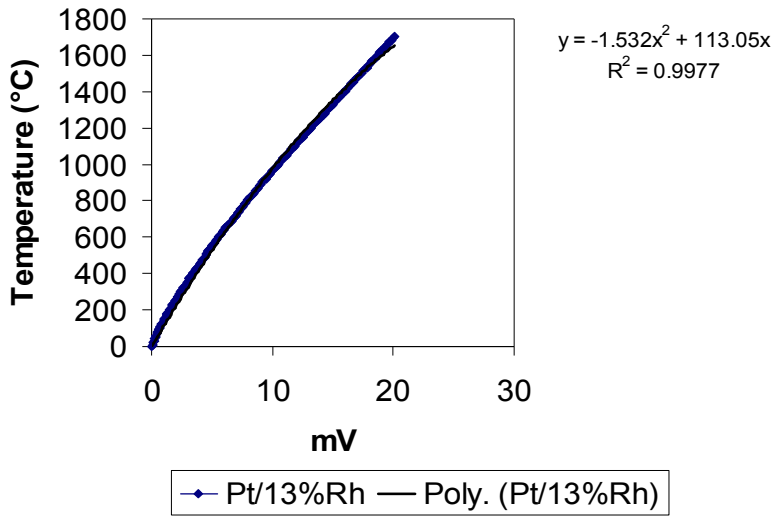

Figure 6-6: Type R Thermocouple Calibration Curve (Data taken from CRC Handbook of Chemistry and Physics, 1992:15-1)

Once temperature conversion has been completed it is recommended that the method proposed by Boddington *et al* (1982, 1986) for the extraction of kinetic data and burn velocities (Leeds Model – Appendix A) be implemented to determine this data about the compositions. However it should be noted that Boddington *et al* (1982) found that the experimental burn velocities were generally higher than those that were extracted from the temperature profiles. Another discrepancy arises in the maximum burning temperature. They attributed this to the finite size of the thermocouples and have proposed various methods to correct for these problems. It is therefore recommended for future work that the effect of thermocouple size be investigated and corrected for using the methods prescribed by Boddington *et al* (1982 and 1986). This phenomenon was also observed by Beck (1984) who also applied the correction.

The possibility of using pyrometry should be investigated for reactions where the temperature exceeds 1700°C, bearing in mind that Laye (1997) has mentioned the problems encountered with spatial convolution of the pyrometer signal and Rugunanan (1991) has mentioned that there are problems associated with changes in the emittance of the sample during combustion and interference from product vapours.

The thermocouples were insulated with thin glass sleeves and the thermocouples held in place by taping them to polystyrene (Figure 6-7).

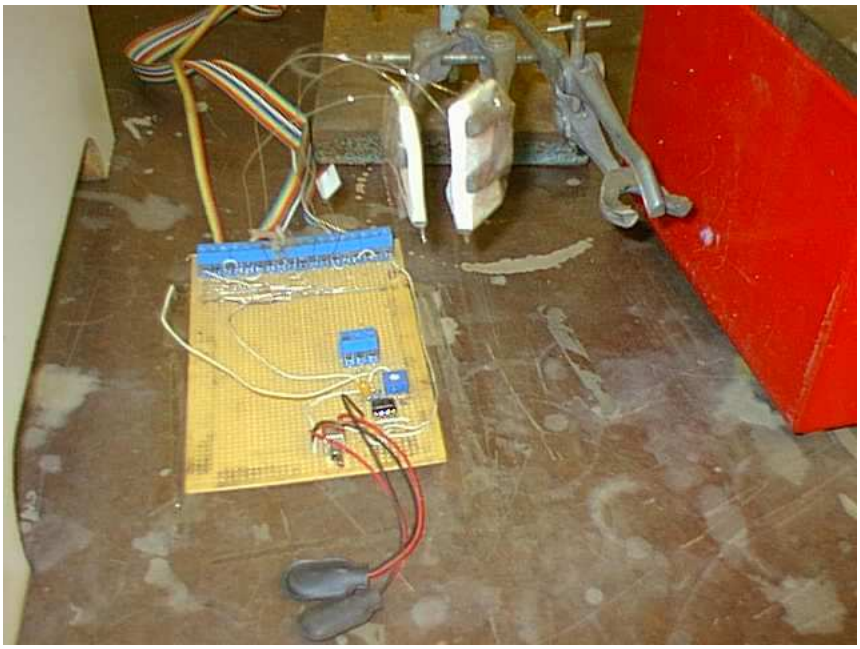

Figure 6-7: Thermocouples and Electronic Interface

6.2.11 Electronic Interface

The electronic interface between the thermocouples and computer was designed and soldered by Dr S. van der Walt and shown in Figure 6-8. The connections were earthed and the thermocouples could be easily interchanged for other thermocouples. An amplifier was added to the first differential channel, but was found to be unnecessary as the data acquisition card had onboard gains of 10, 100 and 1000.

6.2.12 Data Acquisition

An Eagle PC30F (330KHz) card was the chosen data acquisition card for the Intel PIII 650MHz computer (Figure 6-8). The card has 16A/D single ended (8 differential) inputs and 4D/A outputs. Software was developed by Dr S. van der Walt using Delphi. The software allowed for manipulating the sampling frequency, total length of data acquisition time, mode of triggering (manual or electronically), the number of channels being used, and the calibration of the thermocouples should they be changed.

The program also included a data filter which simulates a low-pass filter circuit using a Gaussian filter routine, graphing routines and the ability to extract data to Excel for further manipulation.

Figure 6-8: Data Acquisition Computer

6.3 Experimental Procedures

6.3.1 Weighing and Tumble Mixing of Compositions

All compositions were carefully weighed into large polytops noting the relevant masses. The polytops were then sealed with a lid and then further sealed with laboratory sealing film (parafilm). The polytops were placed within the cavities cut into the polyurethane contained in the tumbler. The tumbler was sealed and the motor switched on. The compositions were tumble mixed for 4 hours unless otherwise stated.

6.3.2 Brush Mixing

After tumbling some of the compositions were brush mixed through an earthed dry sieve. This was done in order to break up the agglomerates and improve mixing.

6.3.3 Visual Interpretation of Burn Characteristics

The propagation and burning characteristics of the mixtures were evaluated using the following "screening" procedure. A rectangular piece of paper was folded along its length and placed on a fire resistant tile. The tile was then placed in the fume cupboard. A small amount (less than 1 g) of the mixture being tested was placed along the fold of the paper from the middle of the paper until the end (Figure 6-9). The paper was lit on the corner of the paper furthest from the mixture and left to burn.

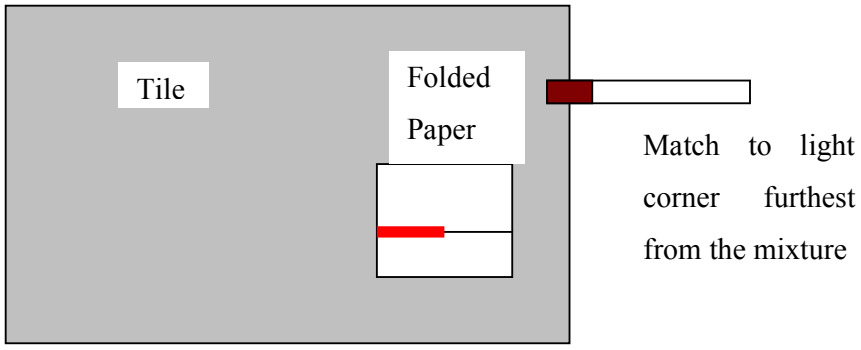

Figure 6-9: Schematic Diagram of Visual Evaluation of the Burn Characteristics of Compositions

The burnt residue was then disposed of in water.

6.3.4 Initial Tube Loading

Initially it was thought to be unsafe to drill into the compositions directly, so a die was designed for a laboratory press to compact the powder into a copper tube (ID 4.35mm) which was already in the aluminium tube (OD 7.5mm). The die is shown in Figure 6-10. The copper tube was placed in the aluminium tube and small holes were

drilled into the tube to allow for insertion of the thermocouples. The tubes were placed in the centre hole of the die and a thin layer of the powdered composition poured into the aluminium tube. The powder was then compacted and the process repeated till the first thermocouple opening was reached. The thermocouple was inserted and covered with powder and once again the powder carefully compacted. The process was repeated until the copper tube was filled. The reason for the incremental compaction of the powder is due to the hydrostatic nature of powder i.e. when a powder is pressed, compaction occurs by particle rearrangement by sliding and by deformation and or fracture. Initially the forces resisting compaction are those holding the agglomerates together augmented by friction between the particles and the die wall. As the pressure increases, the compaction force overcomes the force acting at interparticle contacts (Veale, 1972:139).

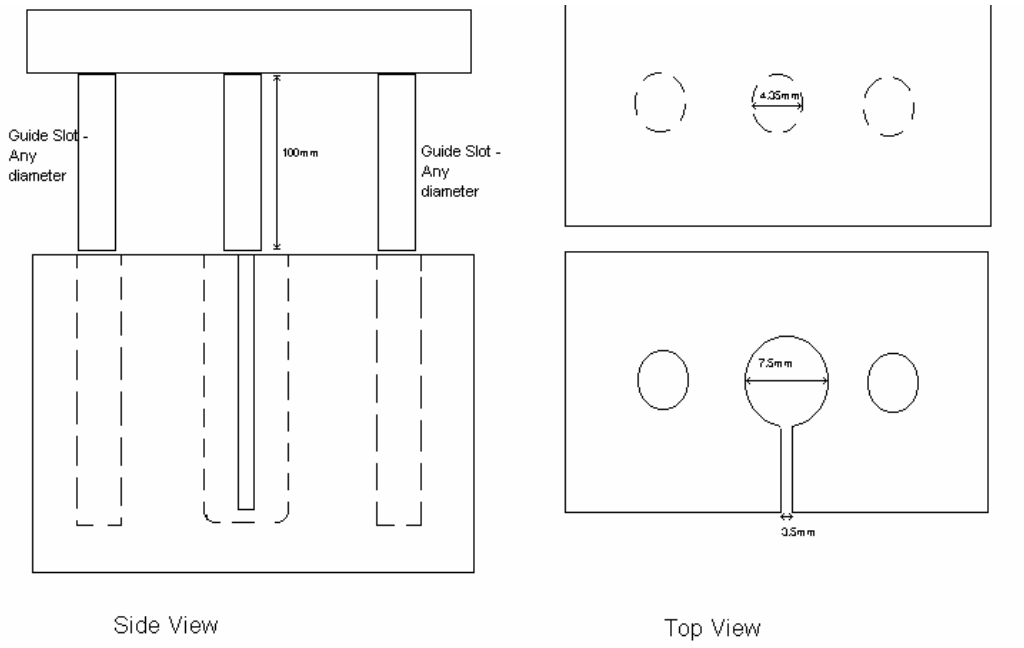

Figure 6-10: Simplified Diagram of Die for the Laboratory Press

However it was found that this method did not work in practice for the following reasons:

- The laboratory press' pressure range was incorrect for the application. A smaller punch would have been more practical.

- The aluminium tubes would bend and stick in the die making removal without damage difficult.
- The thermocouples kept falling out during the powder compaction and the powder would pour out of the openings.
- The powder would break through the bottom of the aluminium tubes.
- The safety of the process was questioned – the powder was loaded and any powder along the sides of the copper tube would undergo huge amounts of friction as the die was lowered (friction and impact ignite the compositions).
- The process was difficult to control for reproducibility.

For these reasons it was decided that it would be better to drill into the aluminium tubes after the detonators were already assembled.

6.3.5 Lead Tube Rolling

The lead tube was crimped shut at one end using a pair of pliers making sure that the end still passed through the first opening in the tube roller. The lead tube was then clamped and a funnel inserted into the open end. The tube was tapped during the incremental filling of the tube with the composition to aid with settling of the powder and help overcome some of the wall friction. Once full, the open end of the lead tube was carefully crimped shut.

The lead tube was then fed through the tube roller. The roller consisted of a number of openings. Each opening corresponded to a different diameter and these decreased in size sequentially. The lead tubes were fed twice to each opening (turning 90° before the second pass) in the prescribed order and drawn down, thereby compacting the powder contained within the tube. It was found that the tube roller left lead trimmings along the sides. These were carefully cut off using a Stanley knife before feeding to the next opening. Figure 6-11 shows the effect of drawing down a lead tube.

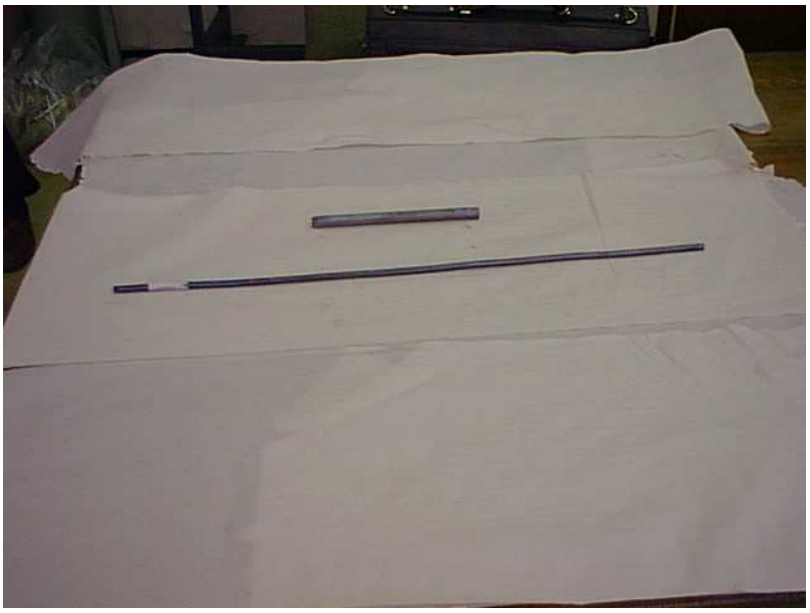

Figure 6-11: Effect of Feeding a Lead Tube through the Tube Roller

The effect of compaction and initial mixture density was not investigated during this investigation due to the nature of the preparation of the delay elements i.e. difficulty to control amount of compaction with tube roller. It is recommended that the effect of compaction be investigated by varying the consolidation pressure, noting the initial density and measuring the burn rate. It would be beneficial to measure the density of the product in order to determine the effect of absorbed gas impurities as a function of initial densities (Section 4.1 vii) and compare these results to compositions based on reactants which have been preheated to remove the absorbed gases.

6.3.6 Detonator Assembly

The 45mm elements were cut from the lead tubes using a pipe cutter. The core diameter of each element was noted. As mentioned previously the core diameter has an effect on the burn speed (Section 4.1 ix). The element was pushed gently to the bottom of the lead tube, followed by the antistatic cup. The antistatic cup prevents friction and the development of static between the end of the shock tube and the composition so as to prevent premature initiation of the composition during handling. Also, it was necessary to include the antistatic cup so as to keep as close to the

commercial system as possible. A hollow cylindrical rubber spacer was fed next, through which the shock tube had been fed. Figure 6-12 depicts the actual sequence of components which are included into a detonator.

Figure 6-12: Detonator Assembly – Component Sequence

The detonators were then carefully crimped to stabilise the position of the components in the detonator and to seal the detonator. In industry the detonators are crimped twice, but in the laboratory the final crimp was omitted as it was found that due to the fact that a gas cylinder was used, the crimping pressure of the final crimp could not be properly controlled. This led to a number of shock tube failures i.e. the shock tube bursts just before the final crimp and the wave fails to travel any further. A completed detonator assembly is shown in Figure 6-13.

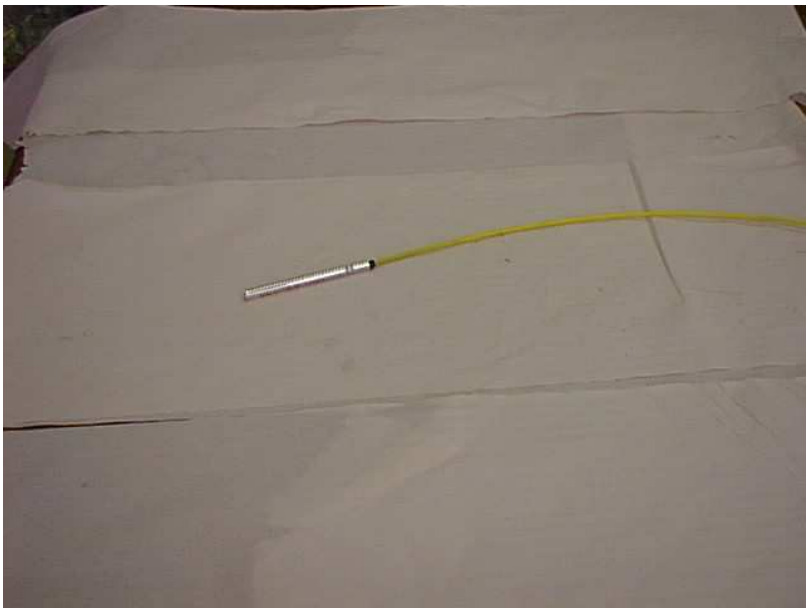

Figure 6-13: Completed Detonator Assembly

6.3.7 Preparation of Detonators for Combustion

The sealed detonator assemblies were then marked for drilling. A thin sharp implement was used with a die to ensure that the detonators were always drilled at the same place and the holes were the same distance apart. The detonator was clamped and a manual hand drill was used to slowly drill in the holes in the prescribed marks. The drilling was done slowly so as to minimise the build up of heat and friction and to control the depth of the hole. The hole was drilled until the composition was reached. A shortcoming of using this manual method is that it produces some error in the hole size and positioning, hence the reason why all burn rates are only reported to the closest mm/s despite the accuracy and dynamics of the other equipment.

As shown in Figure 6-8 the detonator assembly was clamped and the thermocouples inserted into the openings and secured. The placement of the thermocouples is important. Surface or contact applications are inaccurate due temperature influences from the surroundings. Beck (1984) found that by placing the thermocouple junction near the side of the sample channel instead of in the centre lowered the maximum temperature by 50°C. The thermocouples were consistently placed at the side of the

detonator to allow for reproducibility of the temperature profiles, but in future when the temperature profiles are used to determine the kinetic parameters, this effect should be borne in mind. The shock tube was placed in the "mouse trap" and the free end fed into the silencer. The safety screen was also placed in position.

6.3.8 Measurement of Temperature Profiles

The sampling frequency was set at 580Hz for all the measurements with a gain of 1000. It was decided not to have the data acquisition triggered automatically once a threshold temperature had been achieved as Rugunanan and Brown (1994a) found that the triggering level and lack of a meaningful zero value led to the non-reproducibility of temperature profiles. The software was triggered manually and once data acquisition started, the "mouse trap's" electric pulse was initiated manually. The wave travelled down the shock tube and into the detonator assembly to break the membrane of the antistatic cup and initiate the composition. The propagation characteristics of the wave as seen by the wave travelling from thermocouple opening to thermocouple opening was noted. In general the data acquisition period was fixed at 40s, after which the data was saved as a text file for import to Excel for further manipulation. Figure 6-14 contains examples of detonator assemblies that ignited and burned. The thermocouples were visually checked for damage or adherence of combustion products or molten lead. If there was lead or material presence the tips were cut and rejoined.

Figure 6-14: Examples of Detonator Assemblies that Ignited and Burned

It should be noted that Charsley *et al* (1978) found considerable variation in their temperature profiles which they attributed in part, to the uneven nature of the flame front and variations in the microscopic environment of the thermocouple junction. A further avenue of investigation is the derivation of the power function from the temperature profile (Charsley *et al*, 1978). Rugunanan and Brown (1994a, Rugunanan, 1991) noted that the following variables cause the irreproducibility of temperature profiles:

- Inconsistent mixing and packing of the sample
- Variation in the size and placement of the thermocouple junction and
- The triggering level and lack of a meaningful zero value (triggered when temperature exceeded 70°C).

Initially it was thought to embed a thin wire between the antistatic cup and the delay element. As the shock wave passes from the shock tube to the composition, the wire would be destroyed and be used to trigger the data acquisition. This option was ruled out due to the difficulty of embedding the wire in the detonator and connecting it simultaneously to the electronic interface as well the unknown effect of releasing pressure before wave ignites the composition, i.e. the shock tube may not be able to initiate the composition due to the punctured hole ahead of the composition. Furthermore, the wire would need to be replaced after every experiment and will increase cost and time between tests.

A short coming of this measuring method used in this investigation is the puncturing of the detonator assembly. Puncturing of the detonator assembly has three possible effects: It affects the pressure, the temperature attained and the actual burn rate which is observed. This can be seen from the literature. Nosgrove *et al* (1991) have stated that a delay detonator puncture significantly changes the burn rate (up to 40%). In the event of a gassing system, the direction of the gas flow has an effect. The local flame speed also varies as it passes down the delay element. Gassing also influences the flame temperature (Nosgrove *et al*, 1991). Pressure also has an effect on the burning rate (McLain, 1980:58). In Figure 6-14 there is evidence that some material has flowed out of the first hole as a result of gassing. It may perhaps by necessary to modify the setup using Perspex tubes and use photocells or a high speed camera to determine the burn rate. Alternatively the procedure used for the data acquisition

could be triggered by an electric input from the "mouse trap". This will only require puncturing the detonator once for the insertion of the thermocouple (i.e. effect is not felt until wave passes the hole at the downstream end).

6.3.9 Disposal of Detonators

After burning, the detonators were allowed to cool down. The shock tube was cut off. Both the shock tube and the detonator were returned to AEL for disposal. As mentioned previously the combustion products were not analysed during this investigation. It is thus recommended that XRF, XRD, IR and SEM be considered to analyse the combustion products in future.

6.3.10 Numerical Processing of the Data

The measured signal was very noisy because of:

- Mechanical movement of the thermocouple during combustion.
- Interference from the electrical wiring and heavy electrical equipment in the area.
- Turbulence in the molten and gaseous products.

It is recommended that for future work, the occurrence of noise be minimised by shielding the cables.

The "noisy" data was imported into Excel where a template had been drawn up to immediately filter and graph the data. A first order digital filter i.e. $y_n = (1-a)y_{n-1} + ax_n$ was applied to the data (Stephanopolous, 1984:611). The effect of varying the filtration parameter (a) on a 25% Type 3 Si – $PbCrO_4$ composition is illustrated in Appendix B. The value of a affects the maximum voltage attained, but has very little effect on shifting the graphs along the time axis. It was therefore decided that the value of the filtration parameter (a) be fixed at 0.01. The effect of varying a should be borne in mind when extracting kinetic data from the temperature profiles. It would perhaps be necessary in future to investigate different methods of data smoothing. Another reason is that the smoothness of the temperature profile is critical for the subsequent kinetic and thermochemical analysis of the temperature

profiles. Boddington *et al* (1982) have proposed the use of a convolution process based on a least mean squares fit of 25 consecutive points to a second order polynomial. Drennan and Brown (1992b) used a 12-point cubic spline program.

The burn rate was then determined from the temperature profiles as follows:

- The time when the voltage reached 1mV for the first thermocouple was noted.
- The time when the voltage reached 1mV for the second thermocouple was noted.
- The difference between the two times was taken as the time it took for the wave to travel between the first and second thermocouple.
- The distance between the two thermocouples was measured (centre to centre) and
- Thus the burn rate equals the distance over time.

Using the correlation proposed in Section 6.2.10, a voltage of 1mV corresponds to temperature of 115°C. However when comparing the 1.2mV obtained during the heating of the silicone oil to 196°C, it can be seen that the correlation does not yield 196°C, but yields a value of 138°C. This discrepancy may be attributed to the lack of CJC. As mentioned in Section 6.2.10, calibration of the thermocouples are to be conducted using salts with known transition temperatures.

6.3.11 General Safety Precautions

The weighing, brush mixing, burn rate measurements etc. of the compositions were completed behind a thick (8mm) polycarbonate screen. The weighing of the compositions and brush mixing was always done on top of an earthed copper sheet. Personal protective equipment such as leather gloves, lab coats were always worn. Ear muffs were worn during shock tube initiation should a failure have occurred.

6.3.12 Recommended Further Investigations and Complementary Experimental Techniques

The feasibility (availability, safety, cost and time) of augmenting the above procedures and equipment with the procedures and equipment which follow for the investigation of the combustion wave should be investigated:

- The use of time-resolved XRD to monitor when components melt and new crystals are formed. This method has been used successfully by researchers of SHS reactions to identify the composition of chemical phases that appear at a particular moment during the reaction (Varma, 2000).
- The use of quenched samples and SEM to analyse the microstructure. This method has been used to study the way solid rocket fuel burns. A burning sample is dropped into a pool of liquid Ar thereby freezing the reaction before all the starting components have reacted. The quenched sample is then sliced into thin layers and the microstructure analysed using SEM (Varma, 2000).
- The use of a high speed digital video camera that peers through a microscope to observe the microscopic conditions along the combustion front. Varma (2000) have used this technique to great success in evaluating combustion synthesis reactions. This would entail encasing the pyrotechnic material in glass tubes. An added bonus of this set up is that the velocity of the wave can also be determined as the camera has a known shutter speed and the distance the wave has travelled between photographs is known.
- The use of the apparatus designed by AEL to measure pressure during combustion.
- The use of a probe technique (described by Beck, 1984 and Rugunanan, 1991) or hot wire and laser flash heating techniques (Laye, 1997) to measure the thermal conductivity of the mixtures. It should be borne in mind that Laye (1997) has stated that the hot wire and laser flash heating techniques have not rendered satisfactory results.

6.4 Reagent Properties

6.4.1 Silicon

The properties and supplier of the types of Si which were used have been summarised in Table 6-3.

Table 6-3: Silicon Properties and Supplier

Silicon Type	**Supplier**	**Properties**
Type 1	AEL	0.73m^2/g, 28.11µm (standard deviation= 0.39)
Type 2	AEL	2.44m^2/g 12.7µm (standard deviation = 0.15)
Type 3 (12hr import)	AEL	6.39m^2/g 3.53µm (standard deviation = 0.03)
Type 4 (40hr import)	AEL	8.33m^2/g 1.84µm (standard deviation = 0.06)
Type 5 (Dust)	AEL	3.63m^2/g, 9.43µm (standard deviation = 0.22)

6.4.2 Oxidants

Table 6-4 contains a summary of the properties and supplier or methods of preparation of the oxidants which were used.

Table 6-4: Oxidant Properties and Supplier or Method of Preparation

Oxidant	**Supplier or Method of Preparation**	**Properties**
$BaSO_4$	Metallgesellschaft (Pty) Ltd but obtained via AEL	Non-toxic (lethal dose 15g/kg body mass). 99% $BaSO_4$. Retained on 63µm sieve. pH within 8.5-9.5 in aqueous slurry. 0.8-1.3m^2/g. Tapped volume within 55-65ml/100g (AEL Raw Material Specification, 1994). 0.85m^2/g
Pb_3O_4	AEL	0.89m^2/g
Fe_2O_3	Bayer	Spherical, 0.09µm particles, pH within 5-8 in aqueous slurry. 0.002% sieve residue for 0.045mm mesh (Bayer's Paint Shade Card Brochure, s.a.). 0.70m^2/g

Oxidant	**Supplier or Method of Preparation**	**Properties**
MnO_2	Delta EMD	90% is below 70μm. 30.2m^2/g. pH in aqueous slurry – 7.2 (Delta EMD General Certificate, 2000). 15.60m^2/g
$PbCrO_4$	Rolfes Pigments	Middle Chrome L-GXD. 16.70m^2/g
V_2O_5	Rhombus Vanadium Mine	2.4m^2/g
Fe_3O_4	Bayer	0.85m^2/g
$Cu(SbO_2)_2$	Precipitated (Sefanyetso, *s.a.*)	A detailed description of the analysis of this compound follows this Table.
$CuO.Fe_2O_3$	Precipitated (Sefanyetso, *s.a.*)	
$CuO.MnO_2$	Precipitated (Sefanyetso, *s.a.*)	
$CuO.V_2O_5$	Precipitated (Sefanyetso, *s.a.*)	
Sb_2O_3	Antimonox Red Star Associated Additives	3.3m^2/g
Cu_2O	Merck	
CuO (1)	Merck	
CuO (2)	Precipitated from analytical grade $CuSO_4.5H_2O$ and NaOH	
CuO (3)	Foaming Technique (Labuschagne, *s.a.*)	
$(BiO)_2CO_3$	Merck	
ZnO	Merck	
Nanocat® Iron Oxide	Mach I	Amorphous. 250m^2/g, 0.05g/ml bulk density and 3nm (Mach I Product Bulletin, 1995)

$Cu(SbO_2)_2$ Characterisation (Ricco et al, 2002)

As a result of its use in further experimentation and the nature of its preparation, $Cu(SbO_2)_2$ was characterised in detail. The X-Ray Diffraction (XRD) patterns obtained for this oxidant as well as Sb_2O_3 is shown in Figure 6-15. Strangely, the XRD pattern does not correspond to any compound which can be found in the Powder Diffraction File (2000) (PDF 1-50 + 70-88) which is available from the International Centre for Diffraction Data – Newton Square, P.A. despite the compound being known.

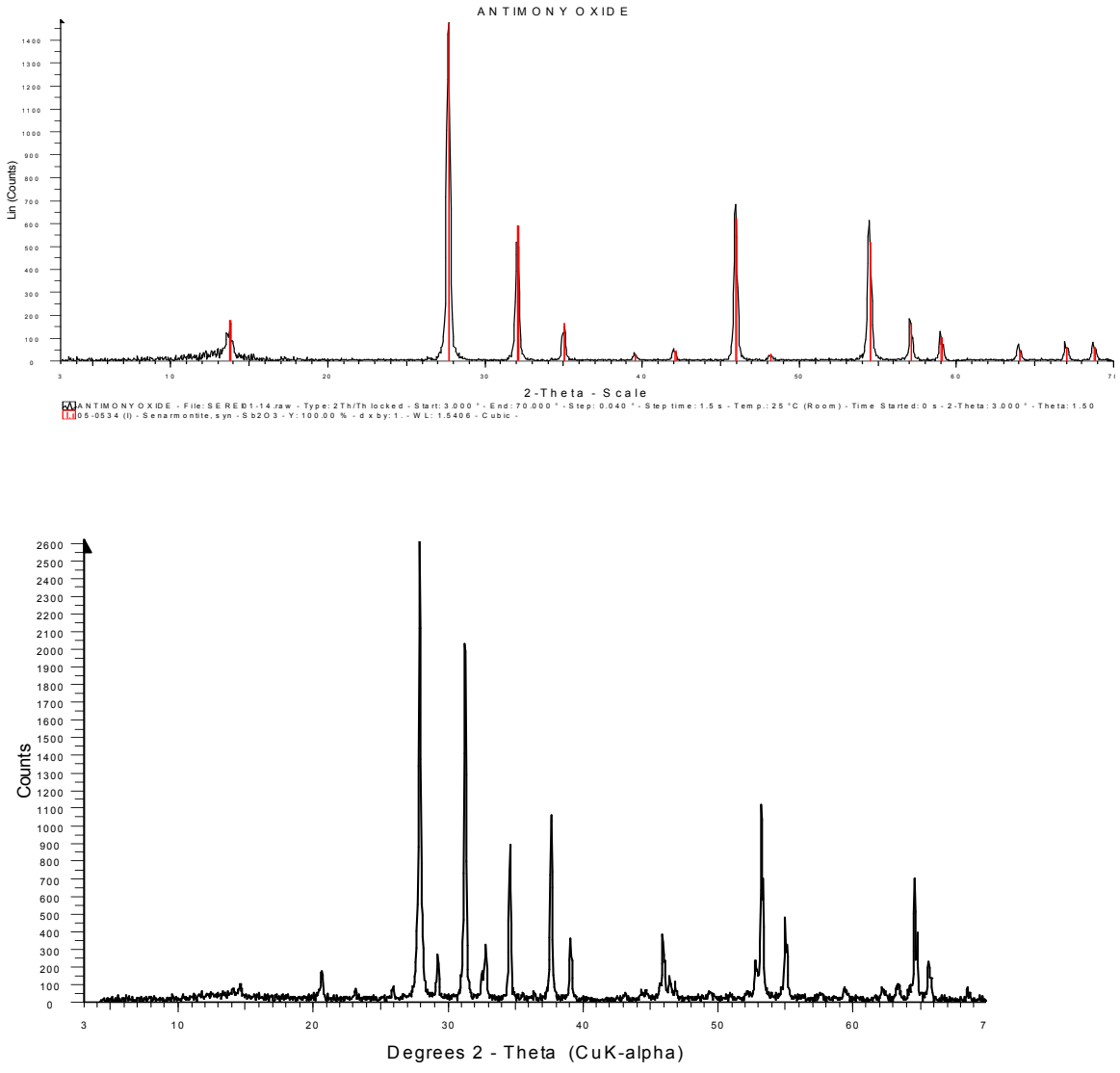

Figure 6-15: XRD Patterns for Sb_2O_3 and $Cu(SbO_2)_2$ respectively

X-Ray Fluorescence (XRF) analysis of the compound and Sb_2O_3 was done by pressing large amounts of the powder in a powder briquette. The results are summarised in Table 6-5. Two samples of the powder were produced to confirm reproducibility of the samples.

Table 6-5: XRF Analysis of $Cu(SbO_2)_2$

%	Sb_2O_3	$CuO.Sb_2O_3$ (1:1)	CuO-Sb_2O_3 (1:1)
Sb_2O_3	97.7	77.7	76.1
CuO	n/d	20.9	20.4

Furthermore, Figure 6-16 is the infrared (IR) scan which was obtained for this compound, CuO and Sb_2O_3. As the spectra for all three are different, it indicates that the compound was indeed formed and was not merely a mixture of Sb_2O_3 and CuO which would have precipitated.

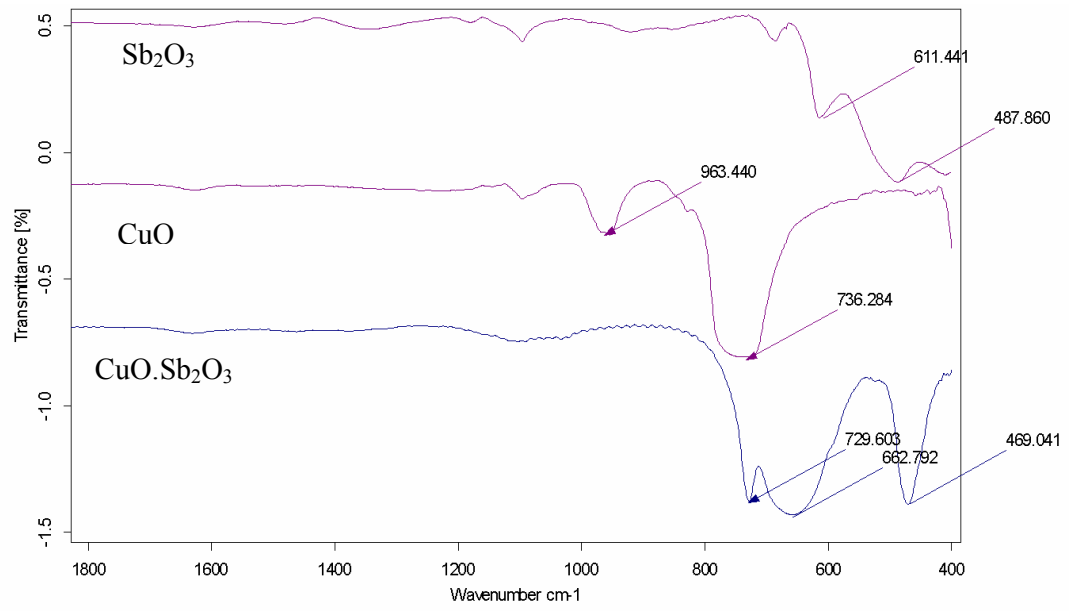

Figure 6-16: IR Scans of CuO, Sb_2O_3 and $Cu(SbO_2)_2$

A particle size analysis of the compound is still to be completed, but BET showed that the compound had a surface area of $9m^2/g$.

Scanning Electron Microscopy (SEM) (Figure 6-17) revealed agglomerated flat particles.

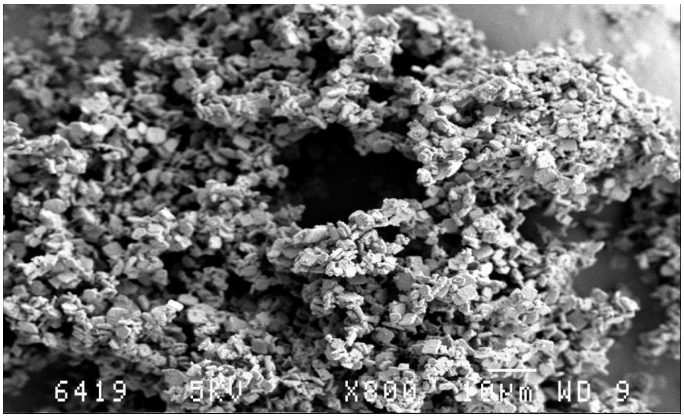

Figure 6-17 SEM Photo of $Cu(SbO_2)_2$

Figure 6-18 shows the results of the TGA/SDTA analysis of the compound. The compound shows exothermic peaks at 460°C and 541°C heated in an air atmosphere. These peaks are not evident in the SDTA/TGA scans of CuO and Sb_2O_3 (endothermic peaks at 990°C for CuO and 648°C and 950°C for Sb_2O_3). This once again indicates that the compound is not purely a mixture of copper oxide and the antimony oxide.

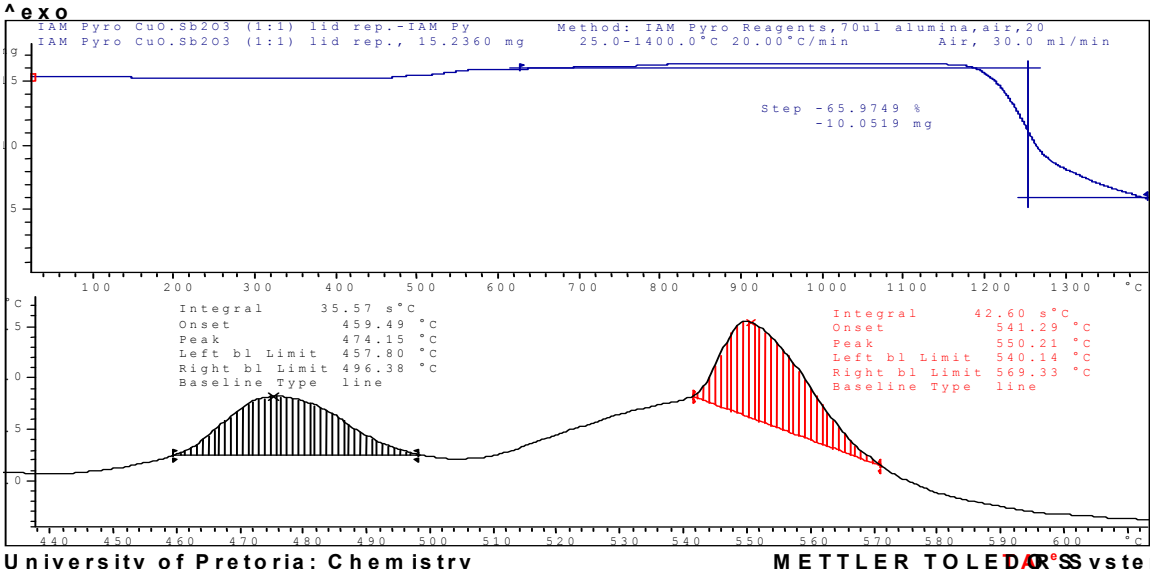

Figure 6-18: TGA/DTA of $Cu(SbO_2)_2$

6.4.3 Additives

Table 6-6 contains a summary of the suppliers and properties of the additives which were used.

Table 6-6: Additive Properties and Suppliers

Additive	**Supplier**	**Properties**
Aluminium Powder	Zimalco (Pty) Ltd	Supramex 2000. Uncoated (natural oxide coat present). 99.5% Al, 95% minimum to pass 106µm sieve and 50% minimum to pass 45µm sieve (Zimalco - Material Safety Data Sheet, s.a)
Nanocat® Iron Oxide	Mach I	Amorphous. 250m^2/g, 0.05g/ml bulk density and 3nm (Mach I Product Bulletin, 1995)
Fumed Silica - Aerosil 200	Degussa	
Wacker® Fumed Silica – HDK20	Wacker-Chemie - Chemimpo	
Fumed Alumina	Degussa	
Fumed Titanium Dioxide	Degussa	
Ultrasil VN3	Degussa	
Nanocat® A Iron Oxide	Mach I	

All other reagents have been described in their relevant section.

7. ALTERNATIVE OXIDANTS

7.1 Thermochemistry of Various Oxidants and Silicon

In order to determine which reactions may possibly occur with silicon as fuel, the heat of reaction, adiabatic temperature and free energy for various proposed reactions were calculated as follows:

- The reactions were assumed to be adiabatic and all calculations were based on complete conversion.
- All relevant data was taken from
    - *JANAF Thermochemical Tables* (1971)
    - Liley, Reid and Buck (1984) Physical and Chemical Data in *Perry's Chemical Engineers' Handbook* and
    - Barin (1989) *Thermochemical Properties of Inorganic Substances*
- The heat of reaction at 298K based on the moles of silicon was calculated by $\Delta H_R = \Delta H_{f,products} - \Delta H_{f,reagents}$. Where ΔH_R is the heat of reaction at 298K (kJ/mol Si), $\Delta H_{f,products}$ is the heat of formation of the respective product (kJ/mol Si) at 298K and $\Delta H_{f,reagents}$ is the heat of formation of the respective reagent (kJ/mol Si) at 298K
- The adiabatic temperature of each reaction was calculated iteratively assuming that all the available energy liberated by the reaction at 298K is available to raise the temperature of the products which leave at the temperature of the reaction. The phase changes are accounted for.

A sample calculation is presented in Appendix C.

The calculated heats of reaction, adiabatic temperature and free energy for all the oxidants with silicon as fuel are given in Table 7-1.

Table 7-1: Calculated Thermochemical Reaction Properties of Various Oxidants with Silicon as Fuel

System	**$\Delta H_{R\ 298K}$ (kJ/mol_{Si})**	**$T_{adiabatic}$ (K)**	**ΔG_{298K} (kJ/mol_{Si})**	**Fuel:Oxidant (Mass ratio)**
V_2O_5 – Si System				
$2V_2O_5 + 3Si \rightarrow 3SiO_2 + 4VO(g)$	-446	2398	-443	0.23
$V_2O_5 + Si \rightarrow SiO_2 + V_2O_3$	-569	1910	-566	0.15
$2V_2O_5 + Si \rightarrow SiO_2 + 2V_2O_4$	-644	1762	-635	0.08
$2V_2O_5 + 5Si \rightarrow 5SiO_2 + 4V$	-287	2166	-285	0.39
Sb_2O_3 – Si System				
$2Sb_2O_3 + 3Si \rightarrow 3SiO_2 + 4Sb(s)$	-431	3657	-434	0.14
$2Sb_2O_3 + 3Si \rightarrow 3SiO_2 + 2Sb_2(g)$	-277	1200	-297	0.14
$2Sb_2O_3 + 3Si \rightarrow 3SiO_2 + 4Sb(g)$	-78	1114	-132	0.14
$2Sb_2O_3 + Si \rightarrow SiO_2 + 2SbO(g)$	323	-	-	0.05
MnO_2 – Si System				
$2MnO_2 + Si \rightarrow SiO_2 + 2MnO$	-648	1350	-659	0.16
$MnO_2 + Si \rightarrow Mn + SiO_2$	-394	1416	-385	0.32
Fe_2O_3 – Si System				
$2Fe_2O_3 + Si \rightarrow SiO_2 + 4FeO$	-332	1408	-386	0.09
$2Fe_2O_3 + 3Si \rightarrow 3SiO_2 + 4Fe$	-357	1155	-358	0.26
Fe_3O_4 – Si System				
$Fe_3O_4 + 2Si \rightarrow 2SiO_2 + 3Fe$	-353	1139	-350	0.24
$2Fe_3O_4 + Si \rightarrow SiO_2 + 6FeO$	-300	1046	-329	0.06

The most thermodynamically favourable reactions have been highlighted in each instance. These mass ratios were used in the preparation of compositions for DTA/TGA analysis. These experiments and their results will be discussed by Sefanyetso (*s.a.*).

It was decided to repeat the above calculations with tungsten as fuel instead of silicon as AEL had expressed that perhaps in the future they would like to experiment with replacing the silicon with tungsten. The results have been summarised in Table 7-2.

From Table 7-2 it can be deduced that tungsten is not as energetic as silicon as a fuel. Tungsten has been used in the past. Charsley *et al* (1978) analysed the thermal properties and temperature profiles of mixtures of tungsten and potassium dichromate. Further work on this system was done by Boddington *et al* (1982 and 1986). In future it would perhaps be necessary to evaluate alternative fuels. Alternative fuels could include Zn, Fe, Mn, Mo. Tribelhorn, Venables and Brown (1995) have studied the use of Zn-fuelled binary compositions with oxidants such as PbO_2, Pb_3O_4, PbO, BaO_2, SrO_2 and $KMnO_4$, but have found it to be unsuitable for delay applications due to the gassy nature of the reactions. Spice and Staveley (quoted by Drennan and Brown, 1992a) have studied Fe-fuelled binary compositions with oxidants such as BaO_2 and $K_2Cr_2O_7$. Drennan and Brown (1992a) studied Mo/Mn-fuelled binary compositions with oxidants such as BaO_2 and SrO_2.

Table 7-2: Calculated Thermochemical Reaction Properties of Various Oxidants with Tungsten as Fuel

System	**$\Delta H_{R\ 298}$ (kJ/mol_W)**	**$T_{adiabatic}$ (K)**	**ΔG_{298} (kJ/mol_W)**	**Fuel:Oxidant (Mass ratio)**
V_2O_5 – W System				
$2V_2O_5 + 3W \rightarrow 3WO_2 + 4VO(g)$	-81	850	-76	1.52
$V_2O_5 + W \rightarrow WO_2 + V_2O_3$	-204	1089	-200	1.01
$2V_2O_5 + W \rightarrow WO_2 + 2V_2O_4$	-279	983	-268	0.51
$2V_2O_5 + 5W \rightarrow 5WO_2 + 4V$	78	-	-	2.53

System	$\Delta H_{R\ 298}$ (kJ/mol_W)	$T_{adiabatic}$ (K)	ΔG_{298} (kJ/mol_W)	Fuel:Oxidant (Mass ratio)
Sb_2O_3 – W System				
$2Sb_2O_3 + 3W \rightarrow 3WO_2 + 4Sb(s)$	-66	878	-67	0.95
$2Sb_2O_3 + 3W \rightarrow 3WO_2 + 2Sb_2(g)$	88	-	-	0.95
$2Sb_2O_3 + 3W \rightarrow 3WO_2 + 4Sb(g)$	287	-	-	0.95
$2Sb_2O_3 + W \rightarrow WO_2 + 2SbO\ (g)$	688	-	-	0.32
MnO_2 – W System				
$2MnO_2 + W \rightarrow WO_2 + 2MnO$	-283	1613	-292	1.06
$MnO_2 + W \rightarrow Mn + WO_2$	-29	447	-19	2.11
Fe_2O_3 – W System				
$2Fe_2O_3 + W \rightarrow WO_2 + 4FeO$	34	-	-	0.58
$2Fe_2O_3 + 3W \rightarrow 3WO_2 + 4Fe$	8	-	-	1.73
Fe_3O_4 – W System				
$2Fe_3O_4 + W \rightarrow WO_2 + 6FeO$	12	-	-	0.40
$Fe_3O_4 + 2W \rightarrow 2WO_2 + 3Fe$	65	-	-	1.59

7.2 Preliminary Experiments

7.2.1 Visual Evaluation of the Burn Characteristics of Various Oxidants

Experimental

The oxidants and mass ratios used in the preparation of the compositions are summarised in Table 7-3. All the compositions were prepared using type 4 silicon.

Table 7-3: Oxidants and Mass Fractions Silicon used for Visual Evaluation of Burn Characteristics

Oxidant	**Mass Fraction Si**	**Oxidant**	**Mass Fraction Si**
Sb_2O_3	0.12	CuO (2)	0.16
$PbCrO_4$	0.15	CuO (3)	0.16
Fe_2O_3	0.08	$CuO.Fe_2O_3$	0.20
Fe_3O_4	0.06	$CuO.Sb_2O_3$	0.14
MnO_2	0.14	$CuO.V_2O_5$	0.25
V_2O_5	0.07	$CuO.MnO_2$	0.21
Melamine	0.83	$Bi_2(CO_3)_3$	0.07
Cu_2O	0.09	ZnO	0.15
CuO (1)	0.16		

All the compositions were accurately weighed and tumbled gently end over end for 2 minutes. The propagation and burning characteristics of the mixtures were visually interpreted using the procedure outlined in Section 6.3.3.

Results and Discussion

The visual observations of the burn characteristics of the compositions are reported in Table 7-4.

Table 7-4: Visual Observations of the Burn Characteristics of Various Oxidants and Type 4 Si

Mixture	**Burn Characteristics**
Fe_2O_3	Very slow burning.
Fe_3O_4	Very slow burning with melting.
V_2O_5	Did not ignite.
$PbCrO_4$	Burned very slow.
MnO_2	Did not ignite.
Sb_2O_3	Burned fast.
CuO (1)	*Ignition required high heat. Slow burning. Combustion wave initially propagates but then self-extinguishes. Cu particles formed after burning.*

Mixture	**Burn Characteristics**
CuO (2)	***Very quick burning. Combustion wave propagates but then self-extinguishes. Cu particles formed after burning.***
CuO (3)	***Easier ignition than CuO (2), but burning is not as quick as CuO (2). Propagation of combustion wave is more stable than for CuO (2). Cu particles formed after burning.***
$CuO.Fe_2O_3$	Burned very slowly.
$Cu(SbO_2)_2$	Burned fast.
$CuO.V_2O_5$	Did not burn.
$CuO.MnO_2$	***Fast burning with stable self propagation of combustion wave.***
Melamine	Did not ignite.
Cu_2O	Ignited but self extinguished.
$Bi_2(CO_3)_3$	Burned very slowly with yellow flame front. Produced a large amount of gas.
ZnO	Did not ignite.

It appeared from these experiments that the freshly prepared CuO may be a replacement for the Pb-based systems. $CuO.MnO_2$ appeared promising for the $BaSO_4$-based system especially due to its inherent self-propagating nature. This was however subject to the results obtained from the burn rate tests.

Nature of the oxidant. The iron oxide-based systems burnt very slowly. That was expected due to the nature of the oxidant as described by McLain(1980:40) and Conkling (1996:681), i.e. high temperature transitions and melting point. The Sb_2O_3-based system burned fast for the same reason – low transition temperature. The surprising result was the slow burning of the $PbCrO_4$ system as $PbCrO_4$ has a low transition temperature.

Hereditary Nature or Method of Preparation. The analytical grade CuO (1) from Merck did not burn nearly as fast as the CuO (2) which was freshly prepared. It would be necessary to analyse the crystal structure in order to determine if this is as a result of the relative "looseness" of the crystal structures for the copper oxides or if other variables are the dominant driving mechanism or are having a synergistic effect i.e.

particle size differences, mechanical enhancement during processing or the addition of particles through impurities which are present.

Addition of Particles or Impurities. It does not appear that the coprecipitated systems showed enhanced reactivity. The $CuO.MnO_2$ system appeared promising for use in the delay elements due to the stable propagation of the combustion wave. The CuO systems however did show different burn characteristics and the copper oxide prepared using the foamed technique (CuO (3)) contained $CaSO_4$ as contaminant as can be seen from the needle shaped crystals in Figure 7-1 which can not be found in Figure 7-2 which was precipitated. This result was confirmed by the XRD and XRF analysis (Appendix D).

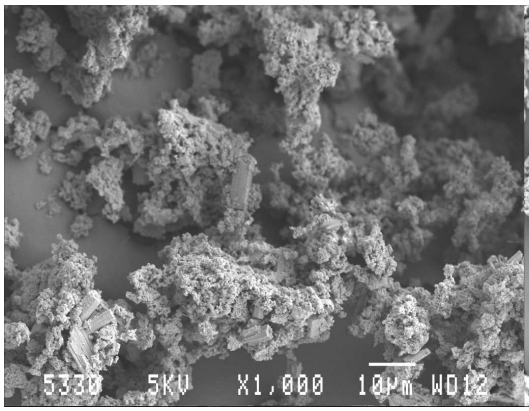

Figure 7-1: CuO prepared by Foamed Technique

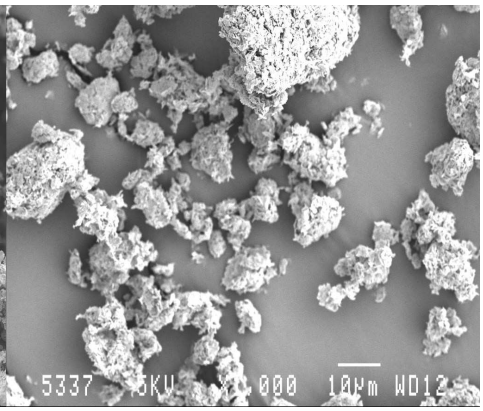

Figure 7-2: Precipitated CuO

It was decided that all the compositions which burnt (excluding $PbCrO_4$, $(BiO)_2CO_3$ and Cu_2O) be submitted to AEL for burn speed measurements.

7.2.2 Industrial Trials

Experimental

Compositions with the mass ratios reported in Table 7-5 were prepared without brush mixing and loaded into lead tubes according to the procedures outlined in Sections 6.3.1 and 6.3.5 (tubes were not rolled). All the compositions were prepared using type

4 Si as fuel. The tubes were drawn down at AEL and the delay elements cut (15mm). The delay elements were assembled into conventional non-electric detonator assemblies with or without starter and sealing elements and the burn time measured using the quality control experimental set up used by AEL.

Table 7-5: Mass Fraction Silicon added for Compositions used in Industrial Trials

Oxidant	**Mass Fraction Si**	**Oxidant**	**Mass Fraction Si**
CuO	0.16	$Cu(SbO_2)_2$	0.14
MnO_2	0.14	V_2O_5	0.07
Fe_2O_3	0.08	$CuO.Fe_2O_3$	0.20
$CuO.\ MnO_2$	0.21	Fe_3O_4	0.06
Sb_2O_3	0.12		

Results and Discussion

The results of trials have been summarised in Table 7-6

Table 7-6: Results of Industrial Trials

Oxidant	**Detonator Assembly Layout**	*Fired / Attempted*	**Core Diameter (mm)**	**Burn Time (ms)**
CuO	With starter and sealing elements	0/3	1.6	
MnO_2	***With starter and sealing elements***	***10/10***	***2.2***	***1776***
MnO_2	***With sealing element***	***10/10***	***2.2***	***1681***
MnO_2	***Without sealing or starter elements***	***0/1***	***2.2***	
Fe_2O_3	With sealing and starter elements	0/3	1.7	

Oxidant	**Detonator Assembly Layout**	*Fired / Attempted*	**Core Diameter (mm)**	**Burn Time (ms)**
$CuO.MnO_2$	With sealing and starter elements	0/3	2.8	
Sb_2O_3	***With sealing and starter elements***	***1/3***	***1.6***	
$Cu(SbO_2)_2$	***With sealing and starter elements***	***10/10***	***2.7***	***1257***
$Cu(SbO_2)_2$	***With sealing element only***	***10/10***	***2.7***	***959***
$Cu(SbO_2)_2$	***Without sealing or starter elements***	***0/3***	***2.7***	
V_2O_5	With sealing and starter elements	0/3	2.7	
$CuO.Fe_2O_3$	With sealing and starter elements	0/3	2.8	
Fe_3O_4	With sealing and starter elements	0/3	2.1	

From Table 7-6 it appears that the only compositions which ignited and burned in detonator assemblies are Sb_2O_3, $Cu(SbO_2)_2$ and MnO_2. CuO apparently does not burn when compacted.

7.2.3 Measurement of Burn Rates – Initial Trials

Experimental

It was necessary to determine the following:

- The burn rate using the setup described in Sections 6.3.8 and 6.3.10
- Whether the use of a starter element is necessary and its effect on the burn rate.

Additional elements were obtained from AEL and the burn rates measured. The elements were incorporated into detonator assemblies according to Section 6.3.6 with or without a starter element and prepared according to Section 6.3.7.

Results

Table 7-7 contains a summary of the compositions which burnt and their burn rates. Detailed experimental results may be found in Appendix E.

Table 7-7: Compositions which Burned during Initial Trials and their respective Burn Rates

Oxidant	**With or without starter element**	**Burn rate (mm/s)**
$Cu(SbO_2)_2$ (first run)	With starter element	9
$Cu(SbO_2)_2$ (second run)	With starter element	25
Sb_2O_3 (first run)	With starter element	3
Sb_2O_3 (second run)	With starter element	2

Unlike the AEL trials, MnO_2 did not burn. This may be as a result of aging of the composition in the delay elements from the time when the AEL trials were run and these runs (3 months). Further experiments using the fresh MnO_2 were conducted and reported in Section 9.1 to determine whether aging had an effect. Furthermore, all the compositions failed to ignite when ignited using shock tubing directly.

There was a wide discrepancy in the burn rate of $Cu(SbO_2)_2$ between the first run and the second run which could be as a result of the aging of the sample or the second run was just a clear outlier. Further experimentation would need to be undertaken under stricter time control to evaluate the extent to which aging affects the burn rate of $Cu(SbO_2)_2$ - Si.

In light of these observations it was decided to continue experimentation with Sb_2O_3, $Cu(SbO_2)_2$, MnO_2 and CuO for AEL's application needs.

8. MODIFICATION OF BURN RATES

8.1 Varying Stoichiometry – Tumble Mixed Compositions

8.1.1 Experimental

Binary mixtures containing 5, 10, 15, 20, 25, 30, 35 and 40% Type 4 Si were prepared for the following oxidants: Sb_2O_3; $Cu(SbO_2)_2$; MnO_2 and CuO. The detonators were assembled and the burn rates were measured using the procedure outlined in Figure 8-1.

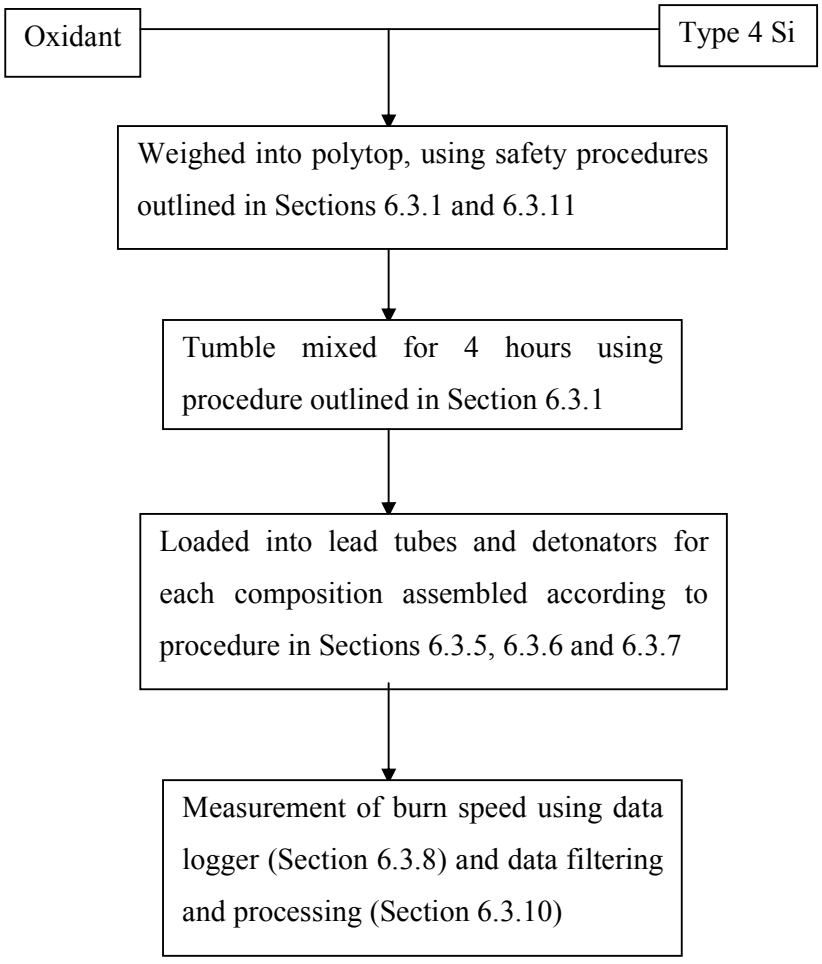

Figure 8-1: Experimental Procedure for Determining the Effect of Varying Stoichiometry for Tumble Mixed Compositions.

8.1.2 Results and Discussion

As can be seen from Table 8-1 the only compositions that ignited and burned contained Sb_2O_3 and $Cu(SbO_2)_2$ as oxidants. Despite the MnO_2-based compositions burning when ignited using a starter element (AEL trials) when they were fresh, they were not directly ignitable using shock tubing despite being fresh. So it appears that this composition cannot be ignited directly using shock tube. The CuO remained unresponsive when compacted despite showing promising burn results during the previous visual burn trials. Rugunanan (1991) found that Cu_2O did not burn when compacted. It was decided that for further trials only $Cu(SbO_2)_2$, Sb_2O_3 and $PbCrO_4$ be considered. All the raw data is reported in Appendix F.

Table 8-1: Summary of Results of Varying Stoichiometry for Tumble Mixed Compositions

Oxidant	**Sb_2O_3**	**$Cu(SbO_2)_2$**	**MnO_2**	**CuO**
Mass % Fuel which ignited	25-35	20-40	No ignition	No ignition

The results of the burn rate measurements of Sb_2O_3 have been summarised in Table 8-2. There were a number of mixture and thermocouple failures so the burn rates reported in Table 8-2 may not be truly representative of the burn rates.

Table 8-2: Effect of Varying Stoichiometry on the Burn Rate of Tumbled Sb_2O_3 – Type 4 Si

Fuel Mass %	**Burn rate (mm/s)**
25%	9
40%	11

The results of the burn rate measurements of $Cu(SbO_2)_2$ is reported graphically in Figure 8-2.

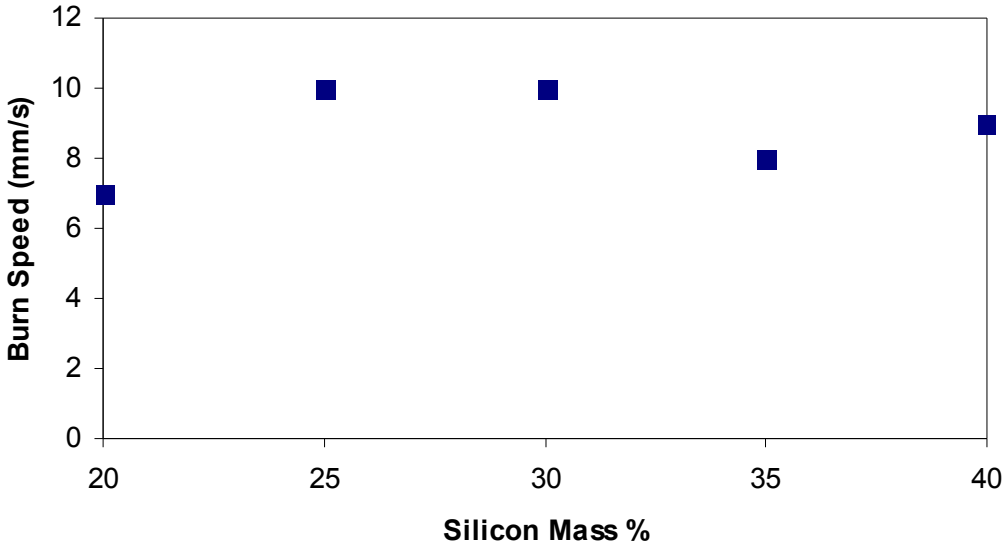

Figure 8-2: Effect of Varying Stoichiometry on the Burn Rate of Tumbled $Cu(SbO_2)_2$ – Type 4 Si

Figure 8-2 shows that the highest measured burn rates occurred at 25 and 30% Si. There is an indication of a local minimum at 35% Si.

As with the Sb_2O_3 experiments, there were a number of mixture and thermocouple failures so the burn rates reported in the Figure 8-2 may not be truly representative of the burn rates. Generally there were two burn rates for each mass percentile and the mean was determined. The standard deviation for these measurements was below 1mm/s as reported in Appendix F.

Whilst looking at the lead tubes and the tumbled compositions it was observed that proper mixing had not occurred as agglomerates of $Cu(SbO_2)_2$, Sb_2O_3 and Si were visible. It was decided to redo these experiments but to brush mix the reagents before loading into the lead tubes so as to break down the agglomerates and improve the mixing of the constituents.

8.2 Varying Stoichiometry – Tumble and Brush Mixed Compositions

8.2.1 Experimental

The mass percentage fuel (Type 4 Si) used for each composition is summarised in Table 8-3. As can be seen from the Table, all the compositions which previously did not ignite for the Sb_2O_3 and $Cu(SbO_2)_2$-based compositions were not repeated.

Table 8-3: Mass Percentage Type 4 Si used for Tumbled and Brushed Compositions

Oxidant	**Mass Percentage Si**
Sb_2O_3	25; 30; 35
$Cu(SbO_2)_2$	20; 25; 30; 35; 40; 45; 50
$PbCrO_4$	5; 10; 15; 20; 25; 30; 35; 40; 45; 50

The detonators were made and burn rates were measured using the procedure outlined in Figure 8-3.

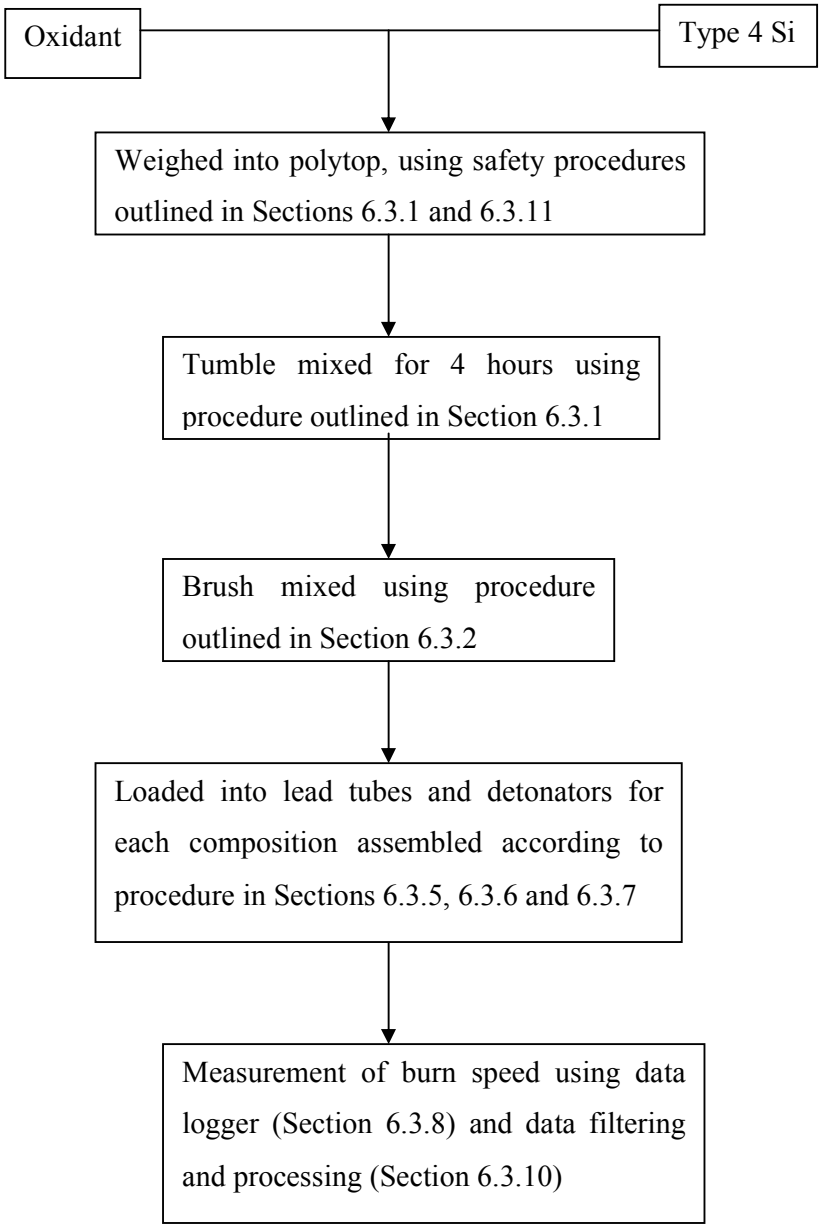

Figure 8-3: Experimental Procedure for Determining the Effect of Varying Stoichiometry for Tumbled and Brushed Compositions

8.2.2 Results and Discussion

Appendix G contains all the experimental data. All the results of the burn rate measurements are reported graphically in Figures 8-4, 8-5 and 8-6.

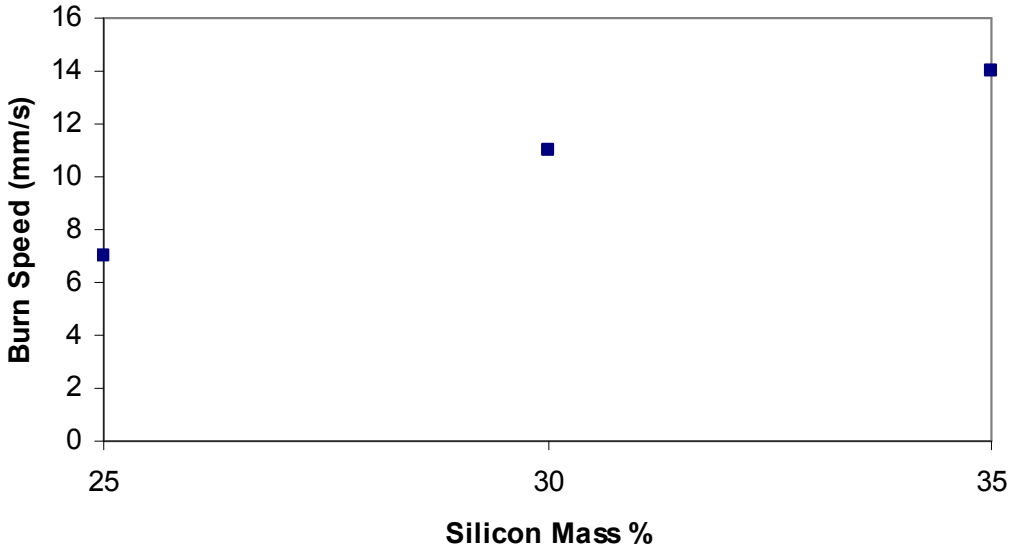

Figure 8-4: Effect of Varying Stoichiometry on the Burn Rate of Tumbled and Brushed Sb_2O_3-Type 4 Si

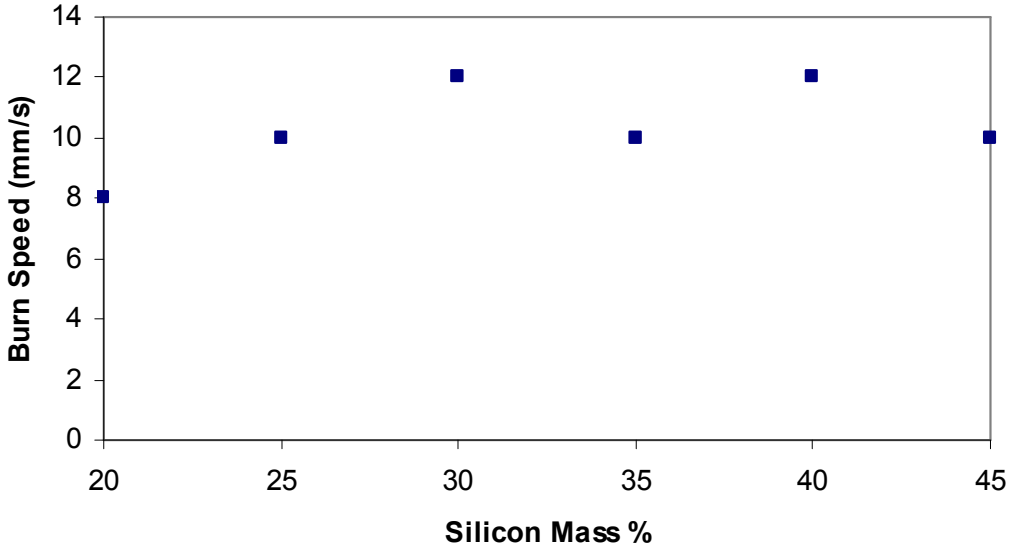

Figure 8-5: Effect of Varying Stoichiometry on the Burn Rate of Tumbled and Brushed $Cu(SbO_2)_2$-Type 4 Si

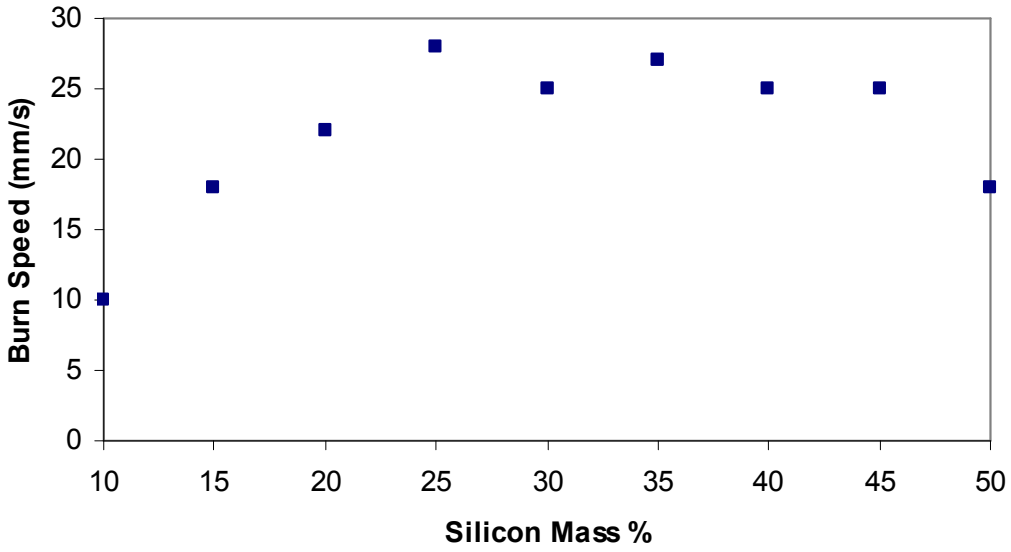

Figure 8-6: Effect of Varying Stoichiometry on the Burn Rate of Tumbled and Brushed $PbCrO_4$-Type 4 Si

Ignition and Burning. Successful ignition and burning were observed for compositions containing Sb_2O_3, $PbCrO_4$, and $Cu(SbO_2)_2$ as oxidants (See Figures 8-4 to 8-6). The burn rates varied in the range 7 – 28 mm/s. Lead chromate burned fastest and Sb_2O_3 slowest under comparable conditions.

Nature of $Cu(SbO_2)_2$ and $PbCrO_4$ curves. Figure 8-5 shows that the highest measured burn rate occurred at 30 and 40% Si with clear lower value at 35% for $Cu(SbO_2)_2$. A similar trend can be found in Figure 9-6 – $PbCrO_4$-Si. This suggests the existence of two local maxima and a local minimum in burn rates (bimodal distribution). This phenomenon is not expected for true solid-solid reactions, where one maximum is expected at or near the stoichiometric ratio. However, this has been observed previously by Al-Kazarji & Rees (1979b) (Section 5.2.1) who found a second peak when using coarser grades of Si and which they attributed to the high pressure generated in the tubes owing to the high temperature of the reaction. They also found that for compositions less than 15%, the rate of reaction was dependent on the pressures formed and the diffusion of the vaporised oxides to the reaction interface. However where the Si content was in excess of 20%, solid-solid mechanisms prevail

and the surface contact area were the controlling variables. Hedger (1983) also found a minimum delay time between 30 and 40% Si for Pb_3O_4-Si systems and attributed it to a change in propagation mechanism. It is felt that this is the case for the $Cu(SbO_2)_2$ and $PbCrO_4$ based compositions. At low oxidant levels the heat transfer takes place by mass transfer of the volatile reaction products, whilst at lower oxidant levels, heat transfer occurs by conduction. As Si is a semi-conductor, more heat is conducted as its ratio is increased, hence the second peak. This would need to be checked by analysing the reaction products.

Comparison of Experimental Burn Rates and Those Reported in Literature. Table 8-4 contains a comparison of the measured burn rates and those reported by Rugunanan (1991) for Si-fuelled compositions with Sb_2O_3 and $PbCrO_4$ as oxidants.

Table 8-4: Comparison of Measured Burn Rates and Those Reported in Literature for Si-Fuelled Compositions with Sb_2O_3 and $PbCrO_4$ as Oxidants

Mass % Si	**Rugunanan (1991) (mm/s)**	**Experimental (mm/s)**
Sb_2O_3		
25% Si	3.3	7
30% Si	6.3	11
35% Si	8.7	14
$PbCrO_4$		
20% Si	7.2	22
30% Si	13	23

Rugunanan (1991) reported that the composition range for Sb_2O_3 which ignited and burned as 20-50% Si. This was not the case for these experiments (Figure 8-4) where only the 20, 25 and 35% Si compositions ignited and burned. It is thought the reason for this was the difference in the method of ignition. Rugunanan (1991) used a starter increment of $KMnO_4$ and Mn, whilst these compositions were directly ignited using shock tube, a relative weak ignition source. As can be seen from Section 7.2.2, a 13% Si composition ignited but it was initiated by incorporating a starter element. This implies that the ignition of Sb_2O_3-based compositions is sensitive to the method of

initiation. Figure 8-4 shows that the burn rate for this composition increased linearly till 35% Si. This implies that the maximum burn rate (specified by Rugunanan, 1991 as being 43% Si) had not yet been achieved but due to the method of ignition could not be determined under these conditions.

Overall the burn speeds measured experimentally were higher. This may in part be due to particle size differences. Rugunanan (1991) reports using a Si with a particle size <53μm whereas a 1.84μm (deviation 0.06) Si was used here. Furthermore, the source of the Sb_2O_3 and $PbCrO_4$ differs which may have affected the burn rate (Section 4.1).

Ignition Reliability. Figure 8-7 depicts the ignition reliability (defined as the fraction of successful ignitions) as a function of mass % Si for all three oxidants. It should be noted that compositions that ignited successfully but did not propagate were still considered as successful ignitions. As can be seen from the Figure, Sb_2O_3 showed unreliable ignition, rendering it unsuitable for the application despite the lower burn rates which were achieved. Commercial applications require a failure rate below or equal to 1 in 5 000. The non-reliability of the compositions at the extreme stoichiometries (e.g. 15% Si and 50% Si) is expected as the probability of finding a Si particle next to oxidant particle is reduced. It would be beneficial to study these extremes in detail.

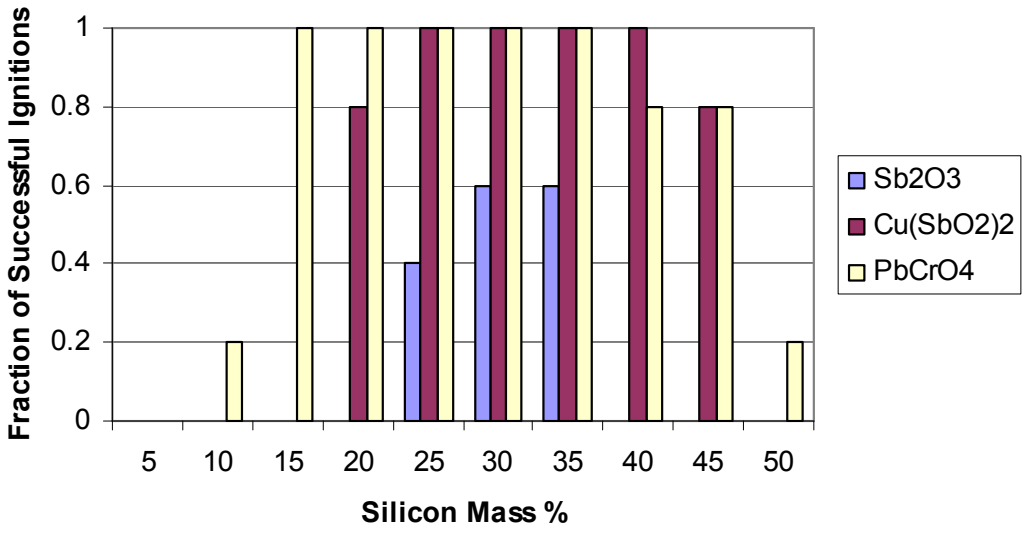

Figure 8-7: Fraction of Successful Ignitions as a Function of Stoichiometry for Tumbled and Brushed Type 4 Silicon-based Compositions for a Total of 5 Attempts

Burn Rate Standard Deviation. The standard deviations reported in Appendix G show excellent repeatability for Sb_2O_3 except at 35% Si where the burn rates varied markedly (standard deviation of 4 mm/s). When comparing the temperature profiles for the runs at 35% Si it was noted that the temperature profiles appear vastly different as a result of lead melting onto the thermocouples during the third and fourth runs. For $Cu(SbO_2)_2$, the standard deviation between runs for each compositions was below 1mm/s. This was not the case for $PbCrO_4$ where the standard deviation was below 2mm/s.

8.3 Varying Fuel Particle Size

8.3.1 Experimental

The reagents and compositions used are given in Table 8-5. All the compositions listed in Table 8-5 were tested with Si types 1, 2, 3 and 5. Other relevant information e.g. particle size etc. is reported in Section 6.4.

Table 8-5: Reagents and Compositions used for Determining the Effect of Varying Si Particle Size

Oxidant	**Mass Percentage Si**
Sb_2O_3	25; 30; 35
$Cu(SbO_2)_2$	20; 25; 30; 35; 40; 45
$PbCrO_4$	15; 20; 25; 30; 35; 40; 45

The detonators were assembled and the burn rates were measured using the procedure outlined in Figure 8-8.

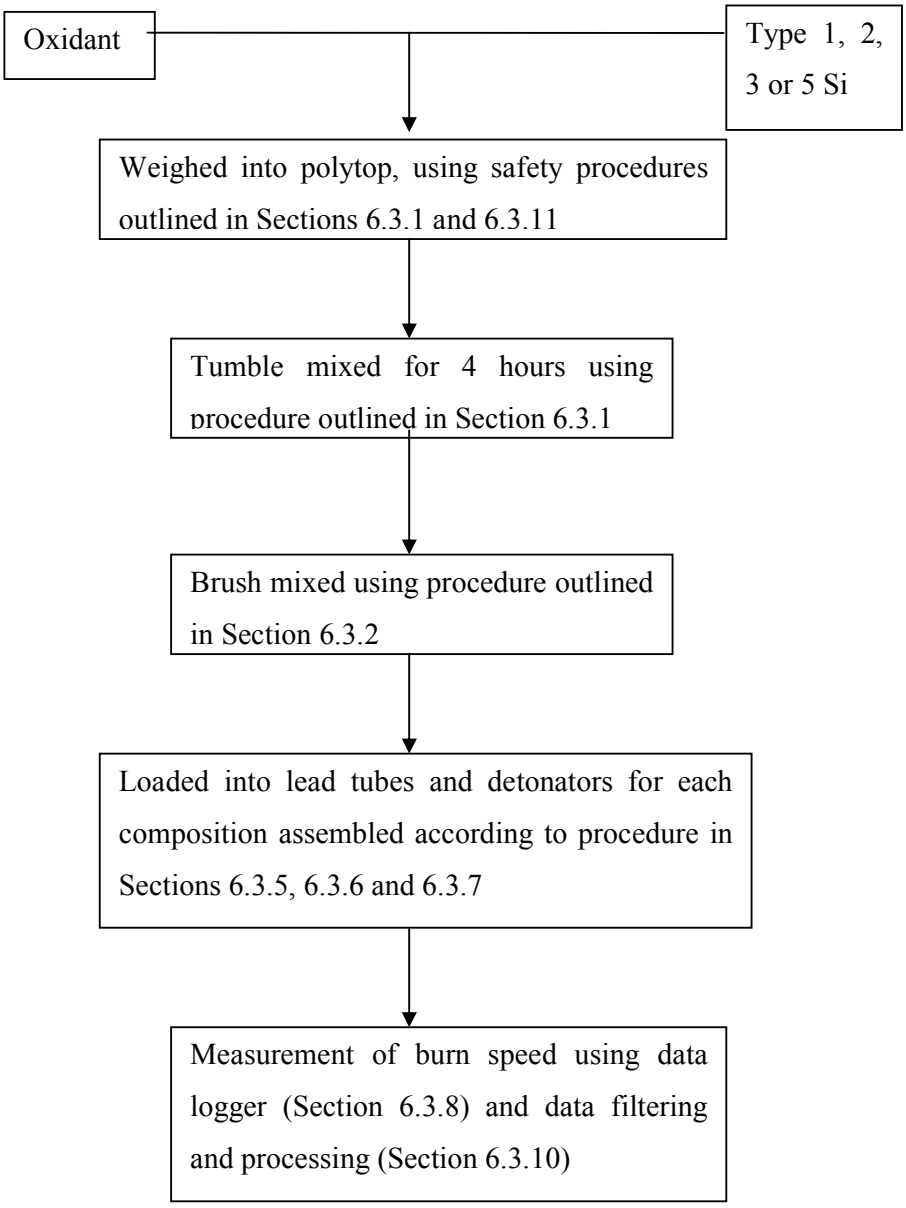

Figure 8-8: Experimental Procedure for Determining the Effect of Varying Stoichiometry and Si Particle Size

8.3.2 Results and Discussion

The experimental data are reported in Appendix H.

Ignition and Burning. It should be noted from the data in the Appendix I that the burning of Sb_2O_3-Si compositions is very dependent on the fuel particle size as

neither type 1, 2, 3 nor 5 Si ignited. This is unfortunate because particle size can not be used to modify burn rates to suit practical application. Rugunanan (1991) on the other hand found that varying the Si particle size for a Sb_2O_3-40%Si composition still resulted in compositions that ignited and that the burn rate increased with increasing specific surface area. Once again it is thought that the difference arises from the method of ignition.

It should be noted that although all the Si types were tried only type 3 and type 4 Si resulted in compositions that ignited (using shock tube directly) with $Cu(SbO_2)_2$ and $PbCrO_4$ as oxidants. Interestingly the reactions for $Cu(SbO_2)_2$ and type 3 Si were less violent and gassy than those for $Cu(SbO_2)_2$ and type 4 Si. All the results of the burn rate measurements for the $PbCrO_4$ and $Cu(SbO_2)_2$- based compositions are reported graphically in Figures 8-9 and 8-10.

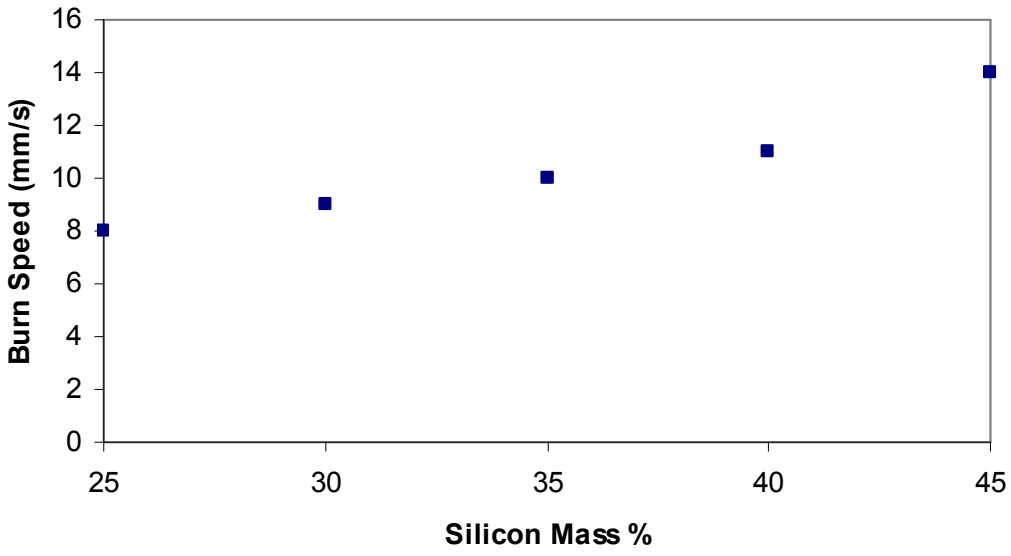

Figure 8-9: Effect of Varying Stoichiometry on the Burn Rate of $Cu(SbO_2)_2$-Type 3 Si

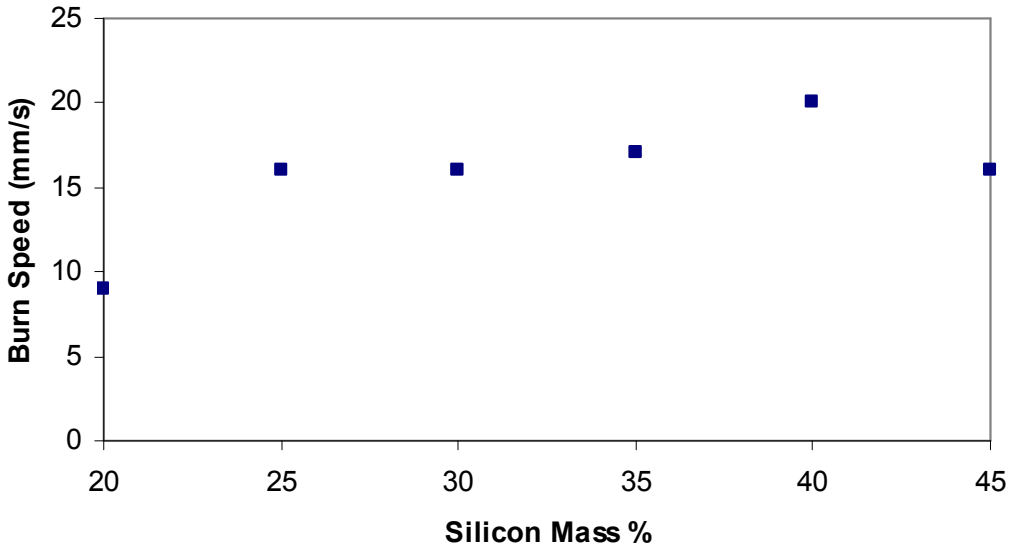

Figure 8-10: Effect of Varying Stoichiometry on the Burn Rate of $PbCrO_4$-Type 3 Si

Another point of interest for the $PbCrO_4$-Si compositions which is not plotted graphically is the ignition of one detonator for the 40% type 5 Si (5th run). No burn rate could be determined as the burn front extinguished as it reached the second thermocouple. This point is unusual as it was the only type 5 Si based composition which ignited. Also interestingly a number of $PbCrO_4$-based compositions (in particular at a high Si content) ignited but failed to propagate beyond the first thermocouple. This may be the result of localised areas of inferior interaction between the $PbCrO_4$ and Si. It was also noted that these compositions were very gassy.

Nature of $Cu(SbO_2)_2$ curve. Figure 8-9 does not show the bimodal distribution that was evident for type 4 Si. This may be due to the different compact density that was obtained due to the different particle size. As observed by Goodfield and Rees (1985) in Section 4.1 vii the compact density in conjunction with oxidant level has a marked effect on the propagation mechanism and they found that the response is complex at intermediate oxidant levels as no one process dominates the heat transfer process. At the intermediate concentration of 35% Si, where the proposed mechanism changeover occurs, the response for the bigger size Si is different due the change in the compact density. This however would need to be confirmed through analysis of the reaction products. The burn rate increases until the highest measured burn rate is reached at ca.

45% Si. It appears that the maximum has shifted to a higher Si content not measured. It would be beneficial to determine whether this was the case by determining the burn rates for compositions with >45%Type 3 Si.

Nature of $PbCrO_4$ curve. Similarly, Figure 8-10 does not show the bimodal distribution that was evident for type 4 Si. It is also felt that similar to the $Cu(SbO_2)_2$-Si system, this observation is also due to the difference in compact density between the type Si and the type 3 Si. The highest measured burn rate occurs at 40% Si with a plateau at 25 and 30% Si. It was observed, in particular for the 25% Si compositions that the reactions were extremely violent and that molten lead had been pushed back up into the shock tube (Figure 8-11). This means that the gas which was produced flowed in the opposite direction to the combustion front. As discussed by Aldushin & Zeinenko (1992) (Appendix A) this plays an important role in the burn rate and affects the nature of the reactions. In order to limit this effect, it is recommended that a sealing element be added to the detonators to limit gas flow in the opposite direction.

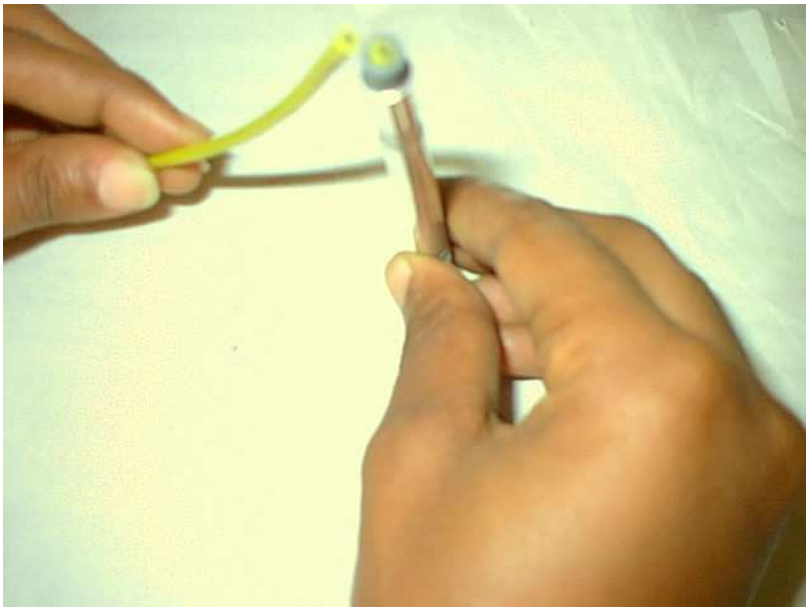

Figure 8-11: Detonator Assembly for which Molten Lead had Flowed Back into the Shock Tube

Ignition Reliability. Figure 8-12 depicts the ignition reliability (defined as the fraction of successful ignitions) as a function of mass % type 3 Si for $PbCrO_4$ and $Cu(SbO_2)_2$

as oxidants. It should be noted that once again compositions that ignited successfully but did not propagate were still considered as successful ignitions. Comparing Figure 8-7 (repeated here) and Figure 8-12 shows that ignition reliability decreases with increasing Si particle size. This may be attributed to the decreased surface area of contact between the Si particles and the oxidant. It should be noted that this may affect the Si mass percentage range which can be applied due to quality control.

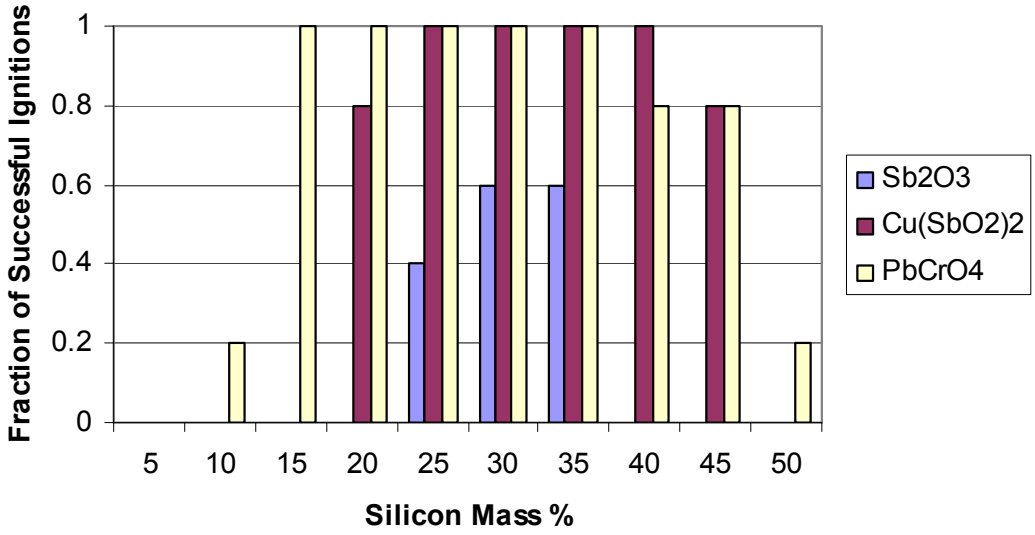

Figure 8-7 (Repeated): Fraction of Successful Ignitions as a Function of Stoichiometry for Tumbled and Brushed Type 4 Si-based Compositions for a Total of 5 Attempts

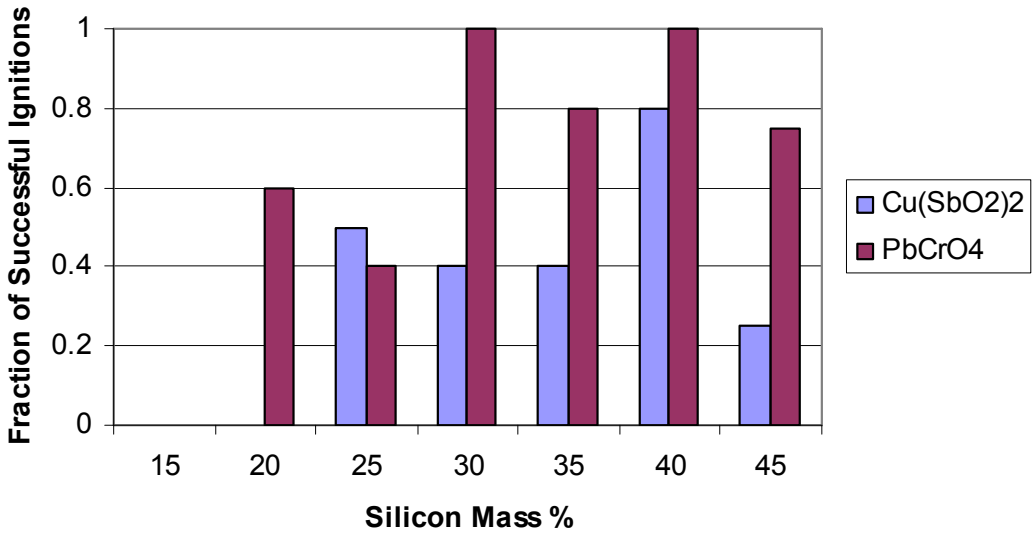

Figure 8-12: Fraction of Successful Ignitions as a Function of Stoichiometry for Type 3 Si-based Compositions for a Total of 5 Attempts

Standard Deviation of Data. The data in Appendix H shows that the standard deviation in the measured burn rates for $Cu(SbO_2)_2$-type 3 Si was below 1mm/s. On the other hand the standard deviation for $PbCrO_4$-type 3 Si was as high as 3mm/s. The voltage profiles appear similar but spurious results were obtained. This may have been the result of the lead melting, the gas formation and the nature of the interaction between the $PbCrO_4$ and Si.

8.4 Varying Oxidant Particle Size

8.4.1 Experimental

Two compositions were prepared using Nanocat® iron oxide and type 4 Si to check whether varying the particle size of the iron oxide would have an effect on the burn characteristics. The compositions were 15% Si and 25% Si. The oxidant was not dried beforehand and was therefore surface hydrated. The detonators were prepared and

subjected to burn rate measurements using the procedure outlined in Figure 8-13. It should be noted that brush mixing was omitted.

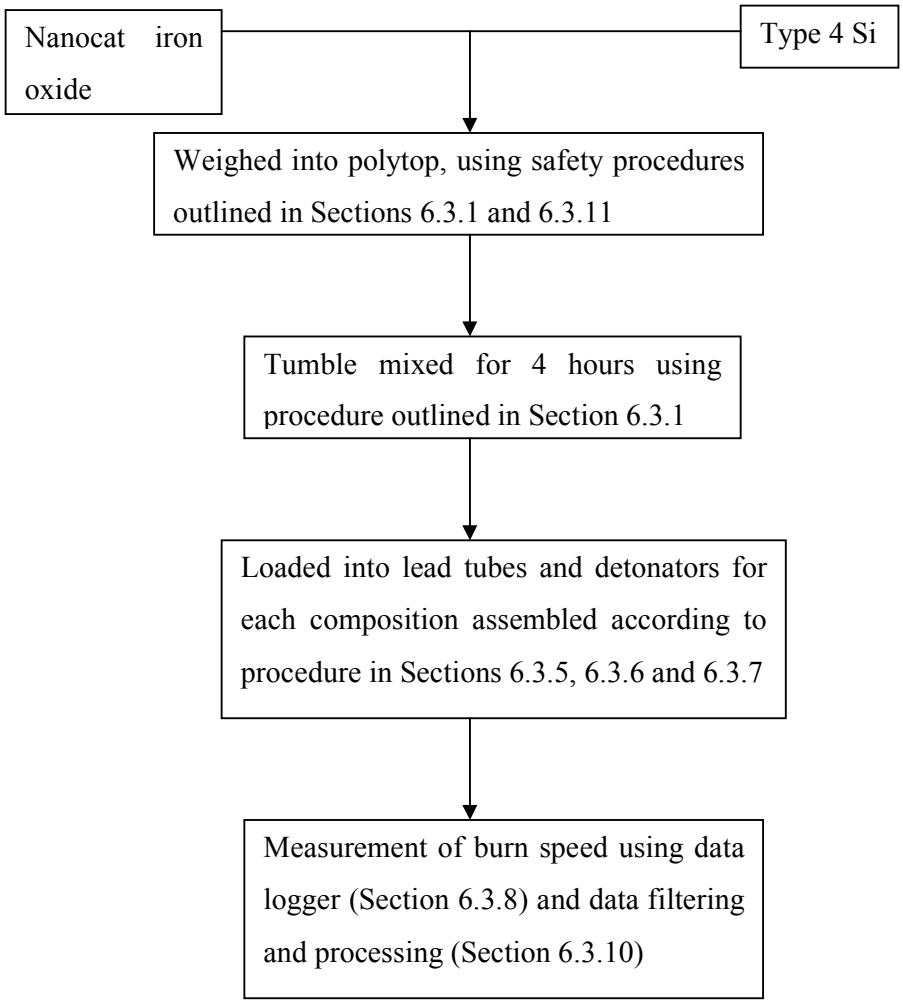

Figure 8-13: Experimental Procedure for Determining the Effect of Varying Oxidant Particle Size

8.4.2 Results and Discussion

A summary of the experimental results is contained in Appendix I. The mixture failed to ignite in all cases. Varying the particle size and origin of the iron oxide did not result in a composition which could be used. The problem with the application of the Nanocat® as an oxidant on its own and not as an additive is the large bulk density of the fine powder. This makes it difficult to process, compact and to prevent segregation of the Si particles after tumbling which happens instantaneously.

8.5 Additives – Aluminium Addition

8.5.1 Experimental

The compositions tested are reported in Appendix J. It should be noted that compositions containing $PbCrO_4$ as oxidant were not tested. The formulations were prepared as follows:

- Two, 5,10 and 20% Al based on the total composition mass was weighed out.
- Of the remaining mass (total composition mass - mass of Al) the relevant percentage of type 4 Si (20-45%) was taken
- The remainder of the mass was the oxidant.

As before, the burn rates were determined according to the procedure outlined in Figure 8-14

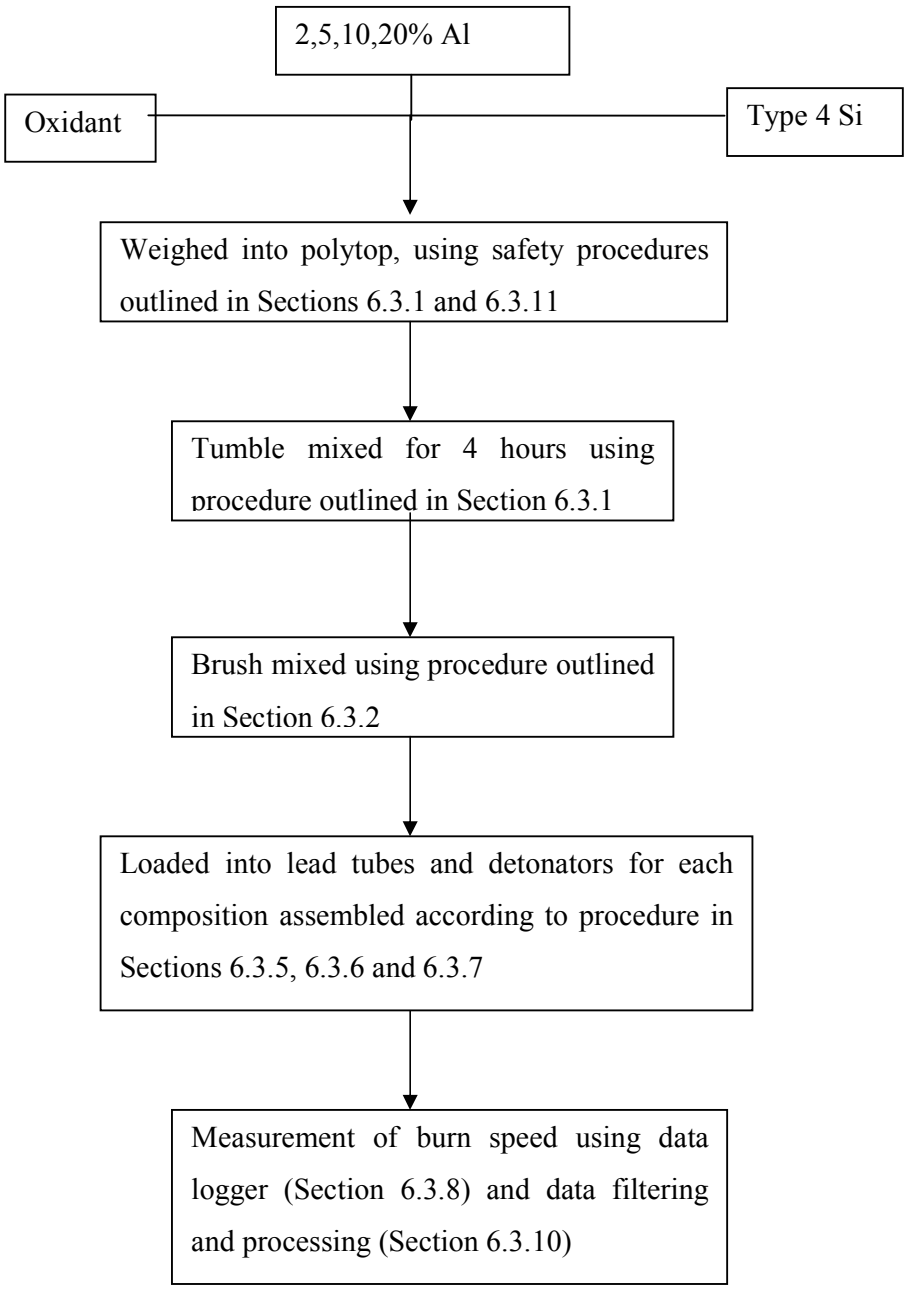

Figure 8-14: Experimental Procedure for Determining the Effect of Al Addition

8.5.2 Results and Discussion

The relevant data on the behaviour of the compositions during burning and burn rates is reported in Appendix J. The burn rate data is reported graphically in Figures 8-15 and 8-16.

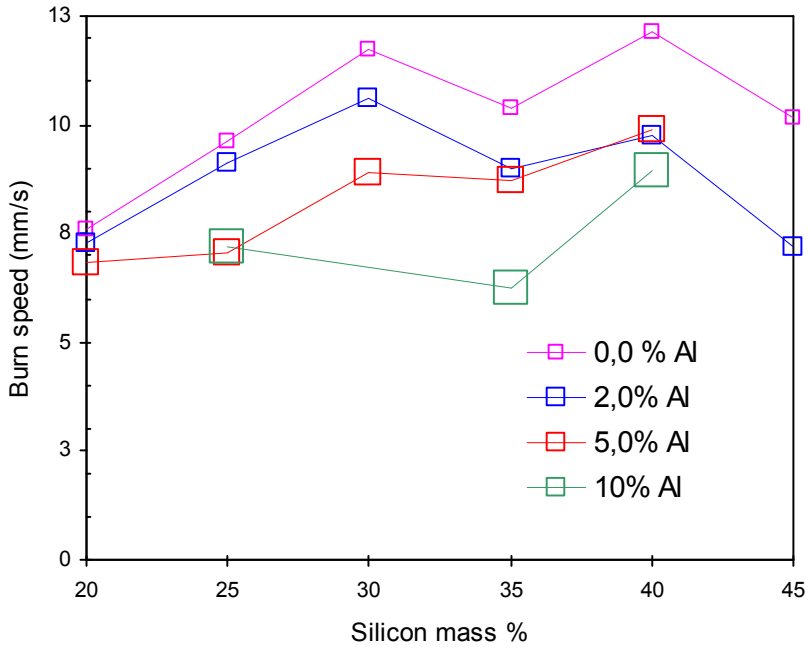

Figure 8-15: Aluminium Addition Decreases the Burn Rate and Ignition Range of $Cu(SbO_2)_2$-Type 4 Si

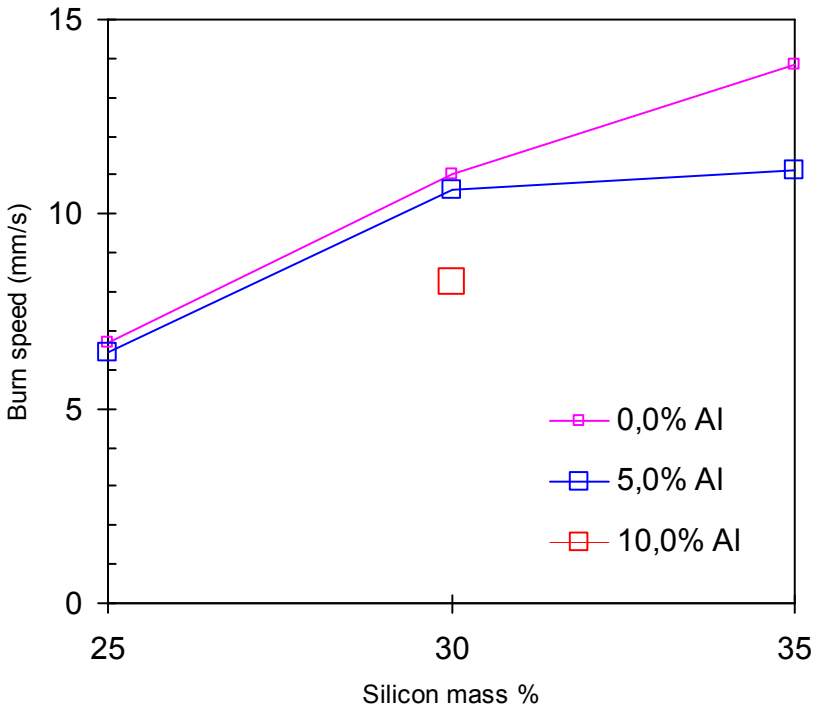

Figure 8-16: Aluminium Addition Decreases the Burn Rate and Ignition Range of Sb_2O_2-Type 4 Si.

Nature of the Curves. Figures 8-15 and 8-16 show that the addition of aluminium powder decreased the burn rate for $Cu(SbO_2)_2$ and Sb_2O_3 instead of increasing it as reported in literature (Section 4.1 iv). Possible reasons for this observation may be:

- The Al acted as a secondary fuel thereby increasing the overall the fuel concentration.
- The presence of the Al may have decreased the available amount of heat for transfer.
- The particle size of the Al was not investigated and may have had an effect.

The highest measured burn rates occurred at 30 (exception – 10% Al) and 40% Si for the compositions with $Cu(SbO_2)_2$ as oxidant. It therefore appears that the bimodal distribution of the burn rates for $Cu(SbO_2)_2$-Si is retained for all the Al addition levels, thereby still indicating that a change in propagation mechanism may have taken place.

Gassiness. It was observed that the gassiness of the burning mixtures increased and the reactions became more vigorous with the addition of Al. Lead was observed to pour out of the opening for the first thermocouple as the wave passed the second opening.

Ignition Reliability. As the proportion of Al which was added increased, the ignition reliability decreased until 10% Al beyond which no compositions ignited. The addition of the Al desensitises the composition to ignition by shock tube. This may also indicate that the Al acts as a secondary fuel.

Standard Deviation of Data. As reported in Appendix J, the standard deviation of the Sb_2O_3-based compositions was not determined due to the low fraction of compositions which actually ignited and yielded a burn rate. The standard deviation of the data for the $Cu(SbO_2)_2$-based compositions was below 2mm/s.

8.6 Conclusions

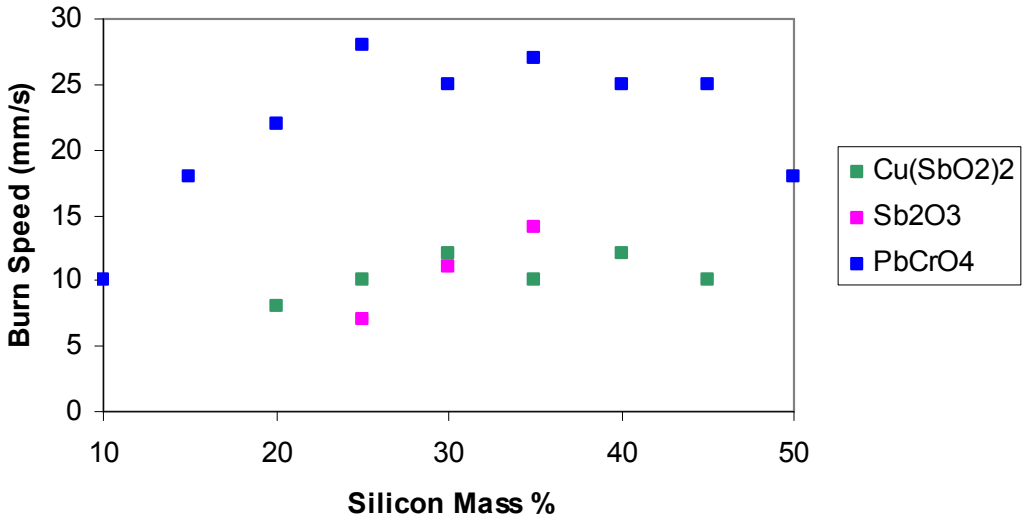

Figure 8-17: Effect of Oxidant on the Burn Rate of Type 4 Si

As shown in Figure 8-17 and the data contained in the preceding sections, the main controlling variable over the burn rate was the nature of the oxidant i.e. in decreasing order of burn rate $PbCrO_4$, $Cu(SbO_2)_2$ and Sb_2O_3. As mentioned previously it would be beneficial to determine the processes which occur during combustion by analysing the combustion products, evaluating the effect of compaction density, core diameter etc. to determine whether the reactions for these oxidants are truly solid-solid reactions and whether there is change in the propagation mechanism at 35% Si for the copper antimonite and lead chromate systems.

Bimodal burn rate distributions were observed for the $Cu(SbO_2)_2$-based compositions as the stoichiometry was varied and Al added. This was not the case when the Si particle size was increased (Figure 8-18). The addition of Al and increasing the particle size decreased the measured burn rates.

The addition of Al reduced the measured burn rates for Sb_2O_3-Si slightly (Figure 8-19). Increasing the Si content on the other hand increased the measured burn speeds within the ignitable composition range. It should be noted that the ignition of Sb_2O_3 is

very dependent on the method of initiation. Increasing the Si particle size and Al content beyond 10% resulted in compositions which were not ignitable by shock tube.

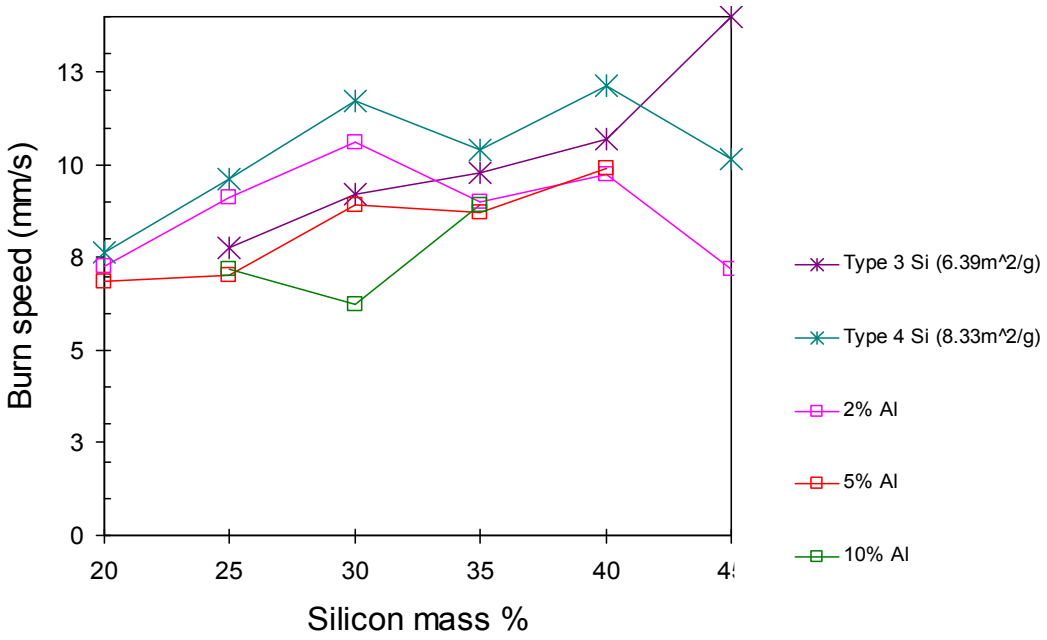

Figure 8-18: Burn Speed Decreases with Increasing Aluminium Addition and Silicon Particle Size for $Cu(SbO_2)_2$-Si

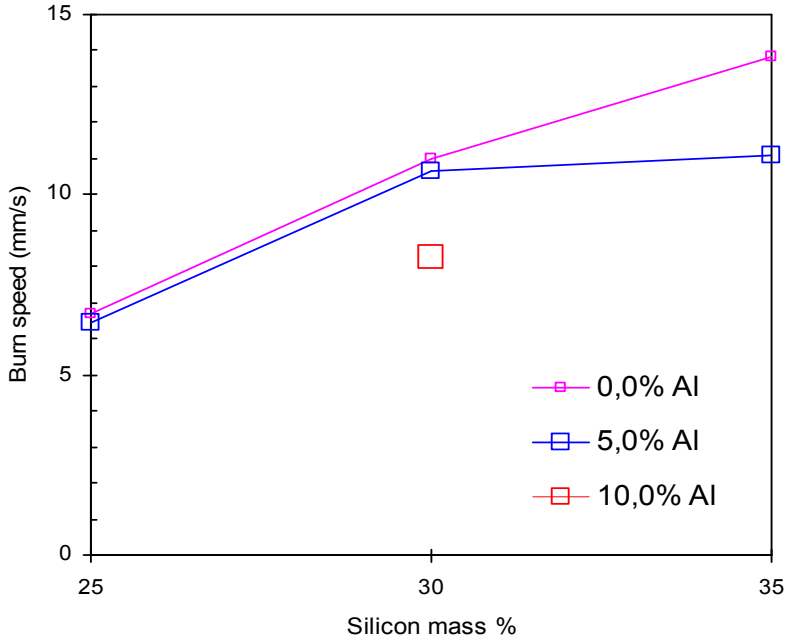

Figure 8-19: Burn Speed Decreases with Increasing Aluminium Content and Decreasing Silicon Content for Sb_2O_3-Si

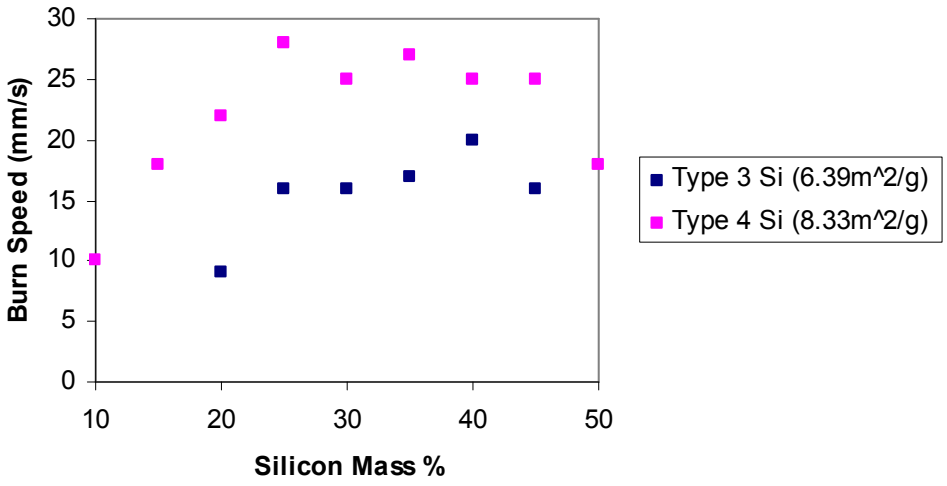

Figure 8-20: Increasing the Silicon Particle Size Decreases the Burn Rate for $PbCrO_4$-Si

A bimodal burn rate distribution was observed for the $PbCrO_4$-Type 4 Si compositions as the stoichiometry was varied (Figure 8-20). Increasing the Si particle size not only reduced the measured burn rate for this composition, but as seen in Figure 8-20, the bimodal burn rate distribution is not evident.

8.7 Applicability and Recommended Further Investigations

As was shown, Sb_2O_3, $PbCrO_4$ and $Cu(SbO_2)_2$ – based compositions are all directly ignitable by shock tube thereby eliminating the need for a "starter" composition. This will create more space in the detonator assemblies. The implementation of $PbCrO_4$ would still require the use of a "sealing" composition to prevent the back-flow of molten lead into the shock tube.

From the reported burn rates for all three oxidants (Appendices G to J), it appears that the only compositions which may be replaced are the "medium" and "slow" compositions i.e. Table 8-6.

Table 8-6: Replacement Compositions for Slow and Medium Compositions Currently in Use

Sb_2O_3 as oxidant	**$Cu(SbO_2)_2$ as oxidant**	**$PbCrO_4$ as oxidant**
"Medium" Composition		
35% Type 4 Si	45% Type 3 Si	15 and 50% Type 4 Si
	25% Type 4 Si, 2% Al	25-45% Type 3 Si
"Slow" Composition		
25% Type 4 Si	20% Type 4 Si 2 & 5% Al	
25% Type 4 Si, 5% Al	25% Type 4 Si 5 & 10% Al	
	35% Type 4 Si 10% Al	
	45% Type 4 Si 2% Al	

The commercial application of Sb_2O_3-based compositions is not advisable due to the large number of ignition failures this composition has exhibited during these laboratory trials. Furthermore, the ignition sensitivity of this composition to varying fuel particle size makes it unattractive should there be a slight difference in the fuel particle size.

$Cu(SbO_2)_2$ has been shown to be a reliable oxidant with a small standard deviation in the burn rate. The burn rates of this composition are easily modified by stoichiometry, particle size and the addition of Al. It appears that it may be a little too fast to replace the "slow" composition (i.e. all the compositions reported in Table 8-6 refer to 7mm/s which is the maximum permissible burn rate for the commercial "slow" composition). This implies that the processing of this composition would need to exact in order to achieve the burn rate. It should be borne in mind that this composition does not require a "starter" element (directly ignitable using shock tube) and therefore longer elements (compared to the "slow" composition) can be used to achieve the desired burn time in the long period delay detonators. It also means that developing an alternative composition for the "starter" composition will be unnecessary. One drawback of using this compound is that its manufacture will require special processing procedures to ensure the safety of workers as the inhalation of Sb_2O_3 (one of the starting reagents) is suspected of causing cancer (Section 5.1.2).

Based on these results it is suggested that the use of $Cu(SbO_2)_2$-based compositions be tested by AEL. The implications of large-scale manufacture of the compound also need to be investigated.

No replacement could be found for the "fast" and "sealing" compositions. It is thought that perhaps a complete change in thinking may be needed and intermetallic reactions be used. Hardt and Holsinger (1973) have found that B and C mixtures with Ti and Zr are self propagating at room temperature with burn rates varying between 0.07 and 97mm/s. They found that the adiabatic temperature must exceed the melting point of the alloy in order to insure a self-propagating reaction (Hardt and Holsinger, 1973). Perhaps the inclusion of one of the above formulations would supply enough energy as a starter for these reactions.

9. DRY MIXING OF FLOW CONDITIONER ADDITIVES

9.1 Powder Processing Problems

The following terms may be used in the description of the various states of undispersed particles:

- Aggregation – describes an association of particles
- Agglomeration – process by which particles grow by collision with other particles
- Flocculation – Reversible aggregation whereby particles are held together loosely with considerable surface separations.
- Coagulation – irreversible aggregation, whereby the particles are held closely together (Hann, 1996:230).

A major problem in the processing of powdered formulations is agglomeration. The agglomeration results in mixtures which are not homogeneously mixed. This in turn affects the burn rate of the pyrotechnic formulations (i.e. constant solid-solid contact and thermal conductivity is not maintained). This problem is compounded when the powders are hygroscopic, waxy or oily or unusually shaped such as needle-type or flake particles. The agglomeration increases as the particle size decreases. Furthermore, moisture content directly increases agglomeration and leads to caking of the powder. This means that most fine-particle powders must be specially handled, i.e. drying at elevated temperatures, screening to break up or remove agglomerates and desiccating to prevent moisture uptake (Tulis, 1980). As mentioned previously (Section 4.1 ix) moisture adsorption affects the burn rate of pyrotechnic formulations (McLain, 1980).

Another related problem occurs when the powders are milled in order to reduce the particle size and during mixing before granulation. The surface areas of the powders are increased and the moisture absorption becomes extensive (Tulis, 1980). Cohesiveness of the powder increases as the moisture content increases (Marinelli & Carson, 1996:1120).

According to Nelson (1996:1099), the strength of the bonds holding the clumps together may increase with storage time because of surface migration of material into the high energy contact region. The migration is as a result of the solubilisation and mobilisation caused by the absorbed vapours. This may explain the phenomenon of slower burning that has been observed in pyrotechnic formulations where the individual constituents of the formulation have been allowed to age before being mixed. Some powders may be treated to decrease the likelihood of these changes and to keep the clumps soft and easy to deagglomerate (Nelson, 1996:1099).

Forces causing primary particles to stick together have been classified as:

- Solid bridging
- Liquid bridging
- Attraction between particles
- Interlocking

Solid bridges form as a result of sintering, solid diffusion or chemical reaction. Liquid bridging results from the presence between individual particles of bulk liquid. Forces of interparticle attraction are electrostatic and Van der Waal's forces. Electrostatic forces arise through charging by contact with charged particles or by friction. Van der Waal's forces arise from electron motion within the atoms and protrude beyond the surface of the particle. These forces are only appreciable where the radii (r) and distance between the particles is small.

The formation of agglomerates by particle interlocking can occur with fibrous or plate-shaped particles but not spheres (Veale, 1972:135-136).

For fine particles (<1μm) the most important agglomerating forces are Van der Waal's and liquid bridging. The tap density of such powders may be as low as 1% of the theoretical density, so particle bridging and extensive void formation occurs. Veale (1972:136-137) has stated that mixing these powders with a fluid and granulating will increase the density to 20% of its theoretical value.

As a result of these forces, powders do not flow easily. Agglomerates move rather than individual particles (Veale, 1972:137). Five common flow problems are:

- *No Flow* – This may occur when a cohesive arch forms at the outlet of the container or a stable rat hole is formed within the container
- *Erratic Flow* – Combination of two no flow conditions.
- *Flooding*- Flooding occurs when fresh material is added to a bulk material (a fine powder) that has formed a stable rat hole.
- *Limited Discharge Rate* – This is a function of the material's air or gas permeability – i.e. material flow is limited by counter flow of gas through the outlet.
- *Segregation* – Occurs when powders are composed of different particle sizes or densities (Marinelli and Carson, 1996:1114).

A further problem during powder processing is the effect of wall friction. The following variables affect wall friction values:

- Pressure – as the pressure acting normal to the wall increases, the coefficient of sliding friction often decreases.
- Moisture Content – As the moisture increases, the more frictional the particles.
- Particle Size and Shape – Fine materials are more frictional and angular particles dig into the wall surface creating more friction.
- Temperature – Higher temperatures result in more frictional particles.
- Time of storage at rest – If allowed to remain in contact with a wall surface, many solids experience an increase in friction between the particles and the wall surface.
- Wall Surface – Smoother wall surfaces are typically less frictional and the corrosion of the surface affects the ability of the material to flow on it (Marinelli & Carson, 1996:1119).

9.1.1 The Use of Additives

In the past small amounts of fine powders have been used as additives to improve the flow properties of a range of powdered insecticides, chemicals, pharmaceuticals, etc. During the mixing the agglomerates are broken down and the fine particles coat the coarser particles of the main constituent and prevent these sticking together. The

coated hydrophobic forms of the fine powder have been used very successfully for this purpose. The fine powders may also be used to absorb the small amount of liquid in the bridges and convert the powder to a mass of dry powder (Veale, 1972:138). These are usually fine powders of sub sieve particle size and include silicates, stearates, phosphates, diatomaceous earth, starch, magnesium oxide, talcum and fatty amines (Tulis, 1980).

The mechanisms by which these conditioners work in inhibiting agglomeration and improving flowability are:

- They form a solid barrier between the powder particles, reducing their attractive forces
- They lubricate the solid surfaces thereby reducing friction between the particles and
- They neutralise electrostatic charge (Tulis, 1980 & Veale, 1972:138).

Electrostatic charge and friction are both potential ignition sources for pyrotechnic compositions and their minimisation will result in safer operating conditions.

Dow Corning Corporation has developed a hydrophobic fumed silica powder, which was called Silanox and Tulanox 500. It has been prepared from a hydrophilic colloidal silica by reacting the latter with hexamethyldisilazane. According to Tulis (1980), this flow conditioner has the following advantages:

- It has an exceedingly light bulk density.
- The particle size is about 1nm.
- The conditioner may be premixed before milling and will allow for the milling of waxy or oily materials.
- The treated powder becomes water repellent, even if initially hygroscopic.
- On a mass basis, the addition of less than 1% of the conditioner is sufficient.
- The resultant powder generally has a higher bulk density after the addition and
- It is chemically inert, even with sensitive pyrotechnic mixtures (Tulis, 1980).

The silica causes a steric methyl field to form on the particles that causes the particles to become hydrophobic. Air is trapped upon the surface of the powder and the water surface then rests on the millions of points of the hydrophobic silica projections coating the powder (Tulis, 1980).

Tulis (1980) has found that the lack of agglomeration and free-flowing characteristic has helped in preventing powder separation and aiding powder fills. Storage of pyrotechnic devices for extended periods has resulted in a high degree of propagation failures due to powder separation within the devices. Tulis (1980) found that this was not the case with the powders treated with the hydrophobic fumed silica.

One disadvantage of this technology is associated with the increased bulk density. The bulk density increase is caused by the fluidisation of the individual particles; they flow and slip past each other readily so that they compact better. If however, the powder stands for an extended period, it becomes thixotropic in nature i.e. it is difficult to achieve instant motion even though once disturbed the powder flows easily. This does not pose a problem where the powders will be fluidised, but should be considered for the dispersal of the powders that are initially tightly contained (Tulis, 1980).

The amount of silica that should be added depends on the material to be fluidised and its particle size. If the particle size is to be reduced, either by milling, deagglomeration etc. additional silica should be added. Incomplete coating will be effective but not optimum, whereas excess silica will not improve the flowability appreciably. Tulis (1980) has found that in some cases it will segregate from the coated particles, floating on the surface as a separate layer.

The Silanox and Tullanox 500 products are old trade names for a product now called CAB-O-SIL TS-500 (Sims, 2000). The CAB-O-SIL TS-500 product has a surface area that varies between 204-245m^2/g (Cabot-Corporation website, 2000).

Wacker-Chemie, on the other hand, produce a high purity fumed silica. When mixed with a powder, even in small amounts, Wacker-Chemie (2000) have stated that their HDK® grades H20 and H2000 can improve the flow properties of powders. The fumed silica accumulates on the surface of the particles, thereby separating the particles and allowing free flow (Wacker HDK® brochure, 2000).

As result of the high specific surface area, the silica can bind moisture on the surface of the hygroscopic powders. This drying effect promotes the free flow of the powder.

Wacker-Chemie (2000) recommend their N20 and T30 fumed silicas for this particular desired effect. They recommend that a concentration of about 0.1 to 3% be used as additive (Wacker HDK® brochure, 2000).

Wacker-Chemie (2000) have summarised their product specifications and determined the charge of the silicas in their range (Table 9-1).

Table 9-1: Wacker HDK® Product Range Specifications (Wacker HDK® Brochure, 2000)

Product	**Electric Charge**	**Surface Modification**	**Surface Area (BET) [m^2/g]**
H20	Highly negative	-$OSi(CH_3)_2$-	170
H1303 P	Negative	-$OSi(CH_3)_3$	100
H2000			140
H3004			210
H1018	Highly negative	-$OSi(CH_3)_2$- PDMS-treated	100
H2015	Positive	-$OSi(CH_3)_2$- PDMS-treated, -NR_2/-NR_3^+ functions	110
H2050	Highly positive	-$OSi(CH_3)_2$- PDMS-treated, -NR_2/-NR_3^+ functions	110
H2150 VP	Highly positive	-$OSi(CH_3)_2$- PDMS-treated, -NR_2/-NR_3^+ functions	110
H3050 VP	Highly positive	-$OSi(CH_3)_2$- PDMS-treated, -NR_2/-NR_3^+ functions	150

A disadvantage of using the Wacker HDK® range is that it may build up an electrostatic charge. It is therefore recommended that when applied to the pyrotechnic mixtures all the equipment used should be properly earthed. Furthermore, Wacker recommend that in order to maintain the structural properties of the silica, gentle conveying methods such as compressed-air diaphragm pumps may be used for conveying over short distances (Wacker HDK® brochure, 2000).

Molecular sieves have been added to powdered mixtures in the past in order to facilitate the drying process before milling. An example where this addition has been advantageous is in the preparation of water-ignitable B-AgF_2 pyrotechnic compositions. Before the size reduction process, molecular sieves (10% on a mass basis) were added to the AgF_2. Subsequent ignition tests revealed that the ignition was much faster, the burn rate reduced and this was even evident after 24 hours (Tulis, 1980).

The molecular sieves remove the moisture from the powders by absorption in an equilibrium process. According to Tulis (1980), for this reason, they should only be used when a continuous drying action is necessary such as in the AgF_2 milling process. They can however be added to powders that are nearly dry. Direct contact with sensitive compositions should be avoided, as the heat of absorption could be sufficient to ignite the mixtures.

Tulis (1980) has added both molecular sieves and the hydrophobic fumed silica to certain milling operations. The molecular sieves are used to dry the particles in the milling process, so that as the particles are fragmented, they are coated with the hydrophobic fumed silica.

9.1.2 Density

The bulk density of a material can be affected by moisture (more moisture makes material more compressible), particle size and shape, temperature (increased temperature results in softer particles which can be compressed) and particle elasticity (Marinelli & Carson, 1996:1121).

The packing of powders under their own weight is expressed as the tap density. Tap density depends on the shape, absolute size and size distribution, surface characteristics and state of agglomeration of the powder (Veale, 1972:138). The apparent density is measured as the mass of powder which fills a given container under free flow (Kaysser and Weise, 1993:114).

9.2 Formulation of Free Flowing Oxidants

9.2.1 Experimental

The experimental procedure which was used has been summarised in Figure 9-1

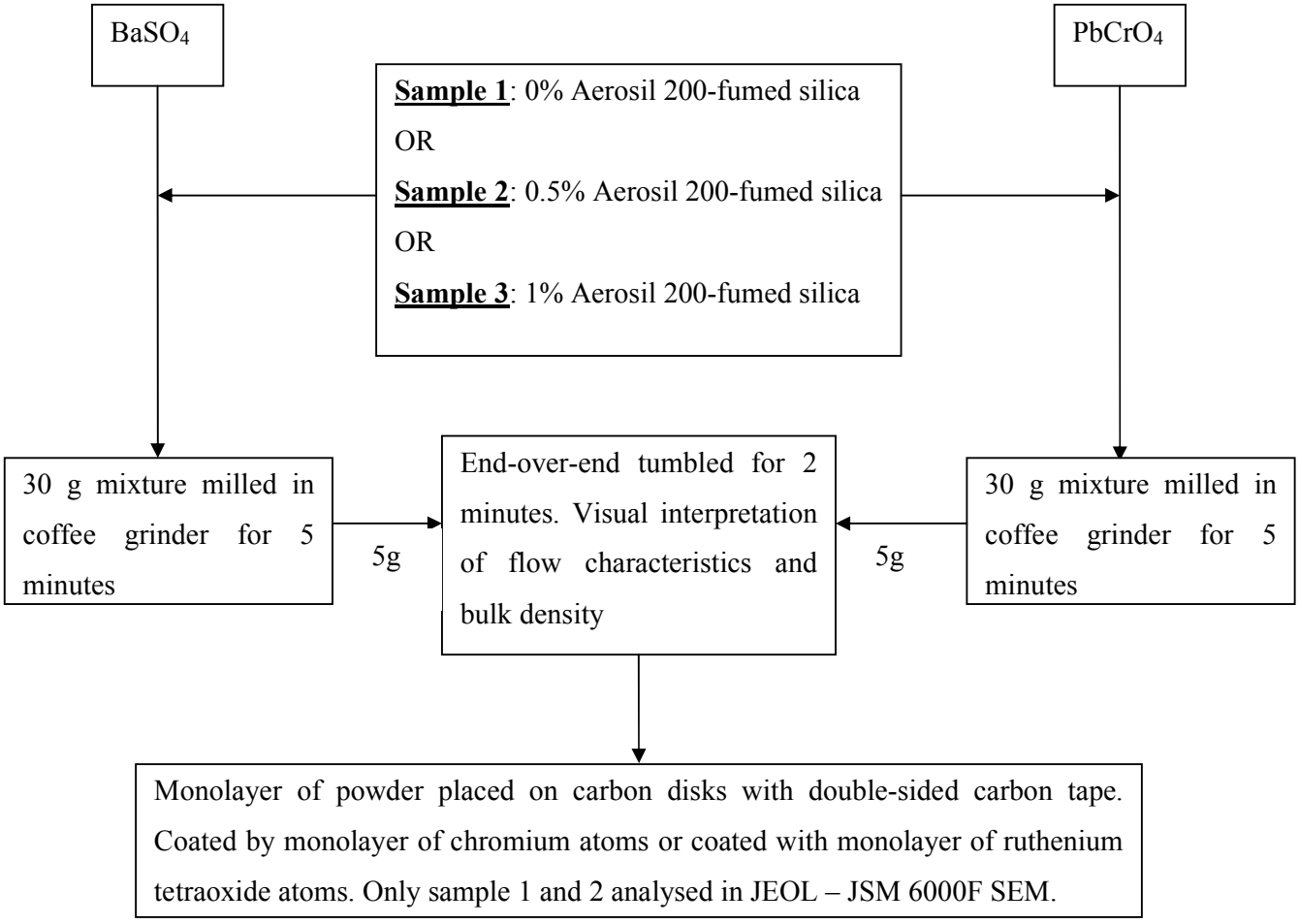

Figure 9-1: Formulation of Free Flowing Oxidants

9.2.2 Results and Discussion

It was observed that the addition of the Aerosil 200 fumed silica led to an increase in the bulk volume which the powders occupied as the fraction of the added fumed silica, increased. This was not expected as theoretically the bulk density was supposed

to increase. The bulk density increase is caused by the fluidisation of the individual particles; they flow and slip past each other readily so that they compact better (Tulis, 1980). It was therefore decided to measure the tapped bulk density of the powders before and after the addition of the nano-sized particles.

No visible difference was observed in the SEM as a result of coating with chromium or ruthenium tetraoxide.

No visible difference was observed in the SEM as a result of the amount of fumed silica which was added (Figure 9-2).

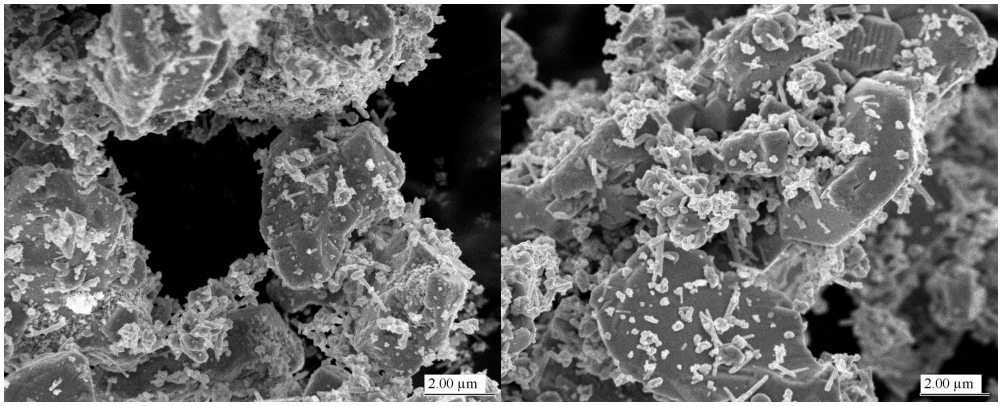

Figure 9-2: Comparison of Sample 1 (left) and Sample 2 (right)

The use of this processing method is limited by the fact that the addition fumed silicas and other inert fine particles, may coat the powders completely and not allow for proper solid to solid contact. This may result in propagation failures. It appeared, though, that this may be overcome through control of the amount which is added and the use of reactive nano-sized particles.

9.3 Formulation of Free Flowing Silicon

9.3.1 Experimental

The experimental procedure which was used has been summarised in Figure 9-3.

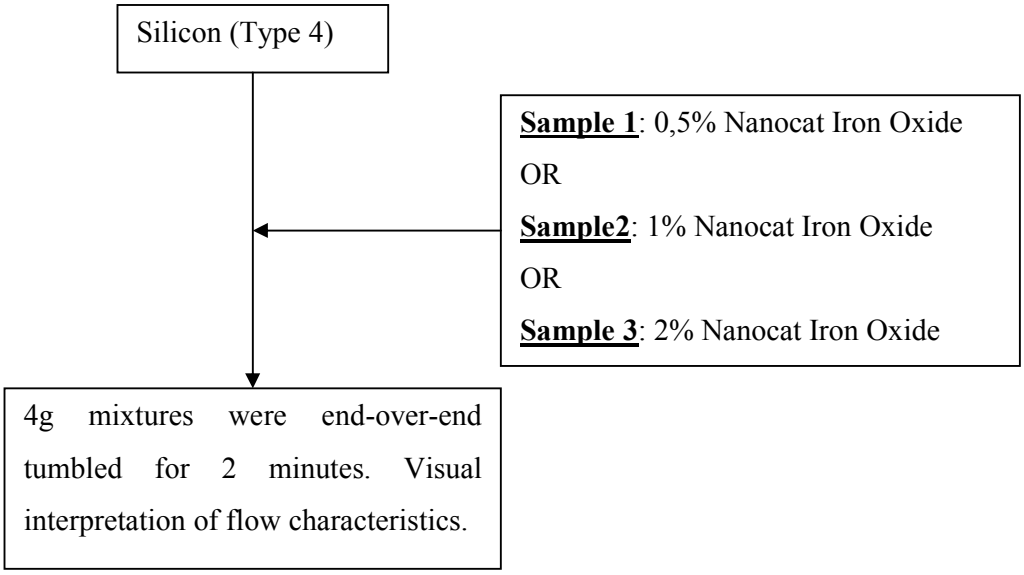

Figure 9-3: Formulation of Free Flowing Silicon

9.3.2 Results and Discussion

The addition of the Nanocat® iron oxide to the silicon did not improve the flow characteristics of the powder regardless of the amount that was added.

9.4 Tapped Bulk Density Measurements

9.4.1 Experimental

Apparatus:

A coffee grinder was used to blend the powders and the tapped bulk density was determined using a measuring cylinder and a mass balance

Reagents:

The reagents that were used may be found in Table 9-2.

Table 9-2: Reagents used in Bulk Density Measurements

Micro or Nano-sized Particles:	**Powders:**
Wacker hydrophobic fumed silica	Silicon
Fumed alumina	Barium sulphate
Fumed titanium dioxide	Antimony trioxide
Ultrasil VN3	
Aerosil 200 – hydrophilic fumed silica	
Nanocat (standard) – Iron oxide	
Nanocat (A) – Iron oxide	

Method:

A 30g mixture containing 1% of the one micro or nano-sized particles and 99% of one of the powders was accurately weighed out and placed in the coffee grinder. A standard of the powder alone was also used. The mixture was then milled in a coffee grinder for 1 minute. Some of the mixture was then placed in the measuring cylinder and the cylinder tapped until there was no powder along its sides and the solids level was distinct. The volume and the mass of the powder in the cylinder were noted and the bulk density calculated.

- *Barium Sulphate.* All the micro and nano-sized particles were used to determine the effect of their addition to the density of the barium sulphate.
- *Silicon.* Only the Wacker fumed silica was tested.
- *Antimony Trioxide.* Only the standard Nanocat was tested.

9.4.2 Results and Discussion

The tap densities that were measured are reported in Table 9-3.

Table 9-3: Modification of the Bulk Densities of $BaSO_4$, Si and Sb_2O_3 using Nanosized Particles

Powder	**Nano-sized Particle (1% Addition)**	**Bulk Density (kg/m^3)**
$BaSO_4$	No additive	1356
	Fumed Alumina	1187
	Fumed Titanium Dioxide	1451
	Ultrasil VN3	1194
	Wacker® Fumed Silica	*1439*
	Nanocat® – standard	1320
	Nanocat® A	1226
Si	No additive	354
	Wacker® Fumed Silica	*358*
Sb_2O_3	No additive	910
	Nanocat®	832

As can be seen, not all the particles used resulted in a higher bulk density. It should be noted that the Wacker® fumed silica addition did however lead to a slightly higher bulk density.

9.5 Addition of Wacker® HDK20 to Silicon compositions with $Cu(SbO_2)_2$, $PbCrO_4$ and Sb_2O_3 as Oxidants

9.5.1 Experimental

The compositions were prepared as follows:

- A batch of type 4 Si (79g) was weighed out and 1% Wacker® fumed silica (0.80g) was added to the Si. The mixture was blended in a coffee grinder for 2 minutes.

- The same procedure as for the preparation of the Si was followed for the preparation of the following powders:
    - 70g $Cu(SbO_2)_2$ and 1% Wacker® fumed silica (0.70g);
    - 65g $PbCrO_4$ and 1% Wacker® fumed silica (0.65g) and
    - 40g Sb_2O_3 and 1% Wacker® fumed silica (0.40g).
- The flow characteristics of mixtures were visually noted after the blending.
- The following pyrotechnic compositions using these batches were prepared – Table 9-4:

Table 9-4: Compositions Containing Wacker® Fumed Silica as Additive

Oxidant and 1% Wacker® fumed silica	**Mass Percentage Si and 1% Wacker® fumed silica**
Sb_2O_3	25; 30; 35
$Cu(SbO_2)_2$	20; 25; 30; 35; 40; 45
$PbCrO_4$	15; 20; 25; 30; 35; 40; 45

- The compositions were tumble mixed for 4 hours and loaded into lead tubes without brush mixing using the procedures outlined in Sections 6.3.1 and 6.3.5.
- Five detonators for each composition were assembled and the voltage profiles measured according to the procedures described in Sections 6.3.6 and 6.3.8 .
- The profiles were filtered and processed according to the procedure outlined in Section 6.3.10.

9.5.2 Results and Discussion

Flow Characteristics. During the mixing and loading of the compositions it was noted that at an addition level of 1% fumed silica the oxidants became free-flowing powders while Si still remained "sticky".

All the relevant data on the behaviour of the compositions during burning and burn rates is contained in Appendix K. The burn rate data have been summarised in Figures

9-4, 9-5 and 9-6 which also compare the data with measured burn rates without the addition of the fumed silica.

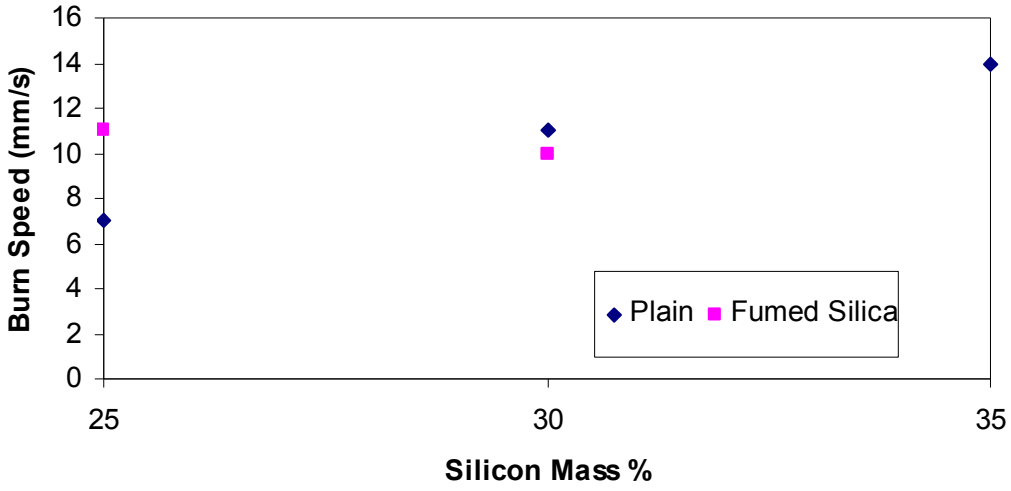

Figure 9-4: Effect of Stoichiometry and Wacker® HDK20 Fumed Silica Addition on the Burn Rate of Sb_2O_3-Type 4 Si

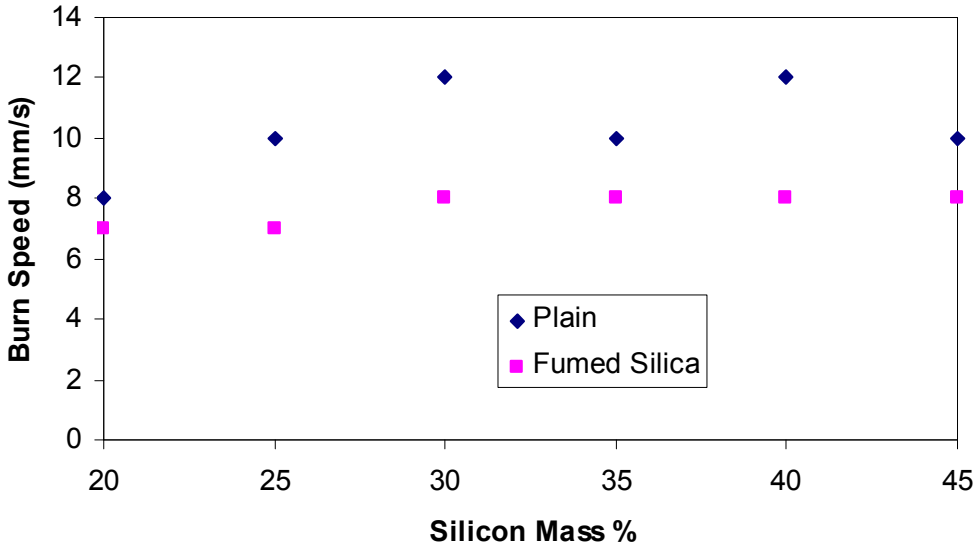

Figure 9-5: Effect of Stoichiometry and Wacker® HDK20 Fumed Silica Addition on the Burn Rate of $Cu(SbO_2)_2$-Type 4 Si

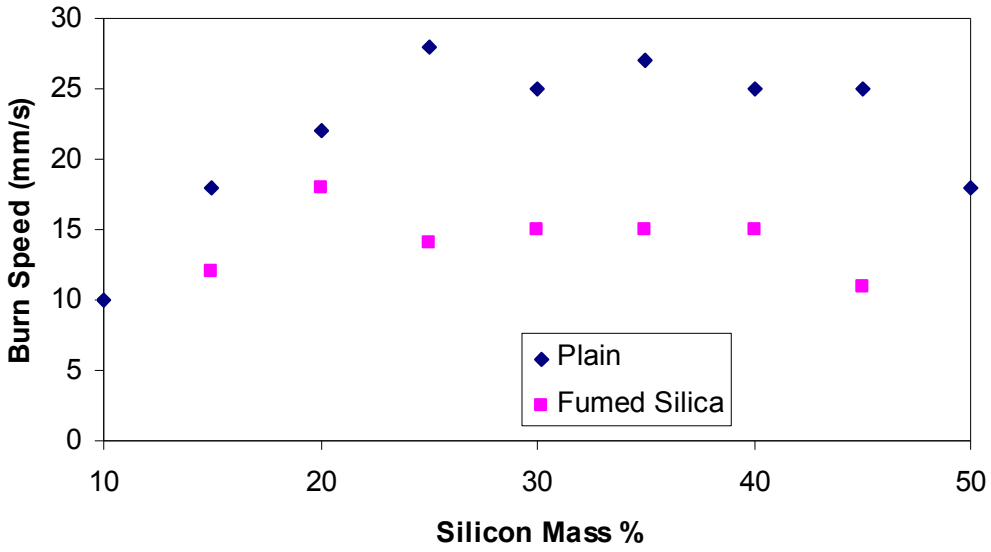

Figure 9-6: Effect of Stoichiometry and Wacker® HDK20 Fumed Silica Addition on the Burn Rate of $PbCrO_4$-Type 4 Si

Ignition and Burning. The compositions ignited and burnt with burn rates varying between 7-18mm/s. The Figures show that the burn rate was reduced significantly with the addition of the fumed silica. This was expected as the fumed silica acts a diluent and absorbs heat.

Nature of the Curves. After reaching the highest measured burn rate at 20% Si (18mm/s) for $PbCrO_4$ as oxidant, the measured burn rate was approximately constant at 15mm/s until 45% Si. This was also the case for $Cu(SbO_2)_2$-Si where the measured burn rates are constant from 30% Si onwards. The constant burn rates despite the change in stoichiometry is a welcome result for the implementation of either $PbCrO_4$ or $Cu(SbO_2)_2$ in industry because it means that should a slight error be made with the Si content the burn rate will remain unaffected.

Ignition Reliability. Figure 9-7 shows the ignition reliability as a function of silicon content with the addition of fumed silica. Comparing Figure 8-7 (repeated here) and Figure 9-7 shows that ignition reliability decreases slightly with the addition of fumed silica. As was seen before, the Sb_2O_3-based composition still remains unreliable in terms of ignitable mixtures, limiting its use (i.e. 25% Si-Sb_2O_3 is no longer ignitable

using shock tube). The occasional composition failed to ignite or the combustion wave failed to propagate.

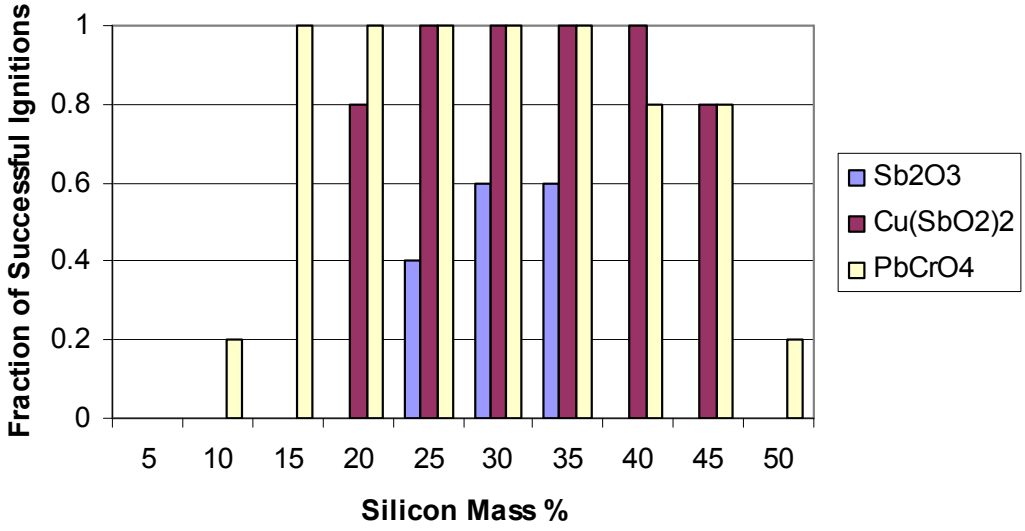

Figure 8-7 (Repeated): Fraction of Successful Ignitions as a Function of Stoichiometry for Tumbled and Brushed Type 4 Si-based Compositions for a Total of 5 Attempts

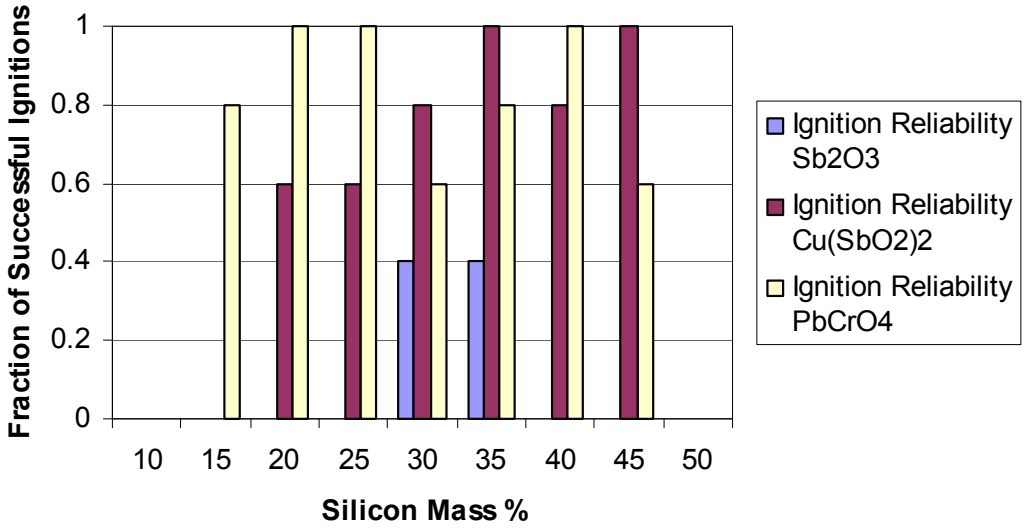

Figure 9-7: Fraction of Successful Ignitions as a Function of Stoichiometry for Type 4 Si-based Compositions with 1% Fumed Silica for a Total of 5 Attempts

Standard Deviation of Data. Generally the standard deviation in burn rate for the $Cu(SbO_2)_2$-based compositions was below 1mm/s. The standard deviation for the burn rates measured for the $PbCrO_4$-based compositions was as high as 3 mm/s.

Yet again it appears that only the "medium" and "slow" compositions can be replaced with the following compositions:

"Slow"	"Medium"
$Cu(SbO_2)_2$ 25% Si, Fumed Silica	$PbCrO_4$ 20% Si, Fumed silica
	$PbCrO_4$ 30-40%Si, Fumed silica

The comments and recommendations which have been made in Section 8.7 apply here and will not be repeated.

10. WET MIXING

10.1 Implications of Implementing Dispersions to Mix Formulations

One method of improving the formulation procedures currently used in practice would be to form stable solid aqueous dispersions of the mixtures. This could minimise the risk of fires, dust exposure and allow for easier mixing and handling of the powders to achieve constant thermal conductivity and solid-solid contact.

Dispersions have been used in industry for the processing of pyrotechnic formulations. Davitt and Yuill (1983) prepared mixtures of Si and SnO_2 by vigorous mechanical stirring of the ingredients in slurry form utilising water. The slurry was then filtered under vacuum and the resulting filter cake dried and sieved to obtain a reasonably free-flowing powder. Boberg *et al* (1997) have also mixed Si and various other reagents in water. The mixtures were oven dried to a water content of 7-10%, then granulated and dried once again to a 0.1% H_2O content.

A proposal (Appendix L) was written detailing what this entailed and a number of suggestions made for experimental work to be conducted using this method for the preparation of the delay compositions.

The problems encountered with powder processing and the reagent properties have already been summarised in Section 9.1 and Section 5.1 respectively. As can be deduced from the reagent properties the powders will have to be processed in weakly alkaline or preferably lower pH values due to the reaction of silicon in alkaline solutions and the dissolution of freshly precipitated antimony trioxide. This will eliminate the use of surfactants which result in a high pH and the precipitation of the oxidant directly onto the Si to promote intimate contact as most hydroxides (excluding iron hydroxides) precipitate at pH values above 8.

An alternative processing route was envisaged upon forming the stable dispersion i.e. the dispersions would be loaded directly into a rigid element, centrifuged to form a

dense sediment. The excess water removed and the elements dried further in the drying rooms available at AEL. An initial laboratory scale simulation was attempted by forming a dispersion of a Si-CuO mixture and filling glass tubes will the dispersions and subjecting the glass tube to centrifugation. The drying and dispersion characteristics of the composition were noted.

10.2 Effect of Addition of Surfactants to Si-CuO

10.2.1 Experimental

Three 20% solid slurries were formed by adding 4g of a type 4 Si-CuO (16% Si) to 16g of water. The slurries were then handled as follows:

- The first slurry or reference slurry was mixed using a high shear mixer at 13000rpm and transferred by pipette to fill glass tubes with varying diameters (ID 2.2, 3, 4 and 5mm). The mass of the glass tubes were noted before the addition.
- A quantity of Tamol (a surfactant obtained from BASF) i.e. 1% of the solids' mass in the slurry was added in the dry form to the slurry. The slurry was then subjected to the high speed shear mixer (13 000rpm) and similarly transferred by pipette to glass tubes with varying diameters.
- Similarly, a quantity of DisperByk i.e. 1% of the solids' mass in the slurry was added to the slurry. The slurry was then mixed using the high shear mixer and once again transferred to glass tubes with varying diameters.

The nature of the dispersions were evaluated visually and the mass of the tubes after the addition of the slurries noted before being centrifuged for 40min at 2500rpm in a small laboratory centrifuge. The height of the solids after centrifuging was measured and the top layer of water removed carefully using a pipette so as to not disturb or remove the solids. The mass of material and the tubes was noted once again. The tubes were then dried for a day in a desiccators under vacuum and with P_2O_5. The mass of the tubes were to be noted after the drying and the slurry visually evaluated for degree of dryness.

10.2.2 Results and Discussion

The experimental data sheet is contained in Appendix M. The initial results have been summarised in Table 10-1.

Table 10-1: Effect of Surfactant Addition to Type 4 Si-CuO

	Reference	Tamol	DisperByk
Initial mass of slurry (g)	**2.2** - 0.267 **3** - 0.626 **4** – 1.168 **5** - 1.851	**2.2** – 0.139 **3** – 0.719 **4** – 1.154 **5** – 1.889	**2.2** – 0.152 **3** - 0.655 **4** – 1.137 **5** – 1.806
Height after initial water removal and centrifuge	**2.2** – 16mm and 10mm at 38mm (Included layer of water i.e. 2 solid layers) **3** – 29mm **4** – 32mm **5** – 33mm	**2.2** – 25mm **3** – 55mm **4** – 60mm **5** – 66mm	Could not be determined as no separation had occurred
Height after drying for a day	*Material for all tubes appeared as if had shot out of tubes due to the production of gas*		

As mentioned previously Si cannot be processed in an alkaline environment due to its violent reaction and the production of hydrogen gas. When formulating a 17% CuO slurry it was found that the pH was 8.78. In the processing of the $Cu(SbO_2)_2$-based compositions, this will also be a problem as even after 4 washes the $Cu(SbO_2)_2$ still resulted in a slurry with a pH of 11.53.

These problems have not been reported by Boberg *et al* (1997) and Davitt and Yuill (1983) and it is thought that this is due to the short time which the Si and oxidants were in contact with water, i.e. were dried immediately. It may perhaps be beneficial to investigate whether this is the case by mixing the ingredients in water using a

surfactant and then drying it immediately by filtration and oven drying at low temperatures. This will affect the burn characteristics due to the presence of the surfactant and the heat pre-treatment of the ingredients before loading into tubes.

11. INCORPORATION INTO A THERMOSET RESIN OR THERMOPLASTIC

11.1 Thermosets and Thermoplastics

Thermosets are formed in a processing mould from moderately large molecular building blocks (reactive precursors) by chemical reaction, whereas with thermoplastics, the finished high-molecular material is merely physically remelted in the mould. This means that thermosets no longer melt and are processed far below their application temperature whilst, thermoplastics can be remelted and must thus be processed at temperatures above their temperatures of application (Schönthaler, 1995:665).

Thermosets that are available include phenolic-, urea-, melamine resins, as well as others based on unsaturated polyester-, diallyl phthalate-, epoxy- and silicone resins. Thermosetting moulding compounds have been compounded from binders and fillers that reinforce the mouldings, economise on resin and broaden the range of application of the resins. An extremely wide variety of materials are used as fillers i.e. organic and inorganic materials. The binders or resins can be combined with the filler. The properties of the cured moulded material are the sum of the properties of the resins and of the fillers, i.e. thus for a given filler, the typical binder properties and for a given binder typical filler properties are also observed (Schönthaler, 1995:665-7).

Thermosets may be manufactured via two routes. The fusion process entails the production of a premix from finely ground solid resin, fillers, etc. The premix is then further compounded on roll mills or extruders. When using roll mills, the fillers are impregnated with the binder and the material is homogenised. According to Schönthaler, (1995:668), the fusion process is best suited for powder or short-fiber fillers. The liquid resin process is used mainly for compounding thermosetting moulding materials that contain long-fiber or macerate fillers (Schönthaler, 1995:668-669). Barr (2000) has stated that addition of the powder may influence the cure rates

of these compounds, but the cure rate may be accelerated by the addition of a catalyst that will react with the silicone.

Silicone resin compounds have been found to satisfy high electrical and thermal requirements and have a high temperature stability, even over long periods. Schönthaler, (1995:675) has reported silicone resins as being very expensive.

The calorific values from the incineration of thermosetting compounds have been reported to be typically about 12 500 – 21 000 kJ/kg (Schönthaler, 1995:665).

Beck (1984) incorporated a small amount of PVC into Sb/$KMnO_4$ system and found that at small additions <1%, the burn rate increased, but larger proportions resulted in a decrease in the burn rate and a very gassy system.

11.2 Reaction of Metal Powders with Fluorine-containing Polymers

The use of fluorine or its derivatives as oxidisers in various propellants and explosives has been recognised for many years. The reaction of fluorine and its derivatives with metals and metal hydrides is used in flares, igniters and incendiaries (Lee *et al*, 1997). According to Lee *et al* (1997) the higher cost of using the fluorine-based oxidisers can be justified by their unique characteristics.

Metal powders such as aluminium, magnesium, titanium and hafnium react exothermically with decomposition products of fluorine containing polymers to produce metal fluorides, generally in the gaseous state yielding a comparatively high flame temperature, enthalpy release and energy density. It has been stated that the decomposition temperature and extent of reaction depends on the size and shape of the metal particles. In general oxidation is retarded by the thin oxide layer which is present on the surface of the metal and reactions with decomposed fluorine compounds are greatly influenced by the quality of the oxide layer (Lee *et al*, 1997).

Lee *et al* (1997) used thermal analysis to determine the ignition temperature and the extent of reaction, i.e. from room temperature to 1000°C at a heating rate of 10°C/min with an Ar atmosphere. A summary of their results is reported in Figure 11-1.

Fluorine containing polymers decompose by depolymerisation to the volatile matter. In general if a reaction occurred the following reactions are expected:

$$2Al + 3CF_2 \rightarrow 2AlF_3 + 3C(s) \text{ for PTFE and}$$

$$4Al + 3(CF_2(Cl)CF_2) \rightarrow 4AlF_3 + 6C(s) + 3Cl \text{ for Kel F}$$

However in the presence of fluorine and oxygen containing compounds, the thermochemical calculations predict AlOF as a major product (Lee *et al*, 1997).

Results and Discussion

Polymers

Melting- 348°C. Complete decomposition – 556°C (PTFE) and 425°C (Kel F).No difference in thermal behaviour due to size but crystallinity has effect

Al/PTFE

20μm – exothermic peak and mass loss at 530°C – reaction not violent enough for useful energetic application. Gradual mass increase till 1000°C.

200nm – strong exothermic peak at 520°C

Al/Kel F

Exothermic reaction 840°C. Major mass loss started at 197°. 661°C – endothermic peak = Al melting

Al/iodoform

Single exothermic reaction at 163°C –decomposition of iodoform. Endotherm at 661°C- Al melting. No reaction or mass gain – depletion of oxidiser due to low melting point of iodoform

Al/DBDPE

Mass loss (85%) at 450°C. Small broad exothermic peak with mass gain at 850°C – weak Al-Br bond compared to Al-F

Ti

Ti/PTFE – strong exotherm at 500°C. Mass gain.

Ti/Kel F – 470 and 630°C

General Comments

- Al- reactions not as exothermic as desired. Increasing exothermicity as increased bond strength of Al-X (X=F, Br, I).
- Ti different to al due to difference in oxide layers – TiO_2 is more porous and diffusion is easier.

Figure 11-1: Summary of Experimental Results Reported for Metal Powders and Halogen-containing Polymers

11.3 Incorporation into Silicone Oil

11.3.1 Experimental

Planning

It was decided to fill silicone oil with some of the powders and one of the mixtures. The maximum amount of powder, which could be added, was determined and used to calculate whether enough oxidant could be added to the silicone oil. The mixtures were also ignited in a fume hood to check the propagation and burning characteristics of the filled oil.

Apparatus and Reagents

The following reagents were used:

- Silicone Oil – VSF 500 (Supplied by Silicon and Technical Products)
- Barium sulphate
- Silicon
- Red lead
- Antimony trioxide
- Antimony trioxide-Silicon mixture (14%Si).

A mass balance was used to accurately determine the mass of each of the reagents. The mixtures were stirred using a glass rod.

Method

Filling of the Silicone Oil

A known mass of the silicone oil was added to a beaker. Each of the powders was added in increments of approximately 0.5g and stirred after each addition. The addition continued until the oil-powder mixtures or pastes appeared to be almost dry

and could not flow. The total mass of powder was then noted and the maximum ratio of powder:silicone oil was determined.

Calculation of the Required Amounts of Silicone Oil and Oxidants

The required amount of each of the oxidants to allow for complete combustion of the silicone oil was calculated based on the silicone oil having the following chemical formula: $SiO(CH_3)_2$.

Burn rate Screening Tests

The mixtures were evaluated using the procedure described in Section 6.3.3.

11.3.2 Results and Discussion

Filling of the Silicone Oil

The maximum ratios of the powders to silicone oil that could be added have been reported in Table 11-1.

Table 11-1: Maximum Ratios Obtained for Filling Silicone Oil

Powder Added	**Mass Silicone Oil Added (g)**	**Mass Powder Added (g)**	**Mass Ratio of Powder to Silicone Oil**
Si	5.125	5.966	1.164
$BaSO_4$	5.180	10.377	2.003
Sb_2O_3	17.427	33.096	1.900
Pb_3O_4	21.285	118.110	5.549
Si-Sb_2O_3 mixture	0.753	1.029	1.367

It is apparent from the Table that more red lead can be added to the oil than any of the other powders.

Required Amounts of the Fuels and Oxidants

A summary of the results is reported in Table 11-2.

Table 11-2: Theoretically Required Mass of Oxidant for Complete Combustion of Silicone Oil

Oxidant	**Theoretical Mass Ratio of Oxidant to Silicone Oil**
$BaSO_4$	13.40
Pb_3O_4	39.76
Sb_2O_3	22.32

When comparing these calculated values with the maximum ratios that could be added experimentally, it can be seen that not enough oxidant can be added to the silicone oil to ensure complete combustion.

Burn rate Screening Tests

The flame front for all the mixtures failed to propagate and was extinguished immediately. Thereby proving that not enough oxygen is available from the oxidants for the combustion of the silicone oil.

11.4 Reaction of a Metal Powder with a Bromine Oxidiser

11.4.1 Experimental

Table 11-3 contains a summary of the supplier and masses of the reagents used.

Table 11-3: Reagents used for Reaction of Al with a Bromine Flame Retardant

Reagent	**Supplier**	**Mass (g)**
Al	Zimalco	1.936
2,3 dimethly-2,3-diphenyl butane (CCDFB)	Peroxid Chemie	1.400
bis-(2,3,4,5-tetrabromophenyl)ether (OCTA)	Dead Sea Bromine	28.000

The amount of Al which was added was based on a 20% excess (mol basis) of Al to the number of moles of Br in the OCTA based on the formation of $AlBr_3$. CCDFB was added to act as a free radical producer at 230°C to enhance reactivity. The amount of CCDFB added was based on 5% of the mass of the OCTA. The OCTA and CCDFB were added together and ground carefully with a mortar and pestle. The mixture was then transferred to a polytop and the Al added. After tumble mixing for 4 hours the propagation and burning characteristics of the mixture was visually interpreted using the procedure outlined in Section 6.3.3. TGA and DTA analysis of the sample was also completed in an air atmosphere (30ml/min) at 20°C/min in an alumina crucible.

11.4.2 Results

The mixture failed to ignite during the visual evaluation of the burn characteristics. So it was decided not to confine the mixtures into a detonator.

The TGA and DTA analysis yielded the data in Figure 11-2. As can be seen from the Figure, similar to the DBDPE used by Lee *et al* (1997) an initial 93% mass loss is obtained starting at 172°C and ending at 638°C with the majority of the mass loss occurring between 400-500°C. A small exothermic peak is evident at 556°C. There is also a small endothermic peak at 658°C which corresponds to the melting point of Al. Unlike Lee *et al* (1997)'s results, no small, broad exothermic peak with mass gain is evident at 850°C.

From the results, it appears that despite the reported exothermicity of the formation of $AlBr_3$, it appears that this is not a viable option for delay compositions. The mixtures based on Al and Br do not ignite and there is large amount of gas produced from the decomposition of the OCTA.

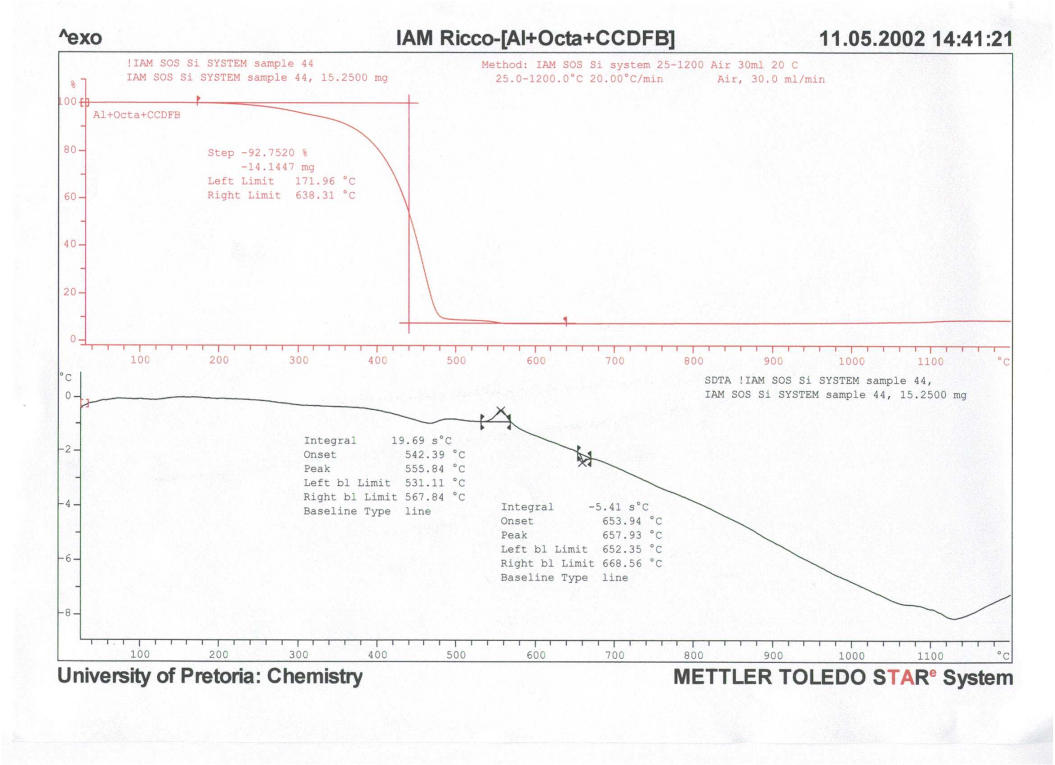

Figure 11-2: TGA/DTA Analysis of Al, OCTA and CCDFB Mixture

12. CONCLUSIONS AND RECOMMENDATIONS

12.1 Review

At present commercial time delay elements manufactured by AEL contain silicon as fuel. It is used in conjunction with three possible oxidisers: red lead, lead dioxide and barium sulphate. The main objective of the investigation was to find alternative oxidants for these time delay elements maintaining the use of silicon as fuel. The required burn speed range was 4 to 250mm/s. The lead compounds need to be replaced because of toxicity concerns during manufacture. The barium sulphate system is plagued with variable ignition and burn rate performance. The requirements for a delay element composition include:

- A constant, repeatable burn speed within a given manufactured batch.
- A "gasless" reaction which is directly ignitable using shock tube (a weak ignition source) and
- A safe, moisture-resistant composition that does not deteriorate with time.

A typical time delay composition comprises of an oxidant, a fuel and processing as well as burn rate moderating additives. These constituents are mixed in powder form and pressed into monolithic delay elements.

In practice, reliable ignition is paramount owing to its safety implications. Repeatable burn rates are very important for efficient use of the explosive during mining and quarrying. Many variables affect the reactivity and thus ignitability and burn rate of time delay compositions. They have been identified and can be divided into three categories:

- *Constituent Material Properties.* These include deviations from the normal crystallographic amorphous structure of the substance, lattice defects in the form of hereditary structures, formation of imperfect structures during transitions or thermal decomposition, impurities and guest particles in the lattice, gases dissolved in the lattice, the nature of the oxidant and fuel and particle shape and size.

- *Compositional Properties.* These include processing and burn rate moderating additives (catalysts, fluxes, binders etc.) and stoichiometry.
- *Processing and End-use Properties.* These include mechanical treatment such as grinding or pressing, degree of mixing, heat pre-treatment, aging, irradiation, compact density, ambient pressure, cross sectional area and surrounding material.

It is essential that a constant thermal conductivity and constant solid-solid contact is maintained to ensure repeatability in terms of burn speed and ignitability.

12.2 Experimental Review

Samples were prepared by tumble mixing followed by brush mixing. Elements were made by filling lead tubes and compacting the powder by drawing down the lead tubes. The compaction of the sample and pyrotechnic core diameter could not be controlled due to the nature of the equipment.

In the laboratory, the compositions were ignited using Exel shock tube, a weak ignition source. During industrial tests (AEL trials) "starter" and "sealing" compositions were used to ignite the delay elements. The "starter" composition is a stronger ignition source.

The burn rate of the compositions was measured using two thermocouples attached via an electronic interface to a data acquisition computer. The thermocouples were inserted a known distance apart into two holes drilled into the detonator assembly that had no explosive charge. The time between the voltage profiles at a fixed voltage was determined and the burn rate calculated. The shortcomings of this method included the drilling processes and the presence of the holes which affects the burn rate of compositions that produce gas. The data smoothing was performed using a first order digital filter. Absolute temperature profiles could not be derived due to the lack of cold junction compensation and thermocouple calibration.

12.3 Conclusions

12.3.1 Ignition.

- The mode of ignition affects the reliability of ignition of the compositions, i.e. MnO_2-Si was ignitable using a "starter" element during industrial trials (AEL trials), but failed to ignite using shock tube directly (laboratory trials). The following oxidants were directly ignitable with shock tube and tested successfully with silicon powders as fuel: Sb_2O_3, $Cu(SbO_2)_2$ and $PbCrO_4$.
- The composition range over which ignition was successful is wider when a strong ignition source is used e.g. the ignitable composition range of Sb_2O_3-Si obtained during this study was markedly narrower than that reported in literature where a stronger source was used.
- The ignition reliability was found to decrease when the fuel particle size increased, e.g. Sb_2O_3-based compositions failed to ignite when types 1, 2, 3 and 5 Si were used.
- The ignition reliability decreased when the addition level of aluminium powder was increased.
- The addition of a low percentage of fumed silica affected the ignition reliability slightly.

12.3.2 Burn Rates

The burn rate was strongly affected by the nature of the oxidant, stoichiometry and the addition of Al and fumed silica. The burn rate data obtained for compositions that were only tumble mixed appears dubious to the presence of agglomerates in compositions. Lead chromate is potentially a suitable alternative to the oxidant currently used in "medium" composition and copper antimonite is potentially a suitable alternative oxidant for "slow" and "medium" compositions that are currently used by AEL. The need for a "starter" composition is eliminated as both the $Cu(SbO_2)_2$ and $PbCrO_4$-based compositions are directly ignitable using shock tube. The $PbCrO_4$-based compositions require the use of a "sealing" composition due to gas

flowing in the opposite direction to which the burn front is travelling. No alternative compositions were found for the "sealing" and "fast" compositions.

Antimony trioxide - Silicon

Stoichiometry. The Sb_2O_3-based compositions exhibited burn rates between 7 and 14mm/s over the stoichiometric range where shock tube ignition was achieved i.e. 25-35% Si for type 4 Si. These burn rates were higher than those reported in literature due to the difference in Si particle size. The compositions exhibited occasional ignition failure rendering them unsuitable for commercial application.

Varying Fuel Particle Size. The ignitability of Sb_2O_3 is very dependent on the fuel particle size i.e. neither type 1, 2, 3 or 5 Si ignited. This is unfortunate because particle size can not be used to modify burn rates to suit practical application.

The Addition of Aluminium. The addition of aluminium reduced the burn rate slightly and resulted in compositions which were gassier.

Copper Antominite-Silicon

Stoichiometry. The $Cu(SbO_2)_2$-based compositions showed a bimodal burn rate variation with stoichiometry. Measured burn rates varied between 8-12mm/s over the composition range which was ignitable (20-45% Si).

Varying Fuel Particle Size. Increasing the silicon particle size decreased the burn speed for copper antimonite-based compositions. Increasing the Si particle size above 3.5μm resulted in compositions which failed to ignite using shock tube. The bimodal burn rate variation with stoichiometry was no longer evident.

Aluminium Addition. The addition of aluminium reduced the measured burn speeds. The bimodal distribution was once again evident for all addition levels of aluminium. The compositions were also gassier.

Lead Chromate-Silicon.

Stoichiometry. The $PbCrO_4$-based compositions had a bimodal burn rate distribution as the stoichiometry was varied with the measured burn rates varying between 10-28mm/s over the composition range which was ignitable (10-50% Si).

Varying Fuel Particle Size. Increasing the silicon particle size decreased the burn speed for the lead chromate-based compositions. Increasing the Si particle size above 3.5μm resulted in compositions that were not ignitable using shock tube.

Iron oxide-Silicon. Despite attempts at varying the size and origin of the iron oxide used, none of the compositions were ignitable using shock tube.

12.3.3 Alternative Processing

Dry mixing with fumed silica as processing aid

As mentioned previously solid-solid contact is very important in obtaining repeatable performance. This is best achieved if the oxidant and fuel individually dispersed in the pyrotechnic mixture. However, solid particles have a strong tendency to agglomerate. Owing to the sensitivity of pyrotechnic mixtures, high shear is avoided during mixing of the compositions. The use of fumed silica to break down agglomerates in the fuel and oxidant before mixing was explored. Even small amounts of fumed silica adsorbed on the individual particle cause separation and agglomerate breakdown. This is visualised by the free flowing nature of the solid powder in the presence of silica. The objective was to achieve complete mixing by tumbling alone. These tests proved that the addition of 1% Wacker® HDK20 (fumed silica) improved the flow characteristics of the $PbCrO_4$, $Cu(SbO_2)_2$ and Sb_2O_3, but the Si remained slightly "sticky".

Reliable ignition and constant burn speeds were achieved with only tumble mixing as a result of the addition of small amounts of Wacker® HDK20. The measured burn

rates were reduced for all the compositions as the fumed silica acted as a diluent. Furthermore the bimodal burn rate distributions which were evident previously for $PbCrO_4$ and $Cu(SbO_2)_2$-based compositions were no longer evident. $Cu(SbO_2)_2$ had a constant burn rate (8mm/s) from 30%Si onwards whilst $PbCrO_4$ had a constant burn rate of 15mm/s from 25-45% Si. This is a welcome result as should a slight error be made with the Si content during processing, the batch will not be ruined as the burn rate remains unaffected. Once again it appears that replacements for "slow" and "medium" compositions have been found.

Wet mixing.

Safe dispersion and intimate mixing of pyrotechnic compositions is in principle also possible in a water medium. The process of particle agglomerate breakdown is further aided by using surfactants as dispersants. For the present situation this option was only considered for the Si-CuO system. Problems were encountered with the high resultant pH of the dispersion. Silicon reacts violently in an alkaline medium. A dispersion of $Cu(SbO_2)_2$ was also found to alkaline.

The mixing of $Cu(SbO_2)_2$, CuO and Si using a dispersions followed by centrifuging into a rigid element is not possible due to the alkaline nature of $Cu(SbO_2)_2$ and CuO and Si reacts violently in alkaline solutions.

Incorporation into a thermoset resin or thermoplastic.

All mixtures failed to ignite when incorporated in silicone oil suggesting the use of more energetic compositions. Al, OCTA and CCDFB failed to ignite and the reported exothermicity of the formation of $AlBr_3$ was not evident. The mixture exhibited a major mass loss during TG/DTA analysis rendering it unviable for use in time delays.

12.4 Recommendations

The following recommendations are made for further work:

Literature Review

- Investigate the effect of introducing impurities into the Si crystal lattice and compare the reactivity of n and p-type reducing agents and n and p-type reducing agents.
- Investigate the types of binders used and the implications of their use.
- Investigate the effect of irradiating the silicon to change conductivity and reactivity. The effects of aging on the burn rate of irradiated samples should be noted.
- Investigate the effect of modifying particle shape and size (by changing precipitation conditions such as concentration, the addition of seed particles and temperature) of $Cu(SbO_2)_2$ on the burn rate.
- Investigate the use of alternative materials (metal-lined polymeric rigid elements) in order to phase out the use of lead drawn elements
- Investigate the effect of mechanical and heat pre-treatment of the reagents on the combustion products and burn rate.
- Investigate the effect of varying compaction by varying the consolidation pressure and initial density. It would be necessary to measure the density of the final product to determine the effect of absorbed gases as a function of initial densities and to compare these results to compositions whose reagents have been preheated to remove the absorbed gases.
- Analyse the effect of varying the pyrotechnic core diameter.
- Determine if the reactions are truly solid-solid reactions
- Analyse the reaction products.

Equipment and Further Analysis

- Evaluate whether an oxide layer has been included in the thermocouple junction by spot welding.

- Modify the data acquisition set up to include cold junction compensation (CJC) before feeding the signal to the computer by installing equipment that models CJC electronically.
- Correct for thermocouple size using the method prescribed by Boddington *et al* (1982 and 1986).
- Investigate the implications of using pyrometry as an alternative temperature sensing device.
- Investigate the possible use of photocells or a high speed camera to measure the burn speed.
- Investigate the effect that different methods of smoothing have on the extraction of kinetic parameters from temperature profiles.
- Convert voltage profiles to temperature profiles.
- Extract kinetic data and burn velocities using the Leeds Method.
- Consider triggering the data acquisition by an electric input from the "mouse trap" and only have one opening for the insertion of a thermocouple.
- Investigate the feasibility of using:
    - Time-resolved XRD to monitor component melting and crystal formation during combustion.
    - SEM to analyse the microstructure of quenched samples (reaction is frozen).
    - A high speed digital video camera to monitor the combustion front and measure burn rate
    - The pressure apparatus available from AEL to monitor pressure changes
    - A probe technique to measure the thermal conductivity of compositions

Alternative Oxidants

- Investigate the effect of aging on $Cu(SbO_2)_2$-Si

Modification of the Burn Rate

- Measure the burn speeds or $Cu(SbO_2)_2$ and $PbCrO_4$-based compositions using commercial detonator assemblies and test facilities.
- Determine the burn rates for >45% Si for Type 3 Si-$Cu(SbO_2)_2$.
- Investigate the implications of large scale manufacture of $Cu(SbO_2)_2$.
- Investigate the use of intermetallic reactions as an alternative to achieve the desired burn rate for the "fast" and "sealing" compositions.

Alternative Processing

- Investigate the possibility of mixing of the constituents in water, using a surfactant and filtering the slurry immediately, followed by oven drying using low temperatures. The effect of surfactant coating and heat pre-treatment of the compositions should be noted.

13. REFERENCES

- Adrian G (1993) Pigments, Inorganic in *Ullmann's Encyclopedia of Industrial Chemistry*, Elvers, B. (editor), VCH Publishers, fifth revised edition, A20, Weinheim, Germany.
- *AEL Raw Material Specification* (1994) Barium Sulphate – "Blanc Fixe N", Document reference 073.
- *AEL Product Specification* (2000a) Delay Composition "*starter, fast, medium and slow"*, Drawn Lead Rod, Single Core, Doc. Ref 281 revision B.
- *AEL Product Specification* (2000b) Delay Composition "*sealing"*, Drawn Lead Rod, Single Core, Doc. Ref 281/01 revision A.
- Albano M P and Garrido L B (1999) Improvement of Ammonium Polyacrylate Adsoprtion on Si_3N_4 Powders by an Aluminium Hydroxide Coating, *Materials Letters,* 38, 431-436.
- Aldushin A P and Zeinenko K I (1992) Combustion of Pyrotechnic Mixtures with Heat Transfer from Gaseous Products, *Combustion, Explosion and Shock Waves*, 27 (6), 700-703.
- Al-Kazaji S S and Rees G J (1978) The Fast Pyrotechnic Reaction of Silicon and Red Lead – Part 1: Differential Thermal Analysis Studies, *Combustion and Flame*, 31, 105-113.
- Al-Kazaji S S and Rees G J (1979a) Differential Thermal Analysis Studies of the Reactions of Silicon and Lead Oxides*, Journal of Thermal Analysis*, 16, 35-39.
- Al-Kazaji S S and Rees G J (1979b) The Fast Pyrotechnic Reaction of Silicon and Red Lead – Heats of Reaction and Rates of Burning, *Fuel*, 58, 139-143.
- Barin I (1989) *Thermochemical Properties of Inorganic Substances*, vol. 2, New York.
- Barr N (2000) *Personal Communication*, affiliated to Dow Corning.
- Baudis U (1985) Barium and Barium Compounds in *Ullmann's Encyclopedia of Industrial Chemistry*, 5th edition, vol. A3, Wolfgang G (Ed), VCH Publishers, Weinheim, Germany.
- *Bayer Paint Shade Card Brochure* (s.a) Inorganic Bayer Pigments: Bayferrox, Document Edition: 6.97.

- Beck M W (1984) Intersolid Combustion Reactions in Pyrotechnic Systems, *PhD Thesis,* Rhodes University, South Africa.
- Beck M W and Brown M E (1986) Modification of the Burning rate of Antimony/Potassium Permanganate Pyrotechnic Delay Compositions, *Combustion and Flame*, 66, 67-75.
- Beck M W (1989) A Preliminary Investigation into the Si/$BaSO_4$ combustion Mechanism*, ICI Explosives Group Technical Report no.684*, Ardeer Site.
- Beck M W and Brown M E (1991) Finite-element Simulation of the Differential Thermal Analysis Response to Ignition of a Pyrotechnic Composition, *Journal of the Chemistry Society of Faraday Transactions*, 87(5), 711-715.
- Beck M W and Flanagan J (1992) *Delay Composition and Device, Patent*, US 5 147 476.
- Beretka J (1984) Kinetic Analysis of Solid-State Reactions between Powdered Reactants, *Journal of the American Chemical Society*, 67(9), 615-620.
- Bergström L (1997) Hamaker Constants of Inorganic Materials, *Advances in Colloid and Interface Science*, 70, 125-169.
- Birchenall C E (1986) Oxidation of Metals and Alloys in *Encyclopedia of Materials Science and Engineering*, vol. 5, Beuer M B (Ed.), Pergamon Press.
- Boberg T, Carlsson S, Ekman B and Karlsson B (1997) *Delay Charge and Element and Detonator Containing such a Charge, Patent,* US 5 654 520.
- Boddington T, Laye P G, Pude J R G and Tipping J (1982) Temperature Profile Analysis of Pyrotechnic Systems, *Combustion and Flame*, 47, 235-254.
- Boddington T, Laye P G, Tipping J and Whalley D (1986) Kinetic Analysis of Temperature Profiles of Pyrotechnic Systems, *Combustion and Flame*, 63, 359-368.
- Boddington T, Cottrell A, Laye P G and Singh M (1986) Times-to-Ignition of Pyrotechnics, *Thermochimica Acta*, 106, 253-261.
- Boddington T, Cottrell A and Laye P G (1989) Combustion Transfer in Gasless Pyrotechnics, *Combustion and Flame*, 79, 234-241.
- Boddington T, Cottrell A and Laye P G (1990) A Numerical Model of Combustion in Gasless Pyrotechnics, *Combustion and Flame*, 76, 63-69.
- Bognolo G (2000) Structure-Performance Relationship, paper presented at *Surfactant Technology and its Applications course*, 2-4 August 2000, University of Pretoria, Pretoria, South Africa.

- Brauer K O (1974) *Handbook of Pyrotechnics*, Chemical Publishing Company, New York, United States.
- Broadbent M (2000) Introduction to Surfactants, *paper presented at Surfactant Technology and its Applications course*, 2-4 August 2000, University of Pretoria, Pretoria, South Africa.
- Brown M E (1989) Thermal Analysis of Energetic Materials, *Thermochimica Acta*, 148, 521-531.
- *Cabot Corporation* (2000), http://www.cabosil, http://www.cabot-corp.com/cabosil, 21/07/2000.
- Cardellini F, Mazzone G and Antisari M V (1996) Solid State Reactions and Microstructural Evolution of Al-Ni Powders During High-Energy Ball Milling, *Acta Mater*., 44(4), 1511-1517.
- Carr D S (1993) Lead Compounds in *Ullmann's Encyclopedia of Industrial Chemistry,* 5th edition, vol. A26, Elvers B (Ed), VCH Publishers, Weinheim, Germany.
- Charsley E L, Ford M C, Tolhurst D E, Barid-Parker S, Boddington T and Laye P G (1978) Differential Thermal Analysis and Temperature Profile Analysis of Pyrotechnic Delay Systems: Mixtures of Tungsten and Potassium Dichromate, *Thermochimica Acta*, 25, 131-141.
- Charsley E L, Chen C, Boddington T, Laye P G and Pude J R G (1980) Differential Thermal Analysis and Temperature Profile Analysis of Pyrotechnic Delay Systems: Ternary Mixtures of Silicon, Boron and Potassium Dichromate, *Thermochimica Acta*, 35, 141-152.
- Churaev N V (1995) Contact Angles and Surface Forces, *Advances in Colloid and Interface Science*, 58, 85-118.
- Conkling J A (1996) Pyrotechnics in *Kirk Othmers' Encyclopedia of Chemical Technology*, J. I. Krosschwitz (Exec. Ed.), John Wiley and Sons, volume 20, 680-697, New York, United States.
- *CRC Handbook for Chemistry and Physics* (1992) Lide D R (Ed), CRC Press, Boca Raton, Florida, United States.
- Crider J F (1982) Self-Propagating High Temperature Synthesis – A Soviet Method for Producing Ceramic Material, 519-526.
- Davies N (1999) Cranfield University, *Personal communication with M Taylor*.

- Davitt, A.L. and Yuill, K.A. (1983), *Delay Composition for Detonators, Patent* US 4 374 686.
- *Delta EMD General Certificate* (2000) MnO_2 Special Sample Request, Request number 860.
- Drennan R L and Brown M E (1992a) Binary and Ternary Pyrotechnic Systems of Mn and/or Mo and BaO_2 and/or SrO_2 Part 2, *Thermochimica Acta, 208*, 223-246.
- Drennan R L and Brown M E (1992b) Binary and Ternary Pyrotechnic Systems of Mn and/or Mo and BaO_2 and/or SrO_2 Part 3. Kinetic Aspects, *Thermochimica Acta*, 208, 247-259.
- Drummond C J and Chan D Y C (1997) van der Waals Interaction, Surface Free Energies and Contact Angles: Dispersive Polymers and Liquids, *Langmuir*, 13(14), 3890-3895.
- Ellern H (1968) *Military and Civilian Pyrotechnics*, Chemical Publishing Company, New York, United States.
- Farminer K W (1973) Silicone Antifoams in Chemical Processing, *Chemical Processing*, October.
- Feng Z, Zhao J, Huggins F E and Huffman G P (1993) Agglomeration and Phase Transition of a Nanophase Iron Oxide Catalyst, *Journal of Catalysis*, 143, 499-509.
- Focke W W (2000a) Introduction to surfaces and interfaces, *paper presented at Surfactant Technology and its Applications course*, 2-4 August 2000, University of Pretoria, Pretoria, South Africa.
- Focke W W (2000b) Particle Suspension Formulation, *paper presented at Surfactant Technology and its Applications course*, 2-4 August 2000, University of Pretoria, Pretoria, South Africa.
- Focke W W and Ricco I M M (2002) *Progress Report: Evaluation of Alternative Oxidants for AEL Time Delay Detonators*, report to AEL.
- Fordham S (1980) *High Explosives*, second revised edition, Pergamon Press.
- Freedman L D, Doak G D and Long G G (1996) Antimony Compounds in *Kirk-Othmers Encyclopedia of Chemical Technology*, 4th edition, volume 3, 385, New York, United States.
- Goodfield J A C and Rees G J (1985) Metal/Oxidant Combustion Reactions: Variation of Propagation Rate with Consolidation Pressure, *Fuel*, 64, 1627-1630.

- Greenwood N N and Earnshaw A (1984) Manganese, Technetium and Rhenium in *Chemistry of the Elements*, Pergamon Press, Oxford, England.
- Greenwood N N and Earnshaw A (1984) Silicon in *Chemistry of the Elements*, Pergamon Press, Oxford, England.
- Guidarelli G, Craciun F, Galassi C and Roncari E (1998) Ultrasonic Characterisation of Solid-Liquid Suspensions, *Ultrasonics*, 36, 467-470.
- Hackley V A, Paik U, Kim B and Malghan S G (1997) Aqueous Processing of Sintered Reaction-Bonded Silicon Nitride: I, Dispersion Properties of Silicon Powder, *Journal of the American Ceramic Society*, 80(7), 1781-1788.
- Hann W M (1996) Dispersants, in *Kirk-Othmer's Encyclopedia of Chemical Technology*, Kroschwitz, J.I. (Exec. Ed.), fourth edition, John-Wiley and Sons, volume 8, New York, United States.
- Hardt A P and Phung P V (1973) Propagation of Gasless Reactions in Solids – I. Analytical Study of Exothermic Intermetallic Reaction Rates*, Combustion and Flame*, 21, 77-89.
- Hardt A P and Holsinger R W (1973) Propagation of Gasless Reactions in Solids – II. Experimental Study of Exothermic Intermetallic Reaction Rates*, Combustion and Flame*, 21, 91-97.
- Hedger J T (1983) Factors Influencing the Pyrotechnic Reaction of Silicon and Red Lead, *Propellants, Explosives, Pyrotechnics*, 8, 95-98.
- Herbst K A, Rose G, Hanusch K, Schumann H and Wolf H U (1985) Antimony and Antimony Compounds in *Ullmann's Encyclopedia of Industrial Chemistry*, 5th edition, vol. A3, Gerhartz W B (Ed), VCH Publishers, Weinheim, Germany.
- Heusch R (1993) Disperse Systems and Dispersants, *in Ullman's Encyclopedia of Chemical Technology*, Elvers, B. (editor), VCH Publishers, fifth revised edition, A23, Weinheim, Germany.
- Howlett S L and May F G J (1974) Ignition Reactions of Boron: I: B-$K_2Cr_2O_7$ and B-Si-$K_2Cr_2O_7$. *Thermochimica Acta*, 9, 213.
- *JANAF Thermochemical Tables* (1971) United States Department of Commerce and National Bureau of Standards, Washington.
- Kaysser W A and Weise W (1993) Powder Metallurgy and Sintered Materials in *Ullmann's Encyclopedia of Industrial Chemistry*, 5th edition, vol. A26, Elvers B (Ed), VCH Publishers.

- Krone U and Lancaster R (1992) Pyrotechnics in *Ullmann's Encyclopedia of Industrial Chemistry*, 5th edition, vol. A22, Elvers B (Ed), VCH Publishers, Weinheim, Germany.
- Labuschagne F J W (s.a.) *Phd Thesis to be submitted*, Department of Chemical Engineering, University of Pretoria.
- Lafuma (2000) Fundamental Mechanisms of Stabilisation or Destabilisation of Disperse Media, *paper presented at Surfactant Technology and its Applications course*, 2-4 August 2000, University of Pretoria, Pretoria, South Africa.
- Laye P G (1997) Tying up Loose Ends, *Thermochimica Acta*, 300, 237-245.
- Lee I, Reed R R, Brady V L and Finnegan S A (1997) Energy Release in the Reaction of Metal Powders with Fluorine Containing Polymers, *Journal of Thermal Analysis*, 49, 1699-1705.
- Liley P E; Read R C and Buck E (1984) Physical and Chemical Data, section 3 in *Perry's Chemical Engineers' Handbook*, 6th edition, McGraw-Hill Book Company, New York.
- *Mach I Product Bulletin* (1995) Nanocat® Superfine Iron Oxide.
- Mailwane H (2000) Dispersing a mixture of Deca-bromobiphenyl Oxide and Antimony Oxide, *Report for CSC 420*, Department of Chemical Engineering, University of Pretoria, South Africa.
- Mani A, Athinarayanaswamy K, Pushpavanam S, Madhu S and Mahadevaiyer Y (1996) pH-Dependent Phases of Electrolytic Antimony Trioxide, *Journal of Material Science Letters*, 15, 2085-2087.
- Marinelli J and Carson J W (1996) Powders, Handling (Bulk) in *Encyclopedia of Chemical Technology,* 4rth edition, vol. 19, Kroschwitz J I (Ed), John Wiley and Sons.
- McLain J H (1980) *Pyrotechnics from the Viewpoint of Solid State Chemistry*, The Franklin Institute Press, Philadelphia, Pennsylvania.
- Mellor J W (1933) The Antimonious Acids and the Antimonites, in *A Comprehensive Treatise on Inorganic and Theoretical Chemistry,* Volume IX, Longmans, Green and co., London.
- Moghaddam A Z and Rees G J (1981) The Fast Pyrotechnic Reaction of Silicon with Lead Oxides: Differential Scanning Calorimetry and Hot-stage Microscopy Studies, *Fuel*, 60, 629-632.

- Nelson R D (1996) Powders, Handling (Dispersion) in *Kirk-Othmer's Encyclopedia of Chemical Technology*, Kroschwitz, J.I. (Exec. Ed.), fourth edition, John-Wiley and Sons, volume 19.
- Nguyen A V (2000) Improved Approximation of Water Dielectric Permittivity for Calculation of Hamaker Constants, *Journal of Colloid and Interface Science* 229, 648-651.
- Nosgrove A H C, Jones A F and King-hele J A (1991) Effects of Solid to Gas Conversion in Detonator Delay Elements, *Combustion Science and Technology*, 76, 133-157.
- Parrott J E and Stuckes A D (1975) *Thermal Conductivity of Technological Materials*, Pion Limited, Bristol.
- Penfold J, Staples E J, Tucker I and Fragnetto G (1996) The Effect of Shear on the Adsorption of Non-ionic Surfactants at the Liquid-Solid Interface, *Physica B*, 221, 325-330.
- Penfold J, Staples E J, Tucker I, Thompson L J and Thomas R K (1998) The Structure and Composition of Mixed Cationic and Non-ionic Surfactant Layers Adsorbed at the Hydrophilic Silicon Surface, *Physica B*, 248, 223-228.
- Pico Technology Application Note (2001)
- Pourbaix M (1966) Silicon in *Atlas of Electrochemical Equilibria in Aqueous Solutions*, Franklin J A (translator), National Association of Corrosion Engineers and Cebelcor.
- Reiter G, Sharma A, Khanns R, Casoli A and David M (1999) The Strength of Long Range Forces Across Thin Liquid Films, *Journal of Colloid and Interface Science*, 214, 126-128.
- Ricco I M M, Sefanyetso S O and Focke W W (2002) An Alternative Oxidant for Silicon-based Pyrotechnic Delay Compositions, *submission for DM Kisch Competition for Innovation*, University of Pretoria.
- Rugunanan R A (1991) Intersolid Pyrotechnic Reactions of Silicon, *PhD Thesis*, Rhodes University, South Africa.
- Rugunanan R A and Brown M E (1991) Reactions of Powdered Silicon with some Pyrotechnic Oxidants, *Journal of Thermal Analysis*, 37, 1193-1211.
- Rugunanan R A and Brown M E (1994a) Combustion of Binary and Ternary Silicon/Oxidant Pyrotechnic Systems, Part I: Binary Systems with Fe_2O_3 and SnO_2 as Oxidants, *Combustion Science and Technology*, 95, 61-83.

- Rugunanan R A and Brown M E (1994b) Combustion of Binary and Ternary Silicon/Oxidant Pyrotechnic Systems, Part II: Binary Systems with Sb_2O_3 and KNO_3 as Oxidants, *Combustion Science and Technology*, 95, 85-99.
- Rugunanan R A and Brown M E (1994c) Combustion of Binary and Ternary Silicon/Oxidant Pyrotechnic Systems, Part III: Ternary Systems, *Combustion Science and Technology*, 95, 101-115.
- Runyan, W (1996) Silicon and Silicon Alloys in *Kirk-Othmer's Encyclopedia of Chemical Technology,* Kroschwitz, J.I. (Exec. Ed.), fourth edition, John-Wiley and Sons, volume 20, New York.
- Sefanyetso S O (s.a.) *MSc Thesis to be submitted*, Department of Chemistry, University of Pretoria.
- Schönthaler W (1995) Thermosets in *Ullmann's Encyclopedia of Industrial Chemistry*, Elvers, B. (editor), VCH Publishers, fifth revised edition, A26.
- Shin H, Agarwal M, De Guire M R and Heuer A H (1998) Deposition Mechanism of Oxide Thin Films on Self-Assembles Organic Monolayers, *Acta Mater*, 46(3), 801-815.
- Sims E. (2000) *Personal Communication*, affiliated to Cabot Corporation
- Snegirev A Y and Talalov V A (1991) Determination of Kinetic Parameters for a Pyrotechnic Mixture, *Inorganic Materials*, 27, 462-467.
- Stephanopolous G (1984) *Chemical Process Control – An Introduction to Theory and Practice*, Prentice Hall, New Jersey.
- Taylor M (2000) Proposed Project in Delay Composition Flow Properties for AEL, *Personal Communication* with W. Focke, affiliated with AEL.
- Taylor R (1986) Thermal Conductivity of Ceramics *in Encyclopedia of Materials Science and Engineering*, Volume 7, Bever M (Ed), Pergamon press, Oxford, England.
- Taylor S J (1994) Computer Modelling of Pyrotechnic Combustion, *PhD Thesis*, Rhodes University, South Africa.
- Triblehorn M J, Venables D S and Brown M E (1995) A Thermoanalytical Study of some Zinc-fuelled Binary Pyrotechnic Systems, *Thermochimica Acta*, 269/270, 649-663.
- Tulis A J (1980) Flowability Techniques in the Processing of Powdered Explosives, Propellants and Pyrotechnics, *Journal of Hazardous Materials*, 4, 3-10.

- van der Avort N (1992) Pigment Dispersion for Water-based Paints and Printing Inks, *ICI Surfactants brochure*, September , document 64-25E/748-191.
- Varma A, Rogachev A S, Mukasyan A S and Hwang S (1998) Combustion Synthesis of Advanced Materials: Principles and Applications, *Advances in Chemical Engineering,* 24, 79-226.
- Varma A (2000) Form from Fire, *Scientific American*, 283(2), 44-47.
- Veale C R (1972) *Fine Powders – Preparation, Properties and Uses*, Applied Science Publishers Ltd, London.
- *Wacker HDK® brochure* (2000) Wacker HDK® Fumed Silica – Thickening and Thixotropy, Reinforcement and Free Flow, Document Edition no. 4955e3.00.
- Wang L L, Munir Z A and Maximov M (1993) Review Thermite Reactions: Their Utilisation in the Synthesis and Processing of Materials, *Journal of Material Science*, 28, 3693-3708.
- Watkins T F, Cackett J C and Hall R G (1968) *Chemical Warfare, Pyrotechnics and the Fireworks Industry*, Pergamon Press, Oxford, England.
- Wolf H U (1985) Barium and Barium Compounds in *Ullmann's Encyclopedia of Industrial Chemistry*, 5th edition, vol. A3, Wolfgang G (Ed), VCH Publishers, Weinheim, Germany.
- Yoganarasimhan S R (1988) Effects of Gas-Phase Mass Transport in the Pyrotechnic System Red Lead-Silicon-Potassium Perchlorate, *Journal of Thermal Analysis*, 34, 937-947.
- Zeulehner W, Neuer B and Rau G (1993) Silicon in *Ullmann's Encyclopedia of Industrial Chemistry*, Elvers, B. (editor), VCH Publishers, fifth revised edition, A23, Weinheim, Germany.
- Zhao J, Huggins F E, Feng Z, Lu F, Shah N and Huffman G P (1993) Structure of a Nanophase Iron Oxide Catalyst, *Journal of Catalysis*, 143, 499-509.
- *Zimalco – Material Safety Data Sheet* (s.a.) Supramex 2000.

14. APPENDICES

APPENDIX A

MATHEMATICAL MODELLING

A1 THERMAL PROPERTIES

A1.1 Thermal Diffusivity

Hardt and Holsinger (1973) have found that despite thermal diffusivities (k/ρc) in theory being independent of compaction pressure, values for compressed and uncompressed powders differ by as much as an order of magnitude which they attribute to the predominance of surface effects. They have also found that the thermal transport properties depend also on the particle size and on the direction of compression (Hardt and Holsinger, 1973).

A1.2 Thermal Conductivity

Parrott and Stuckes (1975:124-126) have made the following generalisations with regards to the thermal conductivity of isotropic oxides:

- Oxides with a lower atomic weight of the cation show a higher thermal conductivity to that of one with a higher atomic weight. This is attributed to the increasing anharmonicity in the lattice vibrations as the atomic weight of the cation becomes increasingly large to that of the oxygen atom.
- The apparent thermal conductivity has been shown to decrease above 300K until about 1000K where it increases due to radiative heat transfer and
- The thermal conductivity for single crystals is higher than that of a polycrystalline substance.
- Small quantities of impurities lower the thermal conductivity, especially around the peak of the thermal conductivity-temperature curve.
- The addition of a second component to form a solid solution greatly decreases the thermal conductivity. The solid solution disturbs the short range order of the lattice and consequently the phonons responsible for heat conduction, with wavelengths of the order of a few interatomic spacings, are effectively scattered by such disturbances.

Cosgrove *et al* (quoted by Parrott and Stuckes, 1975:126) found that the different conditions used in crystal growth affected the thermal conductivity. A decrease was found with decreasing freezing rate and with increasing temperature gradient at the liquid/solid interface. This was attributed to the degree of microsegragation produced in the crystals as the freezing conditions were changed (Parrott & Stuckes, 1975:126-127).

In general the thermal behaviour of the heterogeneous material, unlike that of a solid solution, lies between that of its components and depends on the volume and distribution of each component (Parrott & Stuckes, 1975:128).

For a mixture of 2 components with the materials arranged in parallel slabs, the relationships represented in Figure A-1 hold:

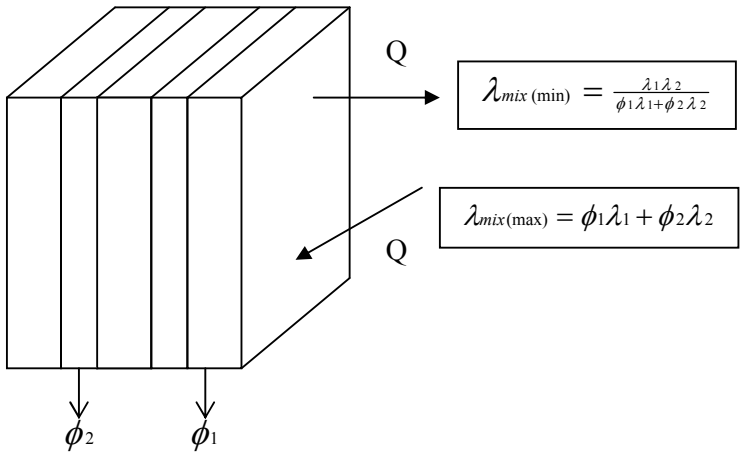

Figure A-1: Simple Parallel-slab Model (Parrott & Stuckes, 1975:130, Godbee and Ziegler, 1966b)

Heat conduction in this arrangement is predominately through the better conductor. However, for heat flow perpendicular to the plane of the slabs the heat flow through each component must be equal but the temperature gradient in each is different as can be seen in Figure A-1. It is dominated by the poorer conductor and is the minimum conductivity of the arrangement (Parrott & Stuckes, 1975:129-130).

Porous Solids

When the thermal conductivity of the fluid is negligible compared to that of the solid, Maxwell's model simplifies to:

$$\frac{\lambda_{mix}}{\lambda_{ccont}} = \frac{1-\phi}{1+\frac{1}{2}\phi}$$

Since the thermal conductivity of air is negligible, porosity levels up to 10-20% merely reduce the observed phonon thermal conductivity. However as the pores are not always spherical, Parrott and Stuckes (1975:133) and Taylor (1986:4921) have found that experimental results can sometimes be fitted rather better to the equation:

$$\lambda_{mix} = \lambda_{cont}(1-\beta_2\phi)$$

A limitation of this expression is that the shape of the pore is not always known. Where the porosity exceeds 25% conduction due to the solid component is reduced by the constriction in the heat flow paths provided by the pores. There are 4 basic heat flow mechanisms that can interact with each other: normal solid conduction, gaseous conduction through the pores, convective heat transfer within the pores and radiation across the pores. Convection can in general be neglected unless the pores exceed about 3mm in diameter; furthermore the contribution due to conduction through the gas is small compared with the solid conductivity (Taylor, 1986:4921-4922). Heat transfer by radiation increases as the pore size increases. As radiation has a T^4 dependence, it plays an increasingly active role at high temperatures. The thermal conductivity will decrease with increasing proportions of glass, liquid and pores although it will start to increase at very high porosities due to the increasing effect of radiative heat transfer (Parrott & Stuckes, 1975:133-134).

Powders

The thermal conductivity of powders is very dependent on the physical texture. For porous samples the low values of thermal conductivity which are obtained are due to the presence of air and also the constriction to heat flow in the solid path at contacts between grains or fibres. Carbon black has a thermal conductivity lower than air due to the presence of a large volume of pores smaller than the mean free path of air molecules. In general, the smaller the particle size, the lower the conductivity. None

of the theoretical models proposed above have good agreement with experimental results as they are too low at room temperature and the experimental conductivities will increase more rapidly with temperature than the model predicts owing to neglect of radiative heat transfer through the air spaces. Lausitz (quoted by Parrott & Stuckes, 1975:145) has commented that although the mathematics is exact, the models used are artificial and radically depart from real powders (Parrott & Stuckes, 1975:144-145).

According to Veale (1972:139) the thermal conductivity of an agglomerated powder in a gas can be calculated by assuming that the heat is transferred by conduction through the solid, by conduction through the gas and by particle to particle radiation. For fine powders, conduction is small owing to the small contact areas between the particles, although these areas may be somewhat increased by the presence of adsorbed layers or preferential condensation of liquid into the saddles between particles. Conductivity is independent of gas pressure as long as the mean free path of the gas molecule is less than the interparticle spacing (Veale, 1972:139-140).

Beck (1984) has used the models proposed by Maxwell and Rayleigh, Russel, Webb, Gorring and Churchill and Kunii and Smith to predict the thermal conductivity of $Sb/KMnO_4$ (quoted in Beck, 1984). He found that the model of Kunii and Smith gave reasonable results.

A2. EXTRACTION OF KINETIC PARAMETERS AND COMBUSTION MODELLING

A number of authors have attempted to mathematically model the combustion wave with mixed success. The earliest theory was based on the Mallard-Le Chatelier theory of propagation, i.e. $v = \frac{\lambda Q}{bc^2 \rho (T_f - T_a)}$ (Quoted by Beck, 1984).

Snegirev and Talalov (1991) have outlined a procedure for recovering kinetic parameters from data of firing a pyrotechnic mixture by an incandescent surface at a constant temperature. They have stated, however, that the combustion time can not be calculated using the kinetic parameters which they derived for the Si-Pb_3O_4 composition as they have not considered the increase in retarding effect of a SiO_2 layer on the Si particles, kinetics of the Pb_3O_4 decomposition and the transport oxidising agent to the zone of combustible material oxidation.

A2.1 Leeds Method for Gasless Pyrotechnic Reactions

Boddington *et al* (1982, 1986) have derived a model for the analysis of temperature profiles for gasless pyrotechnics to obtain information regarding the adiabatic temperature rise and the local instantaneous rate of heat evolution. The model is one of a long cylinder of gasless pyrotechnic mixture, initially and finally at ambient temperature Ta. They have assumed that the temperature excess U=T-Ta over a cross section normal to the axis of propagation is given by:

$$t^* U_{tt} - U_t + G - U t_{th}^{-1} = 0$$

The time $t^* = \lambda / \rho c v^2$ is the rise time of the inert forewave of the profile in the absence of lateral heat transfer. $t_{th} = \rho c / h$ is the thermal relaxation time of the system due to lateral heat transfer. $G = w / c$ is a measure of the local thermal power arising from the heat effects of all the chemical and phase changes. The model is based on the

assumption that the density, thermal conductivity, specific heat capacity etc. are independent of temperature. This model has been further developed by Boddington *et al* (1989, 1990) to allow for a more complex rate law to describe the reaction kinetics at low temperatures and where the global approach used previously predicted too great a reaction rate and to allow for heat loss. The approach is to combine a high temperature diffusion term with an Arrhenius temperature dependence that determines the behaviour at lower temperatures. A limitation of the model is that it makes no allowance for phase changes and is pseudo-one-dimensional (Boddington *et al*, 1989 and 1990).

Drennan and Brown (1992b), Rugunanan and Brown (1994a,b,c), Rugunanan (1991) Beck (1984) have used this method for the extraction of kinetic parameters for binary and ternary mixtures.

A2.2 Combustion Synthesis Reaction Modelling

Munir (1988) has proposed the following equation to calculate the velocity of the combustion front for SHS reactions:

$$v^2 = f(n)\frac{cd}{Q}\frac{RT_c^{\,2}}{E}K_o \exp\left(\frac{-E}{RT}\right)$$

where f(n) is a function of the kinetic order n and T the absolute temperature.

The equation was derived with the following assumptions:

- The thermophysical properties of the product are not strong functions of temperature.
- Convective and radiative heat losses are negligible.
- The width of the reaction zone is narrow in comparison with the thermally affected zone (Munir, 1988).

Varma *et al* (1998) on the other hand have proposed the following equations for the combustion wave velocity in gasless systems:

- For a zero order reaction:

$$v^2 = \frac{2\lambda}{\rho Q}\frac{RT_c^{\,2}}{E}K_o \exp\left(-\frac{E}{RT_c}\right)$$

- For n'th order type kinetics, Varma *et al* (1998) have proposed:

$$v^2 = \frac{(2-n)\lambda}{\rho Q}\frac{RT_c^{\,2}}{E}K_o \exp\left(-\frac{E}{RT_c}\right)$$

This equation is not valid for $n \geq 2$, since it leads to zero (n=2) and imaginary values of velocity for n>2). The origin of this discrepancy is that when the dependence of reaction rate on conversion is sufficiently strong (e.g. for higher order reactions), the reaction rate away from the adiabatic combustion temperature may also be significant. Khaikan and Merzahanov (quoted by Varma *et al*, 1998) derived the following equation for n'th order kinetics:

$$v^2 = \left\{2\left[\Gamma\left(\frac{n}{2}+1\right)\right]^{1-\frac{n}{2}}\left(\frac{n}{2e}\right)^{\frac{n^2}{4}}\right\}\frac{\lambda}{\rho Q}\frac{RT_c^{\,2}}{E}K_o \exp\left(-\frac{E}{RT_c}\right)$$

where $\Gamma(z) = \int_0^\infty e^{-t}t^{z-1}dt$ is the gamma function.

These equations were based on the following assumptions:

- The Lewis number is very small i.e. $Le = \frac{D}{\alpha} <<< 1$. This means that heat conduction occurs much faster than mass diffusion and therefore mass diffusion at a macroscopic scale may be neglected and an average concentration of the reactants in any local region may be used. Density, thermal conductivity and heat capacity are an average of the reactant and product values.
- The temperature and concentration profiles do not change with time (constant pattern propagation).
- There is no heat loss.
- There is one chemical reaction.
- The rate of heat evolution is neglected everywhere except in the narrow zone near T_c (narrow zone approximation) (Varma *et al*, 1998).

This theory applies mainly to kinetic-controlled reactions, but reactions involve many processes. Merzanhov (quoted by Varma *et al*, 1998) compared experimental data with combustion equations for various types of heat sources and concluded that the combustion wave velocity can be represented as follows:

$$v^2 = A(\eta^*, T^*)\exp\left(-\frac{E}{RT^*}\right)$$

Where T^* and η^* are the values of temperature and corresponding conversion which control the combustion front propagation and $A(T^*,\eta^*)$ is a function weaker than the exponential. Merzhanov (quoted by Varma *et al*, 1998) identified 4 types of combustion:

- Combustion with a thin reaction zone (Figure A-2). $\eta^*=1$, $T^* = T_c \approx T_o + \frac{Q}{c}$

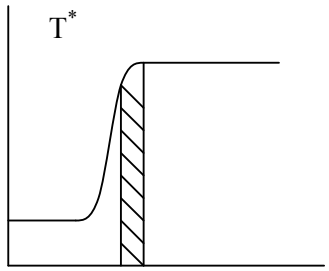

Figure A-2: Temperature Profile for Combustion with a Thin Reaction Zone (Varma et al, 1998)

- Combustion with a wide zone which occurs when a product layer strongly inhibits the reaction (Figure A-3). $T^* = T_o + \frac{Q}{c}\eta^*$, where η^* is determined from:

$$\frac{Q}{c}\frac{\partial\phi(\eta^*,T^*)}{\partial T} + \frac{\partial\phi(\eta^*,T^*)}{\partial\eta} = 0$$

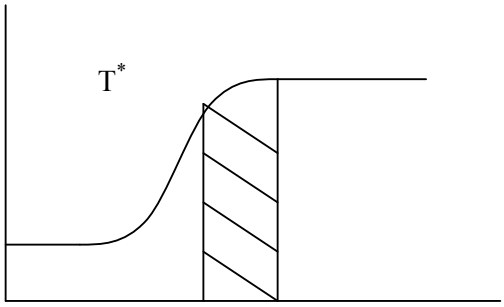

Figure A-3: Temperature Profile for Combustion with a Wide Reaction Zone (Varma et al, 1998)

- Combustion with phase transformations (Figure A-4). $T^*=T_m$ (melting point) and $\eta^* = \frac{(T_m - T_o)}{\left(Q/c\right)}$.

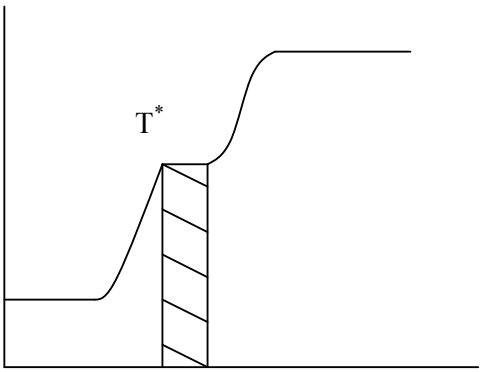

Figure A-4: Temperature Profile for Combustion with Phase Transformations (Varma et al, 1998)

- Combustion with multistage spatially separated reactions (Figure A-5). $\eta^*_1 = 1$ and $T^* \approx T_o + \left(\frac{Q_1}{c}\right)$ where the subscript refers to the first low temperature stage of the complex reaction (Varma *et al*, 1998).

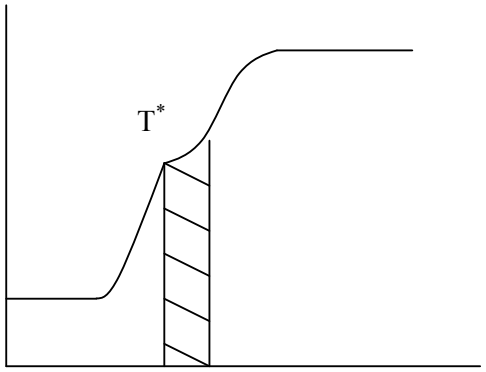

Figure A-5: Temperature Profile for Combustion with Multistage Spatially Separated Reactions (Varma et al, 1998)

Varma *et al* (1998) have further proposed that the temperature profile in the preheating zone be described by:

$T = T_o + (T_c - T_o)\exp\left(\frac{v}{\alpha}x\right)$ where $x \le 0$ and $x_T = \frac{\alpha}{v}$ denotes the characteristic length scale of the combustion wave. The temperature profile in the reaction zone is equal to the combustion temperature.

A2.2.1 Mictrostructural Models

Microstructural models have been developed to account for reactant particle size and distribution, product layer thickness etc and correlate them with the combustion temperature and velocity. The equations used are similar to those in the previous section. However the kinetics of heat release may be controlled by phenomena such as diffusion through a product layer of melting or spreading of reactants. These phenomena often have Arrenhius-type dependencies. The dependence of velocity on particle size has been described as: $v = f(d)F(T)$ (Varma *et al*, 1998)

Four reaction cell geometries have been used in the theoretical models (Varma *et al*, 1998). These include:

1. Alternating lamellae of the two reactants (A and B) which diffuse through a product layer (C) to react i.e. A(s) + B(s) → C(s) (Figure A-6).

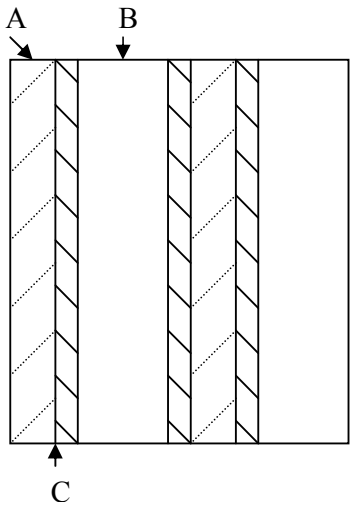

Figure A-6: Reaction Cell Geometry for A(s) + B(s) → C(s) (Varma et al, 1998).

By assuming that the particles are flat, it is possible to neglect the change in the reaction surface area. The characteristic particle size is equivalent to the layer thickness and the relative thickness of the initial reactant layers are determined by stoichiometry. Hardt and Phung (1973) found that $f(d) \propto \frac{1}{d}$

i.e. $v = \frac{0.8\lambda Q}{w_1 a_o \rho c^2 (0.035E - T_o)}$ (all units are British).

Aldushin *et al* (quoted by Varma *et al*, 1998) developed the following kinetic function:

$\phi(\eta, T) = K_o \exp\left(-\frac{E}{RT}\right) e^{-m\eta} \eta^{-n}$ which describes linear (m=0, n=0), parabolic (m=0, n=1), cubic (m=0, n=2) and exponential (m>0, n=0) kinetic dependencies. Combination of these dependencies with the velocity equation yields the following:

i) Power law kinetics (i.e. m=0, n≥0)

$$v = \frac{(n+1)(n+2)}{d^{n+0.5}} F(T)$$

ii) Exponential kinetics (i.e. m>0, n=0)

$$v = \frac{m^2}{(e^m - 1 - m)d} F(T)$$

For a unimodal particle size distribution with particle size distribution function, $\chi(d)$ the effective diameter can be calculation using $d_{eff} = \left[\int_{d_{\min}}^{d_{\max}} d^2 \chi(d) dd\right]^{0.5}$ and used in the above expressions in place of d. For a bimodal distribution, the combustion wave has a two stage structure similar to Figure A1-5, where two combustion fronts propagate in sequence. Using effective particle sizes for fine (d_1) and coarse (d_2) particles the velocity dependence for the leading combustion front is described by:

$U = \frac{F(T)}{\left[d_1^2 m_1 + d_2^2 (1 - m_1)\right]^{0.5}}$ where m_1 is the mass fraction of finer particles (Varma *et al*, 1998).

2. A spherical particle of one reactant (B) is surrounded by a melt of the other reactant (A) and a solid product layer (C) grows on the surface of the particle with the molten reactant diffusing through the product layer i.e. A(l)+B(s)→C(s) (Figure A-7). At a given temperature the concentrations at the interphase boundaries are determined from the phase diagrams of the system (Varma *et al*, 1998).

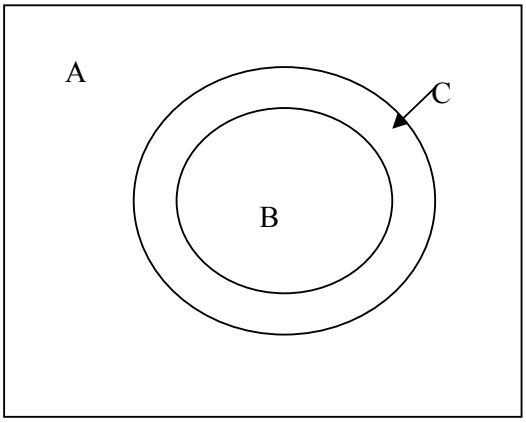

Figure A-7: Reaction Cell Geometry for A(l) + B(s) → C(s) (Varma et al, 1998)

3. Similar to the second cell geometry except that the solid reactant diffuses through an initial product layer to the melt and a liquid product is formed which crystallises in the in the volume of the melt after saturation i.e. A(l)+B(s)→C(l) (Figure A-8). The initial product layer's thickness is assumed to remain constant. Cao and Varma (quoted by Varma *et al*, 1998) reported the combustion wave velocity as being $U = \left[\frac{1}{d}\left(\frac{2}{d}+\frac{1}{\delta}\right)\right]^{0.5} F(T)$ where δ is the thickness of the initial product layer.

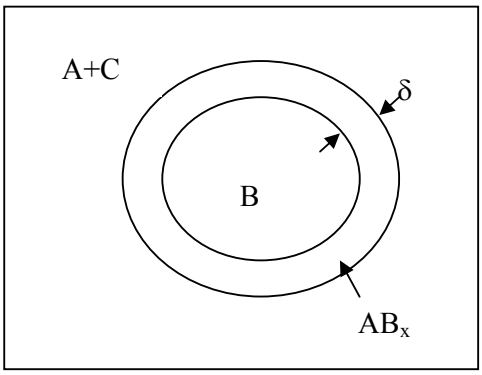

Figure A-8: Reaction Cell Geometry for A(l) + B(s) → C(l) (Varma et al, 1998)

4. Both reactants melt and the liquid product forms in the reaction zone i.e. A(l)+B(l)→C(l) (Varma *et al*, 1998) (Figure A-9). After both reactants melt, their interdiffusion and the formations of a liquid product occur simultaneously. In the kinetic-limiting case, for a stoichiometric mixture of reactants (A and B) the propagation velocity does not depend on the initial reactant particle sizes. For diffusion-controlled reactions the velocity is $v = \frac{b_1}{d} F(T)$ where

$$b_1 = \begin{cases} 1 & \text{if } d < d_B^{st} \\ \dfrac{d^3}{D_{rc}^3 - d^3}\dfrac{v_B MW_B}{v_A MW_A} & \text{if } d > d_B^{st} \end{cases}$$

d_B^{st} is the diameter of reactant B in a corresponding stoichiometric mixture and D_{rc} is diameter of the reaction cell.

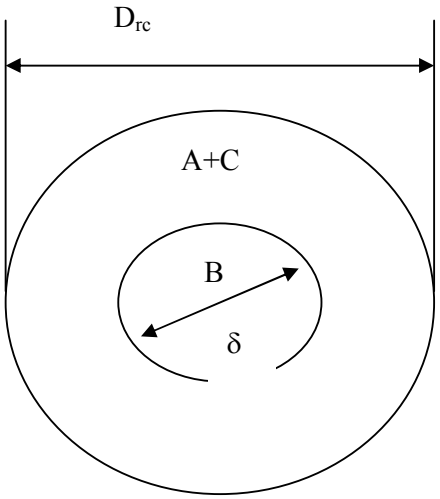

Figure A-9: Reaction Cell Geometry for A(l) + B(l) → C(l) (Varma et al, 1998)

2.2.2 Cellular Models

For cellular models, the reaction medium is divided into a discrete matrix of cells, where the temperature and effective properties are assumed to be uniform throughout the cell. The difference between cellular models and finite difference/element models is that the latter are finite approximations of continuous equations with the implicit assumption that the width of the reaction zone is larger than other length scales (diffusion, heterogeneity of medium etc.). Cellular models have no such assumptions and the local transport processes in a heterogeneous medium is accounted for. Varma *et al* (1998) provide a description of the cellular models which have been reported in literature.

A2.3 Combustion with Gaseous Reaction Products

Varma *et al* (1998) describe the various models which have been derived for filtration combustion, i.e. gas-solid reactions. These models will not be discussed here as they involve the addition of a gaseous reactant which is not the case for pyrotechnic delay reactions, where both reactants are initially solids. However, the model proposed by

Aldushin and Zeinenko (1992) will be discussed to gain an insight into the effect of a gas on the burn characteristics.

It has been shown by Aldushin and Seplyarskii (quoted by Aldushin and Zeinenko, 1992) that the flow of a heat carrier through the reacting medium, in the direction of propagation of the combustion zone, increased the temperature of the zone above the thermodynamic adiabatic combustion temperature. The gas, passing through the reacting mixture, acts as a heat transfer medium, and heats the initial mixture. One characteristic of this system is the inverse relation between the density of the gas flow and the velocity of the reaction wave. In such a system, a state of steady combustion is possible only with spontaneous balancing of the gas separation processes and the effects of the gas flow on the temperature and velocity of propagation of the reaction zone (Aldushin and Zeinenko, 1992).

Based on an isotropic porous pyrotechnic mixture as reacting medium, Aldushin and Zeinenko (1992) have proposed the following equations for the steady combustion front:

$$mc\left(1-\frac{\eta_1 v_1 c_1}{c}\right)T_s' = Qy + \lambda T_s'' + \alpha_2\left(T_g - T_s\right)$$

$$mv_1 c_1(\xi - \eta_1)T_g' = v_1 c_1 y\left(T_g - T_s\right) + \alpha_2\left(T_g - T_s\right)$$

where $m\eta_1 = y$ and $y = K_o \exp\left(-E/RT_s\right) f(\eta_1)$

when $x = -\infty$: $T_s=T_g=T_o$, $\eta_1=0$ and

when $x = \infty$: $T_s=T_g=T_r$, $\eta_1=1$

The above equations are the material and heat balances for the steady combustion wave, counted from right to left, with respect to the spatial variable x and not with the moving reaction front. The terms with dashes are the differentials with respect to x. The parameter, ξ, determines the direction of the gas flow. Depending on the conditions of combustion, the gas can flow in the direction of the moving front ($\xi=1$), or in the reverse direction ($\xi=0$). Aldushin and Zeinenko (1992) have described the detailed derivation of these equations.

Their model is based on the following assumptions:

- The thermophysical properties and the heat of reaction were constant.
- The thermal conductivity of the gas, drop in pressure in the porous layer and heat loss to the surrounding medium were negligibly small.
- Phase transformations did not occur.
- There was no flow of the condensed components.
- The combination of the actual chemical reactions occurring was equivalent to a single overall reaction described by $y = K_o \exp\left(-E/RT_s\right) f(\eta_1)$.
- The boundary conditions were defined by the thermal equilibrium of the phases at large distances from the reaction zone ($x=0$).

From these equations Aldushin and Zeinenko (1992) have derived the following equations:

- The combustion front temperature, T_g:

$$T_g = T_o + \frac{Q}{c_1}\left(1 - \frac{\xi \nu_1 c_2}{c_1}\right)$$

- The combustion mass velocity:

$$m^2 = \frac{\frac{K_o \lambda}{Q}\frac{RT_g^{\,2}}{E}\exp\left(-\frac{E}{RT_g}\right)}{\int_0^1 \frac{(1-\eta_1)d\eta_1}{f(\eta_1)}}$$

According to Aldushin and Zeinenko (1992) the assumption of a narrow chemical reaction zone is consistent with the heat conduction mechanism of combustion wave propagation. During the flow of a gas through the combustion products, this is the only mechanism, whereas when the gas moves with the front, propagation of the reaction can be a convective mechanism, in addition to conduction (Aldushin & Zeinenko, 1992).

Experimentally, Aldushin and Zeinenko (1992) attempted to confirm the possibility of propagation of a steady combustion wave in a porous partially gasified medium and to determine the effect of heat transfer between the gaseous reaction products and the initial material. They used oxygen-containing mixtures based on sodium chlorate

granules. They found that when the flow of the generated oxygen was in the direction of the moving front, the maximum temperature exceeded the combustion front temperature of the products, without taking into account the heat transfer from the gaseous reaction products, but did not exceed the theoretical combustion temperature because of heat losses and the low mass velocity of steady combustion. Furthermore they found that mixtures that burned at a stable constant rate when $\xi=0$ burned at a progressively increasing rate when $\xi=1$. Also, a change in the direction of low for mixtures which were not capable of stable propagation under normal conditions, led to the stabilisation of the combustion. This leads to the assumption that for highly concentrated fuel or compositions of low activity, the change in the direction of gas flow causes the heat transfer mechanism to change. They thus confirmed using the above model experimentally that a steady combustion wave can exist in a porous reacting media composed of chemical sources of pure gases when the gaseous reaction products heat the original material. In this study they have found that the temperature of combustion increases with increasing mass fraction and heat capacity of the released gas and exceeds the adiabatic combustion temperature of the material (Aldushin & Zeinenko, 1992).

Nosgrove *et al* (1991) proposed a model to study the effects of gas production on pyrotechnic compositions. Their model is based on the following assumptions:

- The flow is one-dimensional so that all the variables depend only x the distance down the delay element and on t, the time. This assumption is poor as it neglects heat losses into the detonator wall which is not one-dimensional.
- The temperature of the reacting solid is the same as that of the gas.
- The gas which is released flows under the action of the local pressure gradient according to Darcy's law, but the reacted solid does not move. This implies that permeability is uniform throughout the element length, but the permeability is sensitive to the structure and void fraction of the porous medium which changes as the reaction proceeds.
- Transfer of heat by radiation between the fuel particles may be neglected.
- The gas is an ideal gas.

The resultant equations are:

- Flame Temperature:

$$Tf(\iota) = To + \frac{Q(\rho_0 - \rho_\infty)}{\rho_\infty c_s + (1-\iota)(\rho_0 - \rho_\infty)c_1}$$

- Flame Speed:

$$v^2(\iota) = \frac{\lambda\rho_0(2-l)RT_f{}^2 r(T_f)}{E(\rho_0 - \rho_\infty)^2\left[Q + (c_s - c_1)(T_f - T_0)\right]}$$

They found that the boundary conditions which change as a result of the gas flow can only be used generally to obtain an explicit model and therefore do not describe the effect of the solid to gas conversion and gas flow. They have attempted to solve the problem numerically and found that the direction in which the gas flows and where the detonator is punctured does have an effect on the reaction (Nosgrove et al, 1991).

There has been mixed success for comparing experimental results with these and other theoretical models. The use of simplifying assumptions such as the narrow zone, and one step reaction pose problems. The simplifying assumptions need to be satisfied under experimental conditions in order to obtain intrinsic kinetic data.

A3 TIME TO IGNITION

Boddington *et al* (1986) have measured the times-to-ignition using a temperature-jump technique in order to derive the chemical activation energies. The aim was to raise the temperature of the reagents as quickly as possible from its initial temperature to a temperature, T_a, above the critical temperature. They found that the measurements were not sufficiently precise to discriminate between the various methods which have been proposed by previous authors (quoted by Boddington *et al*, 1986).

A4 COMPUTER MODELLING

Taylor (1994) attempted to use computer modelling to complement the existing experimental techniques used to analyse pyrotechnic compositions. A detailed discussion of his work will not be discussed here.

In summation, Taylor (1994) found the following:

- The one-dimensional model used a simple model (Heat loss through the sides of the column is negligible, heat loss through ends is described by Biot number) and of the column with temperature being calculated at each node at each time step using an explicit method. The method depended on the availability of good kinetic data. It would be beneficial to implement for quick evaluation of compositions.
- The two-dimensional model allows for heat loss and stipulating surrounding material. It had the added advantage of being able to obtain fringe and contour plots and temperature gradients. The model was limited by the quality of the available kinetic data and available computation time.
- The particle-packing model was based on the assumption that the fuel and oxidant particles both had uniform but different radii and that all the particles were spherical.
- The Monte Carlo method incorporated the effect of random packing of the particles on the burn speed.

He recommended that future models allow for the introduction of temperature dependence of properties such as heat capacity etc., non-homogeneous material in the composition (additives), direct incorporation of variables such as compaction and composition and improvement in the models used for kinetic analysis of experimental temperature profiles (Taylor, 1994).

APPENDIX B

EFFECT OF VARYING DATA FILTRATION PARAMETER

APPENDIX C

CALCULATION OF THERMOCHEMICAL REACTION PROPERTIES

APPENDIX D

XRD AND XRF ANALYSIS OF CUO

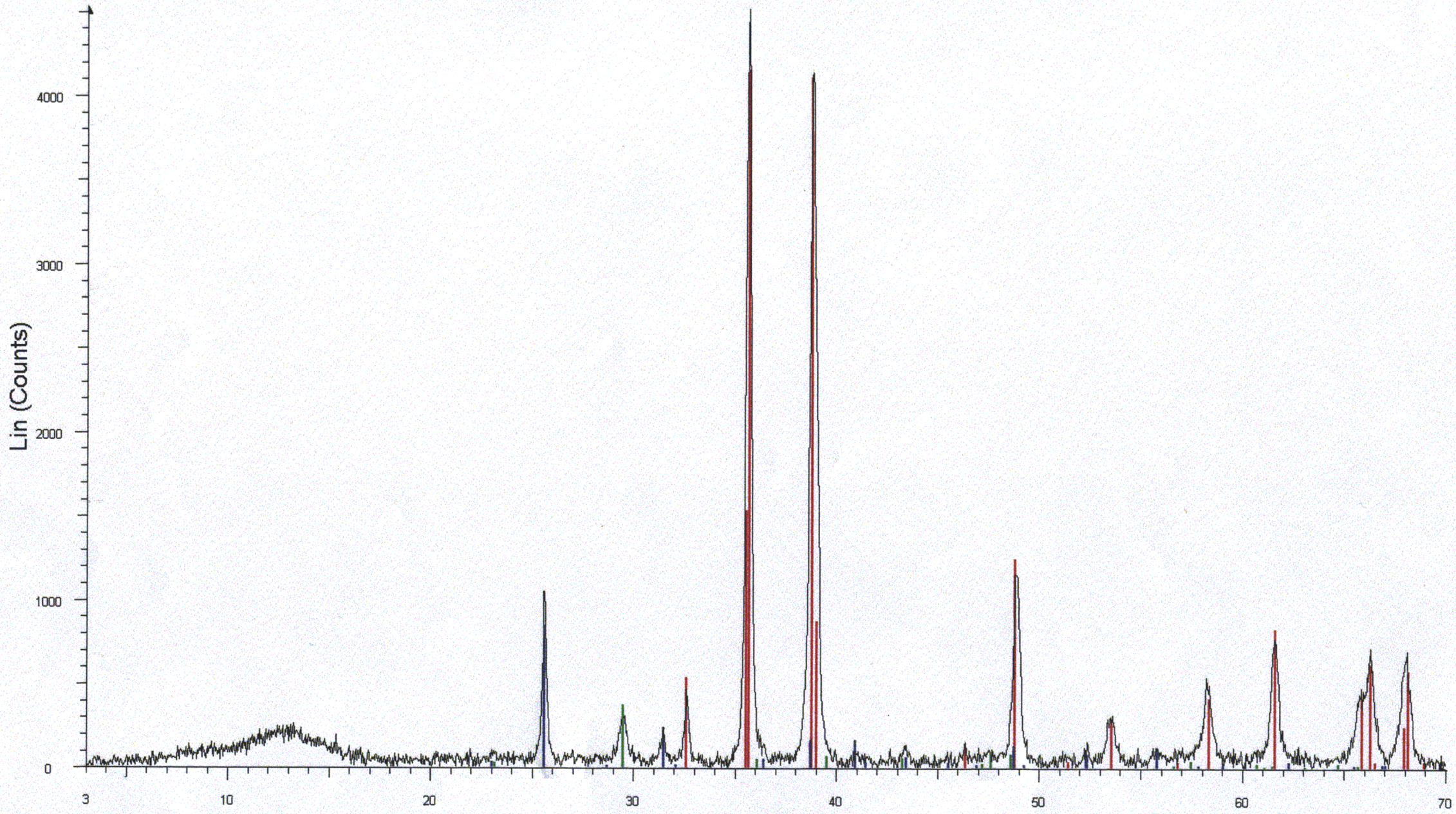

3 - File: RICCO01 .raw - Type: 2Th/Th locked - Start: 3.000 ° - End: 70.040 ° - Step: 0.040 ° - Step time: 1.5 s - Temp.: 25 °C (Room) - Time Started: 0 s - 2-Theta: 3.000 ° - Theta: 1.500 ° - Chi: 0.00 ° - P
48-1548 (*) - Tenorite, syn - CuO - Y: 92.12 % - d x by: 1. - WL: 1.5406 - Monoclinic -
37-1496 (*) - Anhydrite, syn - CaSO4 - Y: 18.75 % - d x by: 1. - WL: 1.5406 - Orthorhombic -
47-1743 (C) - Calcite - CaCO3 - Y: 8.33 % - d x by: 1. - WL: 1.5406 - Rhombohedral -

XRF REPORT:

University of Pretoria
Pretoria 0002 Republic of South Africa Tel (012) 4209111
Fax (012) 43-6867

Faculty of Science
XRD & XRF Laboratory
Department of Earth Sciences
Tel.: (012) 420 2137
Fax.: (012) 362 5219
e-mail: mloub@scientia.up.ac.za

CLIENT: Isabel Ricco

DATE: 20 April 2001

SAMPLES: CuO samples

ANALYSIS:

The sample was mounted on a thin film and analysed using the ARL9400XP+ spectrometer with the wide confidence limit program. Due to the very small sample used these values are not exact but indicative of the impurities present.

%	SAMPLE1	SAMPLE2	SAMPLE3
SiO_2	1.52	n/d	n/d
TiO_2	n/d	n/d	n/d
Al_2O_3	1.92	n/d	n/d
Fe_2O_3	0.49	0.74	n/d
MnO	0.25	0.32	0.53
MgO	1.41	0.36	0.63
CaO	18.5	0.61	0.69
Na_2O	n/d	n/d	n/d
K_2O	n/d	n/d	n/d
P_2O_5	0.21	0.11	0.11
SO_3	19.1	n/d	n/d
Cr_2O_3	940 ppm	n/d	n/d
NiO	0.54	0.29	0.20
CuO	55.5	97.3	97.8
ZnO	0.41	0.27	n/d

If you have any further queries, kindly contact the laboratory.

Analyst:

M.Loubser

APPENDIX E

BURN RATE MEASUREMENTS FOR INITIAL TRIALS

All burn speeds are in mm/s. All runs under 1 were run in Nov 01 and all runs under 2 were run Feb. 02. The samples of PbCrO4 were lost

A) CuO and Si

Method of intitiation	Mass oxidant	Mass Si	Fuel:Total mass ratio	AEL tests	1			2		
					mm	Comment	Burn speed	mm	Comment	Burn Speed
Shock Tube	25.309	4.691	15.63667	Did not ignite	4	Mixture Failure		10	Shock Tube Failure	
Starter					5	Mixture Failure, heat due to starter element		10	Mixture Failure, heat due to starter element	

B) MnO2 and Si

Method of intitiation	Mass oxidant	Mass Si	Fuel:total mass ratio	AEL tests	1			2		
					mm	Comment	Burn speed	mm	Comment	Burn Speed
Shock Tube	17.218	2.789	13.94012	Burnt with sealer,	5	Mixture Failure		10	Shock Tube Failure	
Starter				Burnt with sealer and starter	5	Mixture Failure, heat due to starter element		10	Mixture Failure, heat due to starter element	

C) CuO.MnO2 (Prepared by Serei) and Si

Method of intitiation	Mass oxidant	Mass Si	Fuel:total mass ratio	AEL tests	1			2		
					mm	Comment	Burn speed	mm	Comment	Burn Speed
Shock Tube				Did not ignite	5	Mixture Failure		10	Shock Tube Failure	
Starter					5	Mixture Failure, heat due to starter element		10	Mixture Failure, heat due to starter element	

D) Cu(SbO2)2 (Prepared by Serei) and Si

Method of intitiation	Mass oxidant	Mass Si	Fuel:total mass ratio	AEL tests	1			2		
					mm	Comment	Burn speed	mm	Comment	Burn Speed
Shock Tube				Burnt with sealer,	5	Mixture Failure		10	Shock Tube Failure	
Starter				Burnt with sealer and starte	5	Burnt	9	5	Burnt	25

E) CuO.Fe2O3 (Prepared by Serei) and Si

Method of intitiation	Mass oxidant	Mass Si	Fuel:total mass ratio	AEL tests	1 mm	1 Comment	1 Burn speed	2 mm	2 Comment	2 Burn Speed
Shock Tube				Did not ignite	4	Mixture Failure		10	Mixture Failure	
Starter					4	Mixture Failure, heat due to starter element		10	Mixture Failure, heat due to starter element	

F) Fe2O3 and Si

Method of intitiation	Mass oxidant	Mass Si	Fuel:total mass ratio	AEL tests	1 mm	1 Comment	1 Burn speed	2 mm	2 Comment	2 Burn Speed
Shock Tube	9.161	0.808	8.105126	Did not ignite	5	Mixture Failure		5	Mixture Failure	
Starter					5	Mixture Failure, heat due to starter element		5	Mixture Failure, heat due to starter element	

G) Fe3O4 and Si

Method of intitiation	Mass oxidant	Mass Si	Fuel:total mass ratio	AEL tests	1 mm	1 Comment	1 Burn speed	2 mm	2 Comment	2 Burn Speed
Shock Tube	18.855	1.14	5.701425	Did not ignite	5	Mixture Failure		5	Mixture Failure	
Starter					5	Mixture Failure, heat due to E element		5	Mixture Failure, heat due to E element	

H) Fused V2O5 and Si

Method of intitiation	Mass oxidant	Mass Si	Fuel:total mass ratio	AEL tests	1 mm	1 Comment	1 Burn speed	2 mm	2 Comment	2 Burn Speed
Shock Tube	18.571	1.435	7.172848	Did not ignite	5	Mixture Failure		5	Mixture Failure	
Starter					5	Mixture Failure, heat due to starter element		5	Mixture Failure, heat due to starter element	

I) Deamm V2O5 and Si

Method of intitiation	Mass oxidant	Mass Si	Fuel:total mass ratio	AEL tests	1			2		
					mm	Comment	Burn speed	mm	Comment	Burn Speed
Shock Tube	18.561	1.438	7.19036	Did not ignite	5	Mixture Failure		5	Mixture Failure	
Starter					4	Mixture Failure, heat due to starter element		5	Mixture Failure, heat due to starter element	

J) Sb2O3 and Si

Method of intitiation	Mass oxidant	Mass Si	Fuel:total mass ratio	AEL tests	1			2		
					mm	Comment	Burn speed	mm	Comment	Burn Speed
Shock Tube	17.479	2.539	12.68358	Burnt with starter and sealer	10	Shock Tube Failure		5	Mixture Failure	
Starter					4.5	Burnt	3	5	Burnt	2

APPENDIX F

VARYING STOICHIOMETRY

EXPERIMENTAL DATA FOR TUMBLE MIXED COMPOSITIONS

APPENDIX G

VARYING STOICHIOMETRY

EXPERIMENTAL DATA FOR TUMBLE AND BRUSH MIXED COMPOSITIONS

APPENDIX H

VARYING STOICHIOMETRY AND SILICON PARTICLE SIZE EXPERIMENTAL DATA

APPENDIX I

VARYING OXIDANT PARTICLE SIZE EXPERIMENTAL DATA

APPENDIX J

ALUMINIUM ADDITION

EXPERIMENTAL DATA

APPENDIX K

FUMED SILICA ADDITION EXPERIMENTAL DATA

APPENDIX L

THE USE OF DISPERSIONS AS A PROCESSING ROUTE

PROPOSAL

L1 DISPERSIONS AND DISPERSANTS

Dispersions occur when two or more phases are insoluble or slightly soluble and are dispersed in one another. The continuous or external phase is termed the dispersion medium while the substance distributed in it is termed the internal or dispersed phase (Heusch, 1993:577).

The energy required to produce a dispersion increases with decreasing particle size because their surface area increase and the energy (W) is directly proportional to the surface area (S), i.e.:

$$dW_1 = \gamma_1 dS$$

From the equation, it can be seen that as the surface tension (γ) of the fluid increases, so does the energy required to produce the dispersion. Dispersants lower the interfacial tension between the phases (Heusch, 1993:577). They thus help maintain fine solid particles in a state of suspension and inhibit the particles from agglomeration or settling in the fluid medium.

L1.2 The Dispersion Process

The preparation of a dispersion entails three stages, i.e.

- Wetting the powder into the liquid medium
- Deagglomerating the wetted clumps and
- Preventing reagglomeration or flocculation (Nelson, 1996:1093).

L1.2.1 Wetting the Powders

In order to overcome surface defects such as:

- Lattice defects
- Non-stoichiometry
- Impurity ions
- Dislocations and

- Surface roughness

a solid will tend to adsorb polar molecules such as water i.e. oxygen or hydroxyl radicals cover the exposed surfaces (Focke, 2000a). Despite this, the wetting of powders remains a problem. The wetting process consists of three mechanical steps: adhesion, immersion and spreading. Nelson (1996:1094-1096) has described the fundamentals for the wetting of single particles and clumps. A more detailed discussion of the wetting phenomenon with an approach based on the theory of surface forces has been made by Churaev (1995).

The most common wetting agents are anionic surfactants chosen from the families of alkali, sulphonates, sulphates, ligno sulphates, carboxylates and phosphates. The optimum chain length is between 12 and 18. A wetting agent with a low molar mass has a high diffusion coefficient and thus has a faster rate of wetting. The selection of the wetting agent is important, as the agent may interfere with the drying of the powders in the downstream processing (i.e. in the case of the delay elements the loading of the lead tubes may be affected).

Gas that is drawn beneath the surface of the liquid as a result of a vortex or plunging jet, due to the high shear which is used, may be dispersed into small bubbles which may be stabilised by the wetting agent to form a stable foam. The amount of wetting agent that should also be limited for this reason (Nelson, 1996:1096). Typically only 0.01 to 0.2% (mass basis) of the wetting agent is added to the dispersion (Focke, 2000c)

L1.2.2 Deagglomerating the Wetted Clumps

The particles in a dry powder are held together by the polarisability attraction of adjoining particles, the surface tension at wetted contacts or moderately strong sintering or precipitation bonds. These bonds are formed at the contact points because of the exposure to humidity and temperature cycles during storage before use. Breaking these bonds to fully disperse the submerged and wetted clumps requires high shear stress or mechanical impact. This will result in the formation of a small amount of new surface area that may have a higher adsorptivity and reactivity than the rest of the clump. Methods for the deagglomeration of pigments, which a few of the

constituents in the pyrtechnic formulations are, have been described in ISO 8780 – parts 1-6 (Nelson, 1996:1097-1098).

L1.2.3 Preventing Reagglomeration

Factors Affecting Reagglomeration

The factors which affect dispersion stability have been discussed in detail by Nelson (1996:1100-1104).

- *Polarisability Attraction*

All matter is composed of electric charges which move in response to an external field which can be created by the distribution and motion of charges in nearby matter. The Hamaker constant for interaction energy is a measure of this polarisability attraction between the particles. The determination of the Hamaker constant has been described by numerous authors (Nelson, 1996:1100; Drummond & Chan, 1997; Nguyen, 2000; Bergström, 1997; Reiter *et al*, 1999). Higher constants indicate greater attraction (Hann, 1996:298). The following Hamaker constants have been reported in literature (Table L-1).

Table L-1: Hamaker Constants (Lafuma, 2000)

Particle	**Hamaker Constant (10^{-20} J)**
Silicon	25.5
Water	4.35
Oxides	10.6 – 15.5
Metals	16.2 - 45.5

Nelson (1996:1100) has used the example of two identical spheres with diameter d separated in a liquid by a distance s, to describe the attractive energy, u, due to the attraction, i.e. when s=0 then u becomes infinite. A strongly adsorbed layer of liquid or other solute limits s to s_{min}, which may be set equal to twice the molecular diameter of the liquid, and u to the maximum value (Nelson, 1996:1100).

- *Thermal Jostling or Particle Motion*

If the thermal energy ($u_{thermal}$=kT as per convention) of the particles exceeds the maximum attractive energy u, then the thermal jostling is sufficient to disrupt the agglomerates and often keep the particles dispersed (Nelson, 1996:1100; Hann, 1996:296). Thus by increasing the temperature, agglomerates may be broken and particles may be dispersed. If, however, the particles collide with enough energy and are not well dispersed, they will coagulate or flocculate.

- *Sedimentation*

If the particles are more dense than the liquid medium, then they will move downwards and the bed of particles which is formed compresses toward the state of minimum-included liquid. The property of minimum included water is desirable for the processing of pyrotechnics, as the presence if water in the mixtures affects the burn rate, i.e. small amounts of water have been known to accelerate the burn rate of lead dioxide-silicon mixtures (McLain, 1980:43). If the product of the height of the container and the sedimentation force of the particles (due to gravity or centrifugation) is greater than the thermal energy, then the particles will settle in a dense bed at the bottom (or top if the particle density is greater than the density of the liquid) (Nelson, 1996:1100-1101).

- *Viscous Drag*

The viscosity of the liquid limits the velocity with which the particle can move through the liquid in response to an external force. The balance between the forces on the particle due to gravity and viscous drag determines the terminal sedimentation velocity (Nelson, 1996:1101).

- *Electrostatic Interactions*

Particles with like charges repel each other. The charges may be as a result of hydrolysis (which will be discussed later) of the surface groups or adsorption of ions from the solution. The Stern layer is defined as the layer of solution immediately adjacent to the surface that contains the counterions not part of the solid structure but which are bound so strongly to the surface that they do not exchange with the solution. The plane separating the Stern layer from the next is known as the Stern plane and has a smaller potential than at the surface. At the shear plane, the motion of

the fluid relative to the particle is equal to zero. For particles with no adsorbed surfactant or ions, this plane is at the particle surface. Adsorbed surfactant or ions that are strongly attracted to the particle, prevent liquid motion close to the particle, thus moving the shear plane away from the particle surface. The effective potential at the shear plane is known as the zeta potential that may be used to determine the electrostatic repulsion force. If the electrostatic repulsion exceeds the polarisability attraction at the distance of closest approach, determined by the surrounding fluid, then the particles may be prevented from coming into contact unless they are in a bed of sediment and are pressed together due to its weight (Nelson, 1996:1102-1103).

- *Polymer Chain Interactions*

If the particle is covered with links to polymer chains that are soluble in water, then the particles will be sterically hindered from coming together. If the chains extend a distance of δ_1 into the liquid, then according to Nelson (1996:1103), unlike electrostatic and polarisability interactions which act over large distances, steric repulsive interactions act only when $s<2\delta_1$.

Surface Modification

Reaction or adsorption at the solid surface alters the properties and lead to a surface charge or steric stabilisation.

- *Hydrolysis*

Inorganic particles have a surface charge in water that is a function of the particle's character and the pH. The surfaces of metal oxides, which are the primary constituent of the formulations, can be hydrolysed and take up H^+ or OH^- ions and become charged. Aqueous solutions may sustain potentials as high as 100mV. This potential is a function of the pH. The zeta potential is a measure of the electrostatic potential at the Stern layer that surrounds the particle. The zeta potential for the particle is positive if the solution pH is below the particle's isoelectric pH and negative if it is above the isoelectric pH. According to Nelson (1996:1105) a zeta potential greater than 30mV (positive or negative) is sufficient to keep the particles well dispersed. Lower values may be sufficient for particles with weak attractive forces (Hamaker

Constant close to that of the liquid), but not for particles with strong interactions (Nelson, 1996:1104-1105 & Hann, 1996:294-296).

It is possible to measure the surface charge of a particle using titration. The following points of zero charge or isoelectric pH values have been reported in literature:

- Fe_2O_3 (synthetic or freshly formed in water) – 8.6 (Lafuma, 2000b), 8.0 – 8.7 (Hann, 1996:295)
- Fe_2O_3 (dehydrated) – 5.2 (Hann, 1996:295)
- SiO_2 – 2.2 (Hann, 1996:295).
- Si – above 2, the zeta potential has been reported as being negative (Hackley *et al*, 1997)

This means that at a pH of 7 synthetic or freshly formed Fe_2O_3 will be attracted to Si, whereas dehydrated Fe_2O_3 will not be attracted to Si.

- *Differential Dissolution or Complexation*

In the case of ionic salts, one of the ions making up the lattice may be complexed or hydrated more readily than the other resulting in an imbalance in the particle charge. The surface charge of the particle will thus change with the solution composition as the degree of complexation is affected by additives that adsorb on the surface, complex with the ion or affect the ionic strength and hence the distance over which the particle potential is effective (Nelson, 1996:1105).

- *Chemical Grafting*

Polymer chains which are soluble in the liquid may be grafted onto the particle and provide steric stabilisation. Nelson (1996:1105) has stated that for typical interparticle potentials and a particle diameter of 10μm, steric stabilisation can be provided by a soluble polymer layer with a thickness of approximately 10nm, which can be provided by a polymer tail with a molar mass of 10kg/mol.

- *Surface Coating*

Semisteric stabilisation can be achieved by adding a dense surface coating that contains no occluded solvent, provided that the coating has a Hamaker constant, which is intermediate between the particle and the liquid (Nelson, 1996:1105-1106).

DLVO Theory

The overall stability of the particle dispersion depends on the sum of the attractive and repulsive forces as a function of the distance between the particles. The DLVO theory encompasses the attraction (as mentioned previously is a function of the Hamaker constant) and electrostatic repulsion between the particles (as mentioned previously is a function of the kinetic energy of the particle – thermal jostling; ionic strength, zeta potential and separation distance) but ignores steric stabilisation. The effect of the various variables as predicted by the DLVO theory has been summarised by Hann (1996:299) and can be found in Table L-2.

Table L-2: Effect of Increasing Various Variables on the Coagulation and Flocculation Resistance (Hann, 1996:299).

Variable	**Coagulation Resistance**	**Flocculation Resistance**
Particle size	Increase	Decrease
Surface potential	Increase	Increase
Electrolyte	Decrease	Decrease
Hamaker constant	Decrease	Decrease

Steric Stabilisation versus Electrostatic Stabilisation

Hann (1996:300) has summarised the practical differences between electrostatic and steric stabilisation. This summary may be found in Table.L-3

Table L-3: Practical Differences between Electrostatic and Steric Stabilisation

Steric Stabilisation	**Electrostatic Stabilisation**
Insensitive to electrolyte	Coagulation occurs with increased electrolyte
Effective in aqueous and nonaqueous media	More effective in aqueous media
Effective at high and low concentrations	More effective at low concentrations
Reversible flocculation common	Coagulation is often irreversible
Good freeze-thaw stability	Freezing induces irreversible coagulation

Stabilising Additives

Dispersants consist of molecules, which have one region that is soluble in the liquid and another which is slightly insoluble and attaches to the particles. The adsorbed dispersant prevents agglomeration either by steric stabilisation or by electrostatic stabilisation. The polarisability interactions attract the dispersant molecules from the solution onto the particle surface. If the adsorption sites are equivalent and do not interact with one another, then the fraction of the surface covered by the adsorbate, f, can be described by the following relationship:

$$f = \frac{K_{ads} C_{surf}}{1 + K_{ads} C_{surf}} \qquad \text{(A)}$$

Near monolayer coverage (f>0.95) can only be achieved if $K_{ads}C_{surf}$>19, which can be problematic for some dispersants since the solution concentration cannot be higher than the critical micelle concentration (CMC) (Nelson, 1996:1106-1107). Typical usage levels of high molecular weight dispersants is between 1-10% and for low molecular weight dispersants the level is between 0.5-2% for inorganic powders which the formulations are composed of (Mailwane, 2000).

Positive ions are attracted by the negatively charged surface of the solid particles and therefore will have a higher concentration near the surface than in the bulk. Meanwhile negative ions are repelled from the negative surface and will have a lower concentration near the surface. The ionic attraction or repulsion from the surface affects the non-ionic adsorption coefficient (Nelson, 1996:1107).

Short chain organics that are adsorbed may reduce the polarisability attraction between the particles, provided that its Hamaker constant is between that of the solid and the liquid medium and that the adsorption layer is thick enough. Adsorption does not follow the Langmuir adsorption profile described by equation A in aqueous systems for organic dispersants, as the tails adsorbed molecules at adjacent sites tend to attract each other strongly. Ionisable organic dispersants lose or gain protons in solution if it is within the right pH range. The ionic species may absorb on the

oppositely charged inorganic surface and provide semisteric stabilisation (Nelson, 1996:1107).

Nonionic polymeric units which have been hydrated such as polyethylene oxide are water-soluble and thus adsorb strongly to highly polar materials, whereas alkanes are adsorbed strongly on non-polar materials. The adsorption of these materials cannot be described using the Langmuir theory because the sites are not independent. Dispersants under this class include homopolymers, random block copolymers, diblock copolymers and comb polymers.

- Homopolymers consist of a series of identical segments. If their segments adsorb strongly on the particle, the polymer layer will have a compressed conformation (little occluded liquid) and provide semisteric stabilisation. Less strongly adsorbed homopolymers will coat the particles and be anchored by either loops or tails and provide steric stabilisation.
- Random copolymers consist of random length sequences of soluble segments interspersed with less soluble segments which adsorb onto the particle, while the more soluble segments form loops or tails extending into the liquid. The advantage of this type of polymeric unit over the homopolymer is that due to the separate anchor and soluble segments, there can be better control over the adsorbed layer depth and desorption. Thermal energy drives the motion of the loops and tails and provides a steric barrier. The thickness of this barrier is dependent on the solvent. In a good solvent it is roughly one-third of the fully extended length of the loop or tail.
- Diblock copolymers consist of one sequence of anchor segments and a second sequence of backbone segments. Like random copolymers, the lengths of these segments can be controlled to allow for control of the adsorbed layer depth and soluble segments.
- Comb polymers have a soluble backbone with a number of side chains that contain the anchor group (Nelson, 1996:1107-1108).

Drummond and Chan (1997) have studied the van der Waals interaction, surface free energies and contact angles for the following dispersive polymers and liquids:

- Polymers – Poly(dimethylsiloxane) (PDMS), poly(4-methyl-1-pentene) (TPX), polyethylene (PE), natural rubber and polystyrene (PS)

- Liquids – diiodomethane, 1-bromonaphthalene, 1-methylnaphthalene, bromobenzene, *tert*-butylnaphthalene, liquid paraffin and hexadecane (Drummond & Chan, 1997).

Adsorption of Microparticles

Nelson (1996:1109) has proposed that microparticles which diameters less than a tenth of the particles to be dispersed, can be attached to the larger particles by sintering prior to wet in. According to Nelson (1996:1109-1110), these particles will provide polarisability attraction if their Hamaker constant is midway between the liquid and larger particle or electrostatic attraction if the microparticles have a charge opposite to that of the larger particle. The attached microparticles will prevent the surfaces of the larger particles from coming close together, thus reducing the maximum attractive energy in the same way that encapsulation does (Nelson, 1996:1110). Solid state sintering occurs when a system of loose or compacted powders are subjected to heat treatment below the melting point of all its constituents (Kayser & Weise, 1993:118). Initially it was thought that this method could be used by sintering the Nanocat iron oxide with the silicon prior to dispersing the silicon with another reducing agent. This would allow for intimate contact between the silicon and one of the reducing agents (the Nanocat iron oxide). From the literature it appeared that the Hamaker constants could be in the right range. Despite these factors, this option cannot be used for the following reasons:

- It would entail the use of special crucibles (made from refractories such as ZrO_2 or borides of the transitions metals) which may be expensive
- The high energy cost of the sintering process
- The strong probability that during the sintering process, sufficient energy is added to ignite the mixtures and
- The practical implications of changing the formulation process that significantly in practice i.e. buying new equipment.

In summary, a dispersion can be stabilised if the maximum attractive energy is less than the thermal energy. It should be noted however that the polarisability attraction, electrostatic repulsion and steric repulsion increases with an increase in particle diameter, whereas thermal jostling is independent of the particle diameter.

L2 PROPOSED DISPERSION FORMULATION AIMS

The following aims would have to be achieved by the dispersion process:

- Wet the powders
- Break up particle clusters
- Ensure proper mixing
- Form dense, thin sediment layer of powders once they have settled using centrifugation
- Allow for easy drying
- Minimise the risk of fires when handling the dry powdered formulations downstream
- Allow for reproducible and desired burn speeds of the pyrotechnic formulations. The addition of the wetting agent and dispersant will also affect the amount of oxidising agent which is to be added. This is due to the fact that the carbon and hydrogen atoms in these compounds require oxygen during the burning process of which the oxidising agent is the only source as the reactions occur in sealed containers.
- The surfactant should also be compatible with water.

One of the problems that may be foreseen is that despite the powders being well dispersed in the liquid phase, upon settling, due to the density differences, there will be preferential settling of either the oxidising agent or the silicon. This could be overcome by either:

- Finding a surfactant or surfactant mixture that will not allow preferential settling or
- Shin *et al* (1998) have developed a deposition mechanism of oxide thin films on self-assembled organic monolayers. They developed the model because it has been proved that oxide thin films can be deposited on silicon wafers at low temperatures (<100°C) from an aqueous media using functionalised self-assembled which are ordered arrays of surfactant molecules (long chain hydrocarbons – chain lengths greater than 12CH_2 units) covalently attached to the substrate. The ordering of the surfactant molecules is as a result of the van der Waals interactions between adjacent hydrocarbon chains. It has been found that

both TiO_2 and ZrO_2 films precipitate on the sulphonate-functionalised self assembled monolayers and are adherent and uniform in thickness (Shin *et al*, 1998). This method could be modified to allow for the deposition of the desired reducing agent and not ZrO_2 or TiO_2 on the monolayer. This method would ideal as it allows for proper mixing and intimate contact between the particles – i.e. constant thermal conductivity and contact.

L3 The use of Dispersants and Surfactants for the Dispersion Formulation

L3.1 Finding the Best Wetting Agent

A "flotation" test can be used to determine the effectiveness of the wetting agent. The powder is distributed in the surface of a solution and the time taken by the particles to reach the bottom of the container is measured. This time is inversely proportional to the efficiency of the wetting agent (Mailwane, 2000).

L3.2 Choice of Surfactant – Influence of Surfactant Properties

The choice of surfactant and amount of surfactant used depends on a number of factors, i.e. the chemical nature of the hydrophile, the cmc of the surfactant

The following surfactant properties need to borne in mind when formulating the aqueous dispersions:

- Critical micelle concentration (CMC)- It will be necessary to operate below the CMC in order to avoid overdosing. Surfactants are also most effective at concentrations close to their CMC. The CMC is influenced by chemical structure, nature of counterions, temperature and pH.
- HLB-value – This classification is only used for only for the classification of nonionic surfactants. An increase in hydrophilicity results in an increase in the HLB. The typical HLB range for dispersions is 8-13. It is possible to get a measure of the HLB value from the solubility of the surfactant in water.

- Surfactant Type - Ionic surfactants work by electrostatic forces i.e. repulsion, while nonionic surfactants work by steric repulsion which is good for applications where the medium is polar i.e. water. If increase the electrolyte content of the medium, it will be possible to get close contact and flocculation. Polymeric surfactants are nonionic and contain segments that absorb strongly onto the particle and with a compressed conformation will lead to semisteric stabilisation.
- Water Hardness and Ionic Strength – Anionic surfactants will precipitate out as a result of the water hardness whilst nonionic surfactants will "salt" out of the aqueous solution as a result of the ionic strength (Bognolo, 2000)
- Solubility and Temperature – For ionic surfactants, if the temperature is increased above the Krafft temperature solubility will increase, whilst with nonionic surfactants if the temperature is increased above the cloud point, solubility will decrease.
- Other properties - Foam is an undesired property that can be overcome through the use of antifoaming agents (Broadbent, 2000). For stirred reactors and mixers foam can reduce the batch size. According to Farminer (1973), antifoams based on polydimethyl siloxane fluids have most of the desirable features necessary for controlling foam in any media, i.e. fast knockdown, long lasting action, high efficiency, low cost and ease of handling. These antifoams should, however, not be used where it is dissolved by components of the foaming system e.g. chlorinated hydorcarbon processing. The criteria for successful foam control are:
    - A lower surface tension than the foaming media
    - Insolubility in the foaming media and
    - Dispersibility in the foaming media (Farminer, 1973).

The polarity of the solids will have an effect the type of surfactant that is used. Generally for solids of low polarity long chain alcohols, POE and POE/POP may be used, whilst for highly polar solids alkylphenols, POE, POP/POE, unsaturated alcohols, block copolymers, di- and polyamides may be used (Bognolo, 2000).

L3.4 Method for Choosing the Right Surfactant

The following procedure has been proposed:

- Evaluate the surfactant solubility in the medium without the powders
- Measure the zeta potential of the particles in the medium – not use cationic dispersants if positive and anionic if negative
- Measure the viscosity of highly loaded suspension only powders and liquid (more than 40% solids) – eliminate one with higher viscosity and poor flow characteristics
- Observe sedimentation behaviour of 5 – 10% solids suspension – use only liquid and powders
- Eliminate the surfactant that gives large sediment volume and does not allow for constant and reproducible burn rates
- Check quality of complete dispersion using the British Standard (BS) 3466 (part 4) for metal oxides and ASTM standard B821-92 for metal powders or the methods contained in section 5 (Nelson, 1996:1109).

Due to their synergistic behaviour, it has been recommended that mixtures of surfactants be used. Unfortunately the mechanism of mixed surfactant adsorption is not understood (Penfold *et al*, 1998).

L4 Dispersant and Surfactant Literature for the Dispersion of the Individual Constituents of the Proposed Pyrotechnic Formulations

A vast amount of literature is available on types of dispersants. Comb graft copolymers such as methoxy polyethylene glycol with an acrylic copolymer backbone have been used with great success as a dispersant (Broadbent, 2000). Table L-4 contains examples of organic polymeric dispersants which Hann (1996:303) has summarised.

Table L-4:Examples of Dispersants (Hann, 1996:303).

Type	**Trademark Name**
Poly(meth)acrylates	Alcosperse, Aquatreat, Antiprex, Alcomer, Cyanamer, Belsperse, Goodrite, Acusol, Acumer, Tamol, Daxad.
Polymaleates	Sokolan, Belsperse, Belgard, Belasol, Norasol
Condensed phosphates	
Polysulphonates	Versa TL, Polyfon, Reax, Indulin, Vanisperse, Borresperse and Ultrazine
Sulphonated polycondensates	Lomar, Tamol
Tannins, lignins, glucosides, alginates	Marasperse

Polyacrylates are the most flexible because they are produced in a variety of molecular weights and degrees of anionic charge. Polymaleates are very similar to polyacrylates, but maleic acid is not as easily copolymerised with other functional monomers to allow tailoring for specific applications. Condensed phosphates are not used as much today, due to the role that the phosphates play in the eutrophication of water bodies (Hann, 1996:302).

The following recommendations and studies have already been made and conducted respectively for the dispersion and wetting of the individual powders:

L4.1 Silicon

- Penfold *et al* (1998) used specular neutron reflection to measure the adsorption of the mixed cationic/non-ionic surfactant mixture of $C_{16}TAB/C_{12}E_6$ at the hydrophilic Si/SiO_2/aqueous solution interface. They found that the non-ionic/cationic surfactant adsorbed layer at the Si/SiO_2 interface is a fragmented bilayer. The adsorbed layer can thus be described by three layers. The first layer, adjacent to the solid surface, contains the head groups. The next layer is the associated hydration layer containing the hydrocarbon chains interpenetrating (or

overlapping) from both sides of the interlayer and the third layer adjacent to the fluid phase containing the head groups and hydration. The bilayers were found to be essentially symmetrical, the two headgroup regions appeared identical and the alkyl chain region was less than the dimension of a fully extended chain. This was attributed in part to the fraction of alkyl chains that were in the head group region as a result of the constraints arising from the disparity in head group size between the two surfactants (Penfold *et al*, 1998).

- Hackley *et al* (1997) have compared the dispersion properties of silicon powder with and without the use of surfactants. They found that the untreated silicon powder was easily dispersed and the results obtained were consistent with a model of the particle-solution interface based on the SiO_2-H_2O systems. The suspensions exhibited negative surface potentials at pH values exceeding 2 and were a maximum at pH 9. Furthermore, silicon that had been aged in an electrolyte solution had a higher surface potential, which they attributed to the increase in the surface site density of the Si-OH groups that occurred as a result of slow surface hydrolysis reactions. A summary of their results with various dispersants has been summarised in Table L-5.

Table L-5: Dispersion of Silicon using various Dispersants (Hackley et al*, 1997)*

Dispersant	**Findings**
Daxad 34 – anionic surfactant, linear poly(methacrylic acid) (PMAA)[1]	Had little effect on particle potential – weak interaction with the Si surface. But the adsorption on the negatively charged silicon was functionally similar to the adsorption behaviour for poly(acrylic acid) on Si_3N_4 and PMAA-Na^+ on Al_2O_3 at ph values above their isoelectric pH
Betz 1190 – dimethylamine-epichlorohydrin linear copolymer[2]	Resulted in a shift in the isoelectric pH with increasing polymer concentration (Saturation between 0.1 – 0.5%). Also resulted in a positively charged particle whose electrokinetic behaviour was independent of pH or polymer concentration

Dispersant	Findings
Daxad CP2 - dimethylamine-epichlorohydrin linear copolymer[2]	Similar to results obtained with Betz 1190
Betz 1195 – cross linked form of Betz 1190 with a higher M_r[2]	Similar to results obtained with Betz 1190

[1] A weak acid that dissociates to form an anion. Acid-base properties dependent on the solution pH.

[2] The copolymers are salts of quaternary ammonium compounds and therefore carry a positive charge regardless of the pH.

L4-2 Antimony Trioxide

Mailwane (2000) found during laboratory tests that calsoline oil appeared to be a good wetting agent for antimony trioxide.

L4-3 Iron Oxide

Homopolymers have been found to be ineffective for imparting steric stabilisation as the polymer chain prefers to associate with the solvent molecules of with the surface of the particle and not both at the same time (van der Avort, 1992). van der Avort (1992) has recommended that for metallic iron oxide (red) dispersion surfactants such as Hypermer CG6 (soluble graft copolymer), A109 (modified soluble polyester), PS2 (dispersible polyester) and Atlas G4911 (soluble POE alkyl aryl phenol). These are all nonionic surfactants, which provide steric stabilisation. The recommended dosage for metallic oxides is 1-3% based on the mass of solids (van der Avort, 1992).

L5 Dispersion Evaluation

The degree of deagglomeration can be evaluated using the following methods:

- *Viscosity* – The viscosity of a suspension that contains clumps decreases as the degree of deagglomeration decreases. This is attributed to the fact that the clumps contain occluded liquid and the volume fraction of the clumps is larger than the

volume fraction of the individual particles and so there is less free liquid to facilitate the flow than if the clumps were deagglomerated. This method of evaluation has a few inherent disadvantages, i.e. it is not sensitive in the final stages of deagglomeration.

- *Particle Size Distribution* – The degree of deagglomeration can be monitored using either sieving (particles >20μm) or instrumental particle size analysis for smaller particles.
- *Tinting Strength* – When the particles are well dispersed, they block more light than when there are clumps. Samples have to be taken at various intervals and a fixed quantity of well dispersed contrasting colour pigment added. The samples can then be analysed using a sensitive colorimeter. This method of evaluation cannot be used if the pigment is agglomerated by the sample or the sample and pigment settle out.
- *Grind Gauge* – This method has been described by Nelson (1996:1110). It cannot be used as it involves scraping an excess amount of sample, which is a paste. This may ignite the more sensitive pyrotechnic mixtures. The results obtained using this method are also subject to considerable variations.

The stability to reagglomeration may be evaluated using the following procedures:

- *Microscopy* – The optical microscope may be used for the evaluation of dilute suspensions (<1% solids) of particles 1-10μm. If the dispersion stable, thermal jostling can be seen and the particles will avoid coming close to one another or separate soon after collision.
- *Sediment Volume* – A stable dispersion will result in a thin sediment bed with maximum solids packing and minimum occluded liquid as the particles will move freely past each other to avoid contact as long as possible. Centrifugation will have to be used to force the particles to settle within a reasonable time.
- *Other* Other methods that could be used include the response to electric and acoustic fields, spectroscopy and drift in tinting strength (Nelson, 1996:1110-1111).
- *Ultrasonic Characterisation* – Guidarelli *et al* (1998) used ultrasonic attenuation to analyse suspensions of alumina powder in water at high concentrations (40% vol.). The purpose of their study was to identify weak structural differences that

occur between suspensions with different degrees of deflocculation, obtained by varying the quantity of dispersant around the critical value. This is difficult to be determined using other methods. They found that weakly flocculated suspensions presented lower attenuation than well flocculated suspensions (Guidarelli *et al*, 1998).

Hackley *et al* (1997) have measured the electrokinetic sonic amplitude (ESA) for silicon powder suspensions using an electoacoustic analyser equipped with an autotitrater, overhead stirrer and pH, temperature and conductivity probes. The ESA signal is proportional to the zeta potential and provides a convenient method of determining the polarity and relative magnitude of the charge carried by the particles. The titration data also provide a measure of the particle potential as a function of the pH and can thus be used to determine the isoelectric point (Hackley *et al*, 1997).

The easiest variables to measure for the evaluation of the dispersion would be viscosity, particle size distribution and sediment volume.

L6 DISPERSION PROCESSING EQUIPMENT

Nelson (1996:1098-1099) has described typical design elements for the wet in of powders and wet deagglomeration, the selection of which depends on the application It appears that for the dispersion of the pyrotechnic formulations the equipment in Figure L-1 for the following reasons:

- The disk impeller provides a rapidly refreshed liquid surface by creating a deep vortex. This exposes a new surface area for the powder addition
- The up and downward teeth at the edge of the impeller cause impact, turbulence and cavitation
- The baffles force vertical circulation.
- The equipment promotes rapid wet in due to the low gas pressure, high centrifugal force and the distribution of the powder in a thin and deagglomerated layer on the liquid
- The provision for the flow of clear liquid down the sides of the equipment aids in the prevention of scale and encrustation. Scale forms above the level when

airborne dust sticks to a wall wetted either by vapour condensation of liquid being drawn up the wall by capillary action through previously deposited scale. Encrustation forms near the shoreline of the tank as a result of the wetting and recession due to hydraulic pulses during agitation and then drying near that level. These two properties are undesirable in the processing of pyrotechnic powders as they lead to contamination of the batches which are prepared, the encrustation allows for a dry exposed areas which are easily ignitable and lastly during the processing and subsequent cleaning of the equipment of hazardous powders such as red lead, operators will be exposed directly to the powders (Nelson, 1996:1097&1099).

- A limitation of such a system is the heat that is generated to the high shear. Care should be taken not to have a high solids loading as this will increase the viscosity and hence the shear.

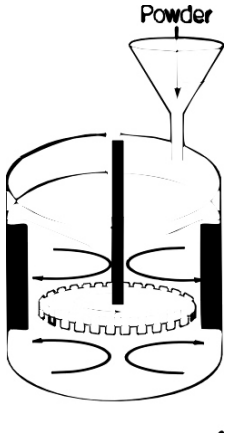

Figure L-1: Processing Equipment for Pyrotechnic Powder Wetting and Deagglomeration (Nelson, 1996:1098-1099).

Penfold *et al* (1996) have studied the effect of shear on the adsorption of a non-ionic surfactant at the silicon/solution interface using a specially constructed shear cell for neutron reflectivity measurements. They found that the hexaethylene glycol monohexadecyl ether ($C_{16}E_6$) there was evidence of shear induced structures in the vicinity of the cell wall. Furthermore at low surfactant concentrations ordered layering of the surfactant separated by solvent-rich regions and extending into the bulk solution was observed, in addition to the adsorbed layer on the solid surface. The

application of Poiseuille shear flow induced a more ordered and well defined structure at the interface (Penfold *et al*, 1996).

APPENDIX M

DISPERSION OF TYPE 4 SI AND CUO

EXPERIMENTAL DATA